An Autonomous Robot for Weed Control
-
Design, Navigation and Control

Tijmen Bakker

An Autonomous Robot for Weed Control

–

Design, Navigation and Control

Tijmen Bakker

An Autonomous Robot for Weed Control

—

Design, Navigation and Control

Tijmen Bakker

"Onbereikbaar is dat wat bestaat, en onpeilbaar, wie kan het doorgronden?"

Prediker 7:24

Voorwoord

Nu dit proefschrift klaar is, wil ik iedereen bedanken die direct of indirect een bijdrage aan dit werk heeft geleverd. Een aantal van hen wil ik hier noemen.

Allereerst wil ik mijn dagelijkse begeleiders bedanken, Jan Bontsema en Kees van Asselt. Kees, jij bent degene die van het dichtst bij alle vreugde en frustratie bij het onderzoek met 'de robot' hebt meegemaakt. Als het maar even kon maakte je tijd vrij om proeven te doen, en mee te denken over de oplossing als we weer eens vastliepen op een of ander technisch probleem. Altijd was je nauw betrokken, je inzet is enorm geweest, heel hartelijk bedankt daarvoor. Verder heb ik door jouw uitgebreide kennis van elektronica van alles van je geleerd. Een paar hoogtepunten wil ik even memoreren: de proef voor het Rijkswaterstaat project waarbij we in de stortregen met jouw auto achter de robot aanreden en voor het eerst zagen hoe de robot keurig autonoom de rand van de parkeerplaats langs de snelweg schoonveegde; en de show op de Agritechnica 2007 die we samen hebben verzorgd, waarvoor jij op de valreep in het beursmagazijn van Schenker Logistics het startprobleem oploste. Dat waren mooie momenten. Jan, hartelijk bedankt voor je begeleiding. Ik heb veel van je geleerd, natuurlijk allereerst over het besturen van 'die kar' die voor jou uiteindelijk toch niets meer was dan een integrator. Met jouw brede kijk op regeltechniek weet je heel goed de praktijk in theorie te vertalen en begrijp je heel goed wat de theorie betekent voor de praktijk, ondanks dat je volgens eigen zeggen 'niet kunt programmeren', maar dat is dan ook niet nodig want 'software lost niets op'. Verder heb ik ook andere dingen van je geleerd, zoals die in de sfeer van het vormgeven van onderzoeksprojecten. Jij hebt een grote bijdrage aan dit onderzoek geleverd en het doet me goed dat je als co-promotor wilt optreden.

Verder wil ik mijn promotoren bedanken, Gerrit van Straten en Joachim Müller. Gerrit, bedankt voor je nauwkeurige en uitgebreide commentaar op mijn teksten en voor je bereidheid om gedetailleerd mee te denken wanneer dat nodig was. Joachim, jouw altijd positieve benadering van het onderzoek heb ik als erg opbouwend ervaren. Ondanks dat je de laatste tijd in Hohenheim bij Stuttgart werkt, maakte je tijd vrij om naar Wageningen te komen en bleef je inhoudelijk betrokken.

Verder ben ik dank verschuldigd aan de bredere begeleidingscommissie waar naast de al genoemde begeleiders en promotoren Kees Lokhorst, Bert Vermeulen en

Jan Willem Hofstee deel van uitmaakten. Jullie inzichten en ideeën waren een waardevolle bijdrage aan mijn onderzoek. Ook wil ik de klankbordgroep noemen: Lammert Bastiaans, Jaap van Bergeijk, Jan Kouwenhoven, Dirk Kurstjens, Bert Lotz, Douwe Monsma, Lie Tang, Anton van Vilsteren en Rommie van der Weide, bedankt voor de input uit de wetenschap en praktijk.

Ook bedank ik mijn collega's bij de leerstoelgroepen Systems and Control en Farm Technology voor de prettige werksfeer. In het bijzonder wil ik ook de AIO's bedanken die zo ongeveer in dezelfde periode begonnen voor de gezellige sfeer waarin het goed delen was van typisch promoveer-ongerief. Rachel, we hebben deze tijd bij elkaar op de kamer gezeten, bedankt voor je gezelligheid, interesse, en voor alle Matlab en Latex tips. Gerard, bedankt voor je waardevolle adviezen en praktische software oplossingen.

Veder bedank ik de mensen die zich ingezet hebben bij het vormgeven van de robot: Frans van Korlaar, Jeroen Kok, Michel Govers, Geerten Lenters, Jordan Charitoglou en Marcel Walvoort. Ook wil ik de studenten bedanken die in het kader van een afstudeervak of stage bij dit onderzoek betrokken waren: studenten Agrotechnologie René van Bruggen, Michel Huls, Micha van Lieshout, Allard Martinet, Jan-Kees de Voogd, Tom van der Walle en Hendrik Wouters; HTS studenten Evert-Jan van den Berg, Jasper Boom, Erik Conijn, Jaap van Dijk, Mohamed El Harchi, Frank Hoving, Erik Janssen, Emiel de Jong, Stijn Knoop, Robin Kramer, Hugo Kruk, Koen Luttikhold, Michael Stauder, Sebastiaan van der Steen, Ivan Timmers, Onno Veldhuyzen, Arjan Vroegop, Pascal Winters en Anne Wiebe de With.

Naast de mensen die direct betrokken waren bij het onderzoek, zijn mensen om mij heen zeker niet minder belangrijk geweest om dit proefschrift te kunnen voltooien. Allereerst wil ik mijn ouders graag bedanken. Jullie hebben altijd ruimte gecreëerd om te kunnen studeren en me gestimuleerd om een studie te kiezen die bij me past, waardoor ik uiteindelijk ook aan dit promotie-onderzoek heb kunnen beginnen. Dat dit bij mij past is ook het resultaat van de interesse in landbouwmachines die kon groeien door al het trekkerwerk wat ik op 'de boerderij' kon doen: ome Jan, bedankt daarvoor. Ook mijn zussen en zwagers wil ik bedanken voor alle interesse, betrokkenheid en steun gedurende dit onderzoek. Rik, ook al kun je dit nu nog niet lezen, bedankt voor alle vreugde die je geeft.

Verder wil ik een ieder bedanken die bij mij op welke manier dan ook betrokken was, hetzij door belangstelling, interesse, gezelligheid, afleiding, meeleven, begrip, vriendschap, of hoe dan ook. Twee vrienden wil ik speciaal noemen: René van der Linde en Albert Folmer, jullie hebben deze hele periode met mij meegeleefd. Het doet me goed dat jullie mij als paranimf terzijde willen staan.

Tenslotte, last but not least, Krista, bedankt voor je meeleven en meedenken bij het maken van dit proefschrift, dank voor je support!

Contents

Chapter 1

Introduction

1.1   Scope and motivation

Major factors driving the presently increasing interest in non-chemical weed control are: concern about herbicides polluting ground and surface water, human health risks from herbicide exposure or residues, effects on the flora and fauna, development of herbicide resistance and the lack of approved and effective herbicides for minor crops such as vegetables. Inter-row weeds, which are those growing between crop rows, are relatively easily controlled by non-chemical means. Inter-row cultivation using tines with hoe blades is the most common method. But to control intra-row weeds, which are the weeds that grow within the line of row crop plants and are not affected by inter-row cultivation, a large amount of labor is needed for manual weeding. Currently no equipment is available that replaces manual weeding completely. The labor required for manual weeding involves high costs and it is often difficult to organize. The mean input of manual weed control in organic grown crops in the Netherlands is ca. 45 h ha^{-1} for planted vegetables, but increases to more than 175 h ha^{-1} for direct-sown onion (Van der Weide et al., 2008). In 1998, on average 73 hours per hectare organic grown sugar beet were spent on hand weeding in the Netherlands (Van der Weide et al., 2002). Sørensen et al. (2005) calculated that by maintaining an altered crop plan and introducing new robotic weeding technology, the labor demand can potentially be reduced by 85 percent for organic sugar beet production. Furthermore, technology solving this problem may provide a means of reducing agriculture's current dependency on herbicides, improving its sustainability and reducing its environmental impact (Slaughter et al., 2008).

Replacing manual weeding by a machine requires advanced technology, because the machine has to establish where crop plants or weed plants are located and has to remove the weeds with a precisely controlled device. So, in general, research is firstly concentrating on answering the question how weeds in the intra-row area can be detected and removed by advanced technology.

The required precision of the removal of weeds from the intra-row area limits the attainable capacity (which is equivalent to driving speed) of the solutions for automatic intra-row weeding. With the increasing labor costs for the driver and the expected high investment costs for such technology, still considerable operating costs per hectare are expected. Therefore, research in this area secondly is concentrating on answering the question how to do intra-row weed control cost-effectively if the issue of automatical detection and removal is solved.

Automatic discrimination of crop and weeds is done by e.g. discriminating structured patterns (crop) from unstructured (weed), seed mapping, measurement of spectral reflectance and by machine vision (Bontsema et al., 1998; Griepentrog et al., 2005; Vrindts et al., 2002; Gerhards and Sökefeld, 2001; Åstrand, 2005; Blasco et al., 2002; Lamm et al., 2002; Nieuwenhuizen et al., 2007). A number of these methods are combined with a non-chemical actuator to remove weeds from the row (Bontsema et al., 1998; Kielhorn et al., 2000; Blasco et al., 2002; Home, 2003; Åstrand, 2005; Gobor and Schulze Lammers, 2006; O'Dogherty et al., 2007; Tillett et al., 2008). While the results are promising, these advanced methods are hardly applied in machines in practice. The intra-row weeder of Garford (Garford, 2008) applies the methods of Tillett et al. (2008). The machine of Radis Mécanisation (Van der Schans et al., 2006) discriminates between crop and weed based on a difference in height: From plants above a certain height it is assumed that these are crop plants. The latest machine can be only used in transplanted crop, where crops have lead on the weeds regarding their size. The applicability of this discrimination method is limited.

To attain acceptable operating costs for advanced intra-row weed control, technology is developed that can perform intra-row weeding autonomously. This robotization of intra-row weed control fits into a broader scope of research and development of automatic guidance for agricultural applications in open fields. Automatic guidance of agricultural vehicles has received already the attention of researchers from the early days of the tractor (Wilson, 2000; Reid et al., 2000). Systems that follow furrows to guide a machine across the field were already diagrammed in patents in the early 1920s (Reid et al., 2000). The most apparent motivation for research to automatic guidance is to relieve the operator from continuously making steering adjustments while maintaining the attached or towed implement at some level of acceptable performance. The economic objective to carry out field operations with minimum costs has led to tractors with more power and implements with higher capacity by both higher working width and speed and higher complexity e.g. when multiple operations like tillage and seeding and fertilizer application are combined in one machine. These developments made the task of the operator more complex and the need to relieve the driver more apparent. Typical early approaches for guidance with respect to a directrix generated by the previous path of operation mentioned by (Wilson, 2000) are: wheels attached to mechanical linkages pin-connected to the tractor straddling the marker furrow (Grovum and Zoerb, 1970), mechanical fingers mounted on the cutter bar of a windrower (Parish and Goering, 1970), a furrow engaging device ahead of the tractor's front wheel and attached to the steering linkage (Kirk et al., 1976) and optical sensors mounted

for non-contact sensing of the furrow wall (Harries and Ambler, 1981). Mechanical feelers which mechanically follow a ridge, furrow or crop are commercially available (Reid et al., 2000; Tillett, 1991). The use of low cost devices that mechanically follow a furrow has been strictly limited for a number of reasons including reliability, particularly in stony soils or where the furrow has become eroded, the requirement to perform headland turns manually, and safety (Tillett, 1991). Another type of early approaches for guidance used a directrix generated by fixed points in the field like buried leader cables (Telle and Perdok, 1979) and radio beacons (Searcy et al., 1990). The cost of the buried cables is difficult to justify on large fields that are not intensively farmed, and the cost of signal processing plus line of sight limitations has limited the application of radio beacons (Wilson, 2000).

Current research for automatic guidance concentrates mainly on two recent technologies: machine vision and GPS. Machine vision systems provides both offset and heading information to the control system. Typical papers on the development of computer vision of vehicle guidance are Reid and Searcy (1988), Marchant (1996), Gerrish et al. (1997), Billingsley and Schoenfisch (1997) and Søgaard and Olsen (2003). Computer vision has great potential, but encounters sometimes difficulties in obtaining the required features from an image caused by e.g. changes in the level of ambient lighting, partial shadowing and blurring due to movement of the camera Wilson (2000). With GPS the location of the vehicle and the location of a path in a field that the vehicle must follow can be determined in absolute coordinates, from which the relative location of the vehicle to the path can be calculated. GPS based guidance requires that absolute coordinates of the path to be followed are known. However, those coordinates can be transferred from earlier operations or can be generated automatically parallel to and one working width apart from a first manual driven path. Precise GPS with an accuracy of less then 2 cm using carrier phase information requires in addition to the mobile receiver a fixed base station receiver at a known location close to the work area. The costs of such GPS systems are still considerable. The main limitations are the consistent positioning accuracy in the range of centimeters at field conditions where the GPS signal is obscured e.g. in the presence of buildings or trees. Typical developments of GPS based guidance are the work of O'Connor (1997), Bell (1999), Van Zuydam (1999), Noguchi et al. (2001a), Thuilot et al. (2002) and Rekow and Ohlemeyer (2007). O'Connor (1997) showed centimeter-level path tracking with a tractor in the field of a linear path and U-turns made between the parallel linear pathes automatically. Bell (1999) showed path following control with a tractor on realistic non-linear farm trajectories. Nowadays most tractor manufacturers can supply GPS-based guidance for their tractors. Also, there are a number of companies that

deliver GPS based guidance that can be retrofitted to existing tractors (Trimble, 2008a; SBG-Innovatie, 2008). Recently tractor manufacturer John Deere included automatic headland turning in their commercially available driver assisted steering system (Rekow and Ohlemeyer, 2007).

Both GPS and vision also have been used to develop autonomous agricultural machinery. John Deere developed a GPS based autonomous orchard tractor in cooperation with Autonomous Solutions Inc (Torrie et al., 2002). Demeter, a New Holland Speedrower (selfpropelled swathmower) harvested nearly 100 ha of crop autonomously (Pilarski et al., 2002). The "Automaatje" robot vehicle developed to perform light tasks in the field could drive autonomously in a field based on RTK-DGPS (Van Zuydam and Achten, 2002; Thoma, 2005). Stentz et al. (2002) tested a computer controlled tractor supervised remotely by a human while it autonomously drove seven kilometers in an orange groove. Recently small autonomous scouting vehicles like the Cropscout (Van Henten et al., 2004), WURking (Hofstee et al., 2007) and Sietse (Van Evert et al., 2006) have been developed mainly for competition in autonomous navigation in between maize rows in the Field Robot Event (Van Straten, 2004; Van Henten and Müller, 2007). Tasks currently performed by one tractor driver with a big machine could be replaced in the future by a number of small sized field robots. The small size of field robots is expected to have positive effects on environment, energy use and weather dependency but also on the economics of farming. Economic factors include the lower incremental investments in machines and production profit when components can be mass produced (Blackmore et al., 2005; Bakker et al., 2006).

Only a few concepts of robotic systems are specially developed for weed control and have been tested under field conditions. Jørgensen et al. (2006) showed a robotic tool carrier for weeding that demonstrated row following ability at the Field Robot Event 2007 but results are not published yet. Bak and Jakobsen (2004) describes an agricultural robotic platform with four wheel steering for weed detection that employs GPS as the main sensor for guidance. Its useability for e.g. soil cultivation tasks like mechanical hoeing is limited due to its limited power. The results show the performance of the path following control on different path shapes. Åstrand and Baerveldt (2002) developed and tested a robot that employs one vision system to guide the robot along the rows and another to identify a crop among weeds plants. The last one is used to control a weeding-tool that removes the weeds in between the crop plants in the row. In an outdoor test on about 80 meters of a rape field the typical lateral offset error measured by the row recognition vision system was about $\pm$ 2 cm at the front of a vehicle, and from earlier indoor tests it was concluded that

an error of $\pm$ 1 cm could be expected at the rear at the weeding tool position. The robot has four major systems: the robot control system, the row recognition system, the plant identification system and the weeding system. A test in a greenhouse with sugar beet with no weeds showed that all sub-systems worked well together: The robot was able to do weed control in the seedline between the crop plants in a sugar beet row. Hague and Tillett (1996) and Tillett et al. (1998) transformed an originally manually driven commercially manufactured vehicle for use on horticultural plots into a robotic platform for plant scale selective operations like mechanically removing or destroying weeds. The autonomous vehicle uses vision, wheel encoders, a pair of piezo-resistive accelerometers and a solid-state compass. The sensor data was fused using a Kalman filter. The reported standard deviation of the offset of the vehicle was 20 mm. The vehicle has been operating on sets of four and eight plant beds of 40 m in length, including three and seven headland turns respectively with good reliability. Crop plant positions of a young transplanted crop were detected by machine vision and sprayed by an array of solenoid valves. Tillett et al. (1998) reported good results with machine vision based navigation under selected experimental conditions, meaning consistent lighting and without long shadows, a flat field with only minor disturbances and a healthy crop with no large areas of missing crop and virtually no weed infestation. They assess the developed row guidance method as being applicable for mechanical hoe guidance after improvement to correct for variable lighting conditions and developing necessary sensing and control strategies, which they showed in later papers (Tillett and Hague, 1999; Tillett et al., 2002; Tillett and Hague, 2006). They argue that the advantage of applying this technology to manually driven tractors is that the operator can intervene under especially difficult conditions. Tillett et al. (1998) judge that full autonomy requires much higher levels of reliability. Autonomous operation might need a secondary independent location system like DGPS for reasons of safety and liability by which field boundaries can be marked out.

1.2   Research objectives

Notwithstanding all the research already performed on technology required for autonomous weeding, the issue of autonomous weeding is not yet solved. There are no autonomous weeders on the market, while the problem of manual weeding is still apparent. Research to autonomous platforms for weed control focussed mainly on autonomous navigation related issues, but the design of a complete autonomous weeding system considering all implications of full autonomy was not yet worked out

systematically. The availability of a mobile platform resulting from such a design is a necessary condition to contribute the problem of autonomous weeding. The most extensive research on robots for autonomous weeding of Tillett et al. (1998) and Åstrand and Baerveldt (2002) both demonstrated vision based guidance under field conditions, where only Tillett et al. (1998) showed autonomous headland turning. While Tillett et al. (1998) suggested a secondary independent location system for reasons of safety and liability like RTK-DGPS, they did not implement this yet. From research and practical availability of tractor guidance we know that with RTK-DGPS based steering assistance of robust guidance of tractors is possible (O'Connor, 1997; Bell, 1999; Noguchi et al., 2001a; Thuilot et al., 2002), also on the headland (Rekow and Ohlemeyer, 2007). With the increasing number of tractors equipped with this technology, RTK-DGPS measured row location information from seeding with an RTK-DGPS equipped tractor system could be available soon for navigation with an autonomous weeder. While Bak and Jakobsen (2004) explored RTK-DGPS based navigation with a platform for weed control on various path shapes in isolation, results from autonomously navigating in a field were not yet shown.

The objective of this research is to replace manual weeding in organic farming by a device working autonomously at field level. Developing such a device is considered as a design problem. So the main research question was how to design a device working autonomously at field level to replace manual weeding. The resulting concept design led to the following autonomous navigation related research questions:

- How to detect crop rows by machine vision.
- How to perform path-following control with a four-wheel steered robotic vehicle.
- How to navigate autonomously in a field given crop row locations and field and headland boundaries.

1.3   Outline of the thesis

The thesis is outlined as follows:

Chapter 1 is the general introduction.

Chapter 2 describes the design of the autonomous weeder starting from the objective using a systematic design approach. The requirements formulated in this chapter were investigated by Kok et al. (2003) by means of interviewing specialists

including researchers and organic farmers. It results in a four-wheel steered robotic platform.

Chapter 3 describes a vision based row detection system that can detect crop rows of sugar beet. Detection of sugar beet crop rows by machine vision is needed for crop row following.

Chapter 4 describes the control design for path following with the four wheel steered robotic platform that was tested using GPS.

Chapter 5 presents the results of autonomous navigation on a field based on GPS while mapping crop rows with the camera. It describes the control system implementing a hybrid deliberate architecture with a reactive behavior based layer.

Chapter 6 presents the conclusions of this research and the perspectives for further research.

Chapter 2

Systematic Design of an Autonomous Platform for Robotic Weeding

Abstract

The systematic design of an autonomous platform for robotic weeding research in arable farming is described. The long term objective of the project is the replacement of hand weeding in organic farming by a device working autonomously at field level. The distinguishing feature of the described design procedure is the use of a structured design approach, which forces the designer to systematically review and compare alternative solution options, thus preventing the selection of solutions based on prejudice or belief. The result of the design is a versatile research vehicle with a diesel engine, hydraulic transmission, four-wheel drive and four-wheel steering. The robustness of the vehicle and the open software architecture permit the investigation of a wide spectrum of research options for intra-row weed detection and weeding actuators.

Keywords: structured design, machine vision, GPS, robotics, intra-row weed control, autonomous weeding, organic farming.

2.1 Introduction

Automation of agricultural machinery is seen as a means to reduce cost in current and future field operations. Some authors have proposed multipurpose mechanical frames (Manor, 1995), while others presented automated agricultural machinery (Pilarski et al., 2002; O'Connor, 1997; Noguchi et al., 2001a; Nagasaka et al., 2004) or smaller autonomous vehicles for specific applications (Blackmore et al., 2005; Bak and Jakobsen, 2004; Tillett et al., 1998; Jørgensen et al., 2006).

Automation of mechanical weed control in arable farming is one example that could contribute to sustainable food production at lower cost. Weeds in agricultural production are mainly controlled by herbicides. As in organic farming the use of herbicides is prohibited, weed control is a major problem. While there is sufficient equipment available to control the weeds in between the rows (inter-row weeding), weed control within the rows (intra-row weeding) still requires a lot of manual labor. This is especially the case for crops that are slowly growing and shallowly sown like sugar beet, carrots and onions. In 1998, on average 73 hours per hectare sugar beet were spent on hand weeding in the Netherlands (Van der Weide et al., 2002). The required labor for hand weeding is expensive and often not available. Autonomous robotic weed control systems could replace this labor and could also reduce agriculture's current dependency on herbicides, improving its sustainability and reducing its environmental impact (Slaughter et al., 2008).

Different robotic applications have different requirements and for the same robotic application even different assessments can be made when deciding about the technology to be incorporated as has been described by different researchers (Vestlund and Hellstrom, 2006; Bak and Jakobsen, 2004; Jørgensen et al., 2006). While those studies provide great insight in requirements and the assessments made about the available technology to be incorporated, the method used to achieve a final solution stays unclear. This paper presents the design of an autonomous platform for weed control research using a systematic design method from mechanical engineering. In doing so, an overview is given of alternative solutions for components of the system presented in the literature, and the benefits of applying a systematic design method are explored.

Objective

Problem definition phase

Function structure

Alternatives definition phase

Concept solution

Forming phase

Prototype
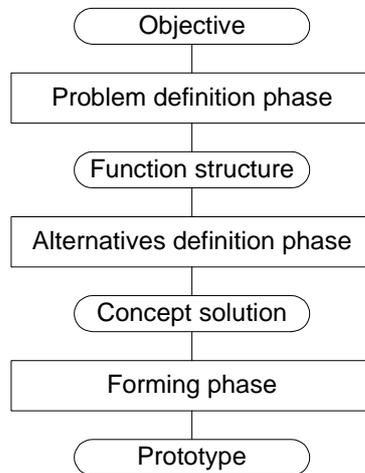
Figure 2.1: The design process

2.2 The design procedure

2.2.1 Method

The autonomous weeding robot is designed using a systematic design method described by (Van den Kroonenberg and Siers, 1998). This method belongs to a class of methods using a phase model of the product design process. These methods describe the product design as a process consisting of different phases at different levels of abstraction (Roozenburg and Eekels, 2003). The phases are (1) 'problem definition phase', (2) 'alternatives definition phase' and (3) 'forming phase' (fig. 2.1). The results of the respective phases are a function structure, a concept solution and a prototype, respectively.

The problem definition phase starts with defining the objective of the design. In the problem definition phase a set of requirements is established, that can be split into fixed and variable requirements. A design that does not satisfy the fixed requirements is rejected. Variable requirements have to be fulfilled to a certain extent. To what extent these requirements are fulfilled, determines the quality of the design. The variable requirements are also used as criteria for the evaluation of possible concept solutions. The last part of the problem definition phase consists of the definition of the functions of the robot. A function is an action that has to be performed by the robot to reach a specific goal. In our case, important functions are 'intra-row weeding' and 'navigate along the row'.

The functions are grouped in a function structure, which represents a solution on the first level of abstraction (fig. 2.2). The function structure consists of several functions. Every function can be accomplished by several alternative principles, e.g. mechanical and thermal principles for weed removal.

In the alternatives definition phase, possible alternative principles for the various functions are presented in a morphological chart (fig. 2.3 and 2.4). The left column lists the functions and the rows display the alternative principles. By selecting one alternative for each function and by combining these alternatives, concept solutions are established. These concept solutions are represented by lines drawn in the morphological chart. The best concept solution is selected using a rating procedure.

In the forming phase the selected concept solution is worked out into a prototype.

2.2.2 Application for the weeding robot

According to the ultimate research objective, formulated as 'replacement of hand weeding in organic farming by a device working autonomously at field level', the first step in the problem definition phase was to establish the set of requirements. For this purpose interviews were held with potential users, scientists and consultants related to organic farming. The resulting requirements are listed below.

Fixed requirements:
- Replacing hand weeding in organic farming.
- Applicable in combination with other weed control measures.
- Manual control of the vehicle must be possible for moving the vehicle over short distances.
- Weeding a field autonomously.
- Ability to work both day and night.
- The weeding robot must not cross the field boundaries.
- The weeding robot must be self restarting after an emergency stop.
- The weeding robot informs the farmer when stopped definitely, e.g. due to security reasons or when the task is finished.
- The weeding robot sends its operational status to the user at request.
- The weeding robot must function properly in sugar beet.

Variable requirements:
- Removing more than 90 percent of the weeds in the row.

- The costs per hectare need to be comparable to the costs of hand weeding or less
- Damage to the crop is at least as low as with hand weeding.
- Wheel pressure of the weeding robot must be not higher than for mechanical weeding.
- Energy efficiency at least as high as mechanical weeding.
- Noise emission not higher than mechanical weeding.
- Safe for people, animals and property.
- Supervision requirement at least lower than hand weeding.
- Complexity of operation not higher than mechanical weeding.
- Reliable functioning.
- Suitable as research platform.

The requirement 'Suitable as research platform' requires some explanation. There are many open questions related to autonomous vehicles in the agricultural area. Some of these are related to the behavior in obstacle avoidance, safety manoeuvres, intelligent turns at the headland, intelligent driving strategies for covering a field or in multi-vehicle environments, and freedom in positioning of implements by manoeuvring the vehicle. In order to allow the investigation of such issues, it is desirable to have a platform with more degrees of freedom, than perhaps ultimately needed. In addition, changes in construction should be easy.

After establishing the set of requirements the functions of the weeding robot were identified. These functions were grouped into a function block scheme. This scheme is represented in figure 2.2. Functions located in parallel lines can be performed simultaneously.

The navigation system consists of four functions. Firstly, the weeding robot should constantly determine whether it is located in- or outside the field borders. Secondly, if within the field borders, it should determine whether it is on a headland or not. Thirdly, in case it is not on the headlands, it should navigate along the row and perform the intra-row weeding. Fourthly, if the weeding robot arrives on the headland, it should stop the intra-row weeding and start to navigate to the next crop rows to be weeded. This sequence repeats until the whole field, except the headlands, is weeded. Weeding of the headlands is left out of consideration. An increasing number of farmers in the Netherlands do not grow sugar beet at the headlands because they think it is not cost-effective.

In the alternatives definition phase possible alternative principles for the various functions are listed in a morphological chart (figures 2.3 and 2.4). Four people
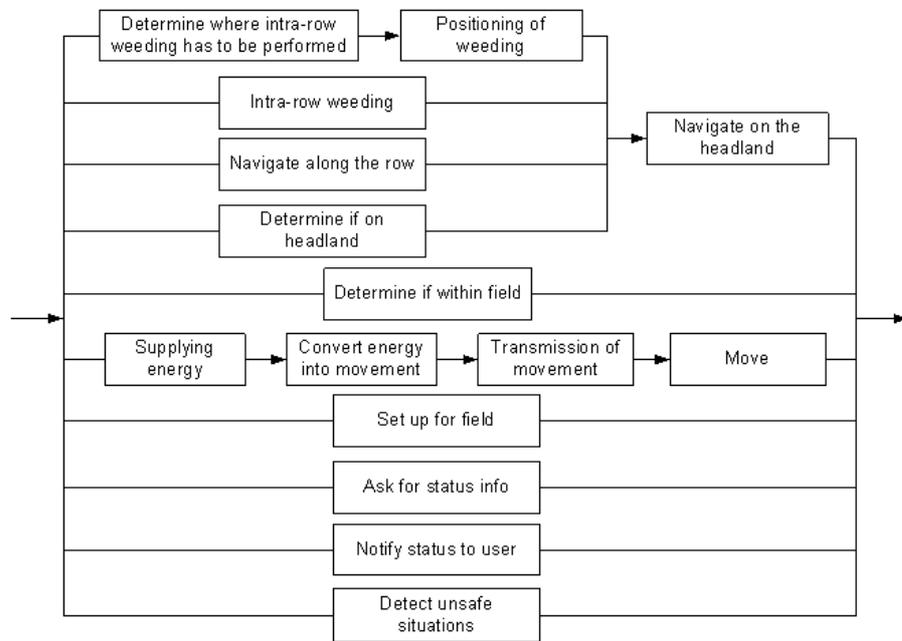
Figure 2.2: The function structure

involved in the project drew lines indicating possible concept solutions in the chart. These concept solutions were then weighed against each other in consultation based on their expert knowledge, using the variable requirements listed above. The concept solution indicated by the line in figures 2.3 and 2.4 is the final concept solution. Finally, in the forming phase the concept solution was worked out into a prototype.

2.2.3   Results of the design process

Determine where intra-row weeding has to be performed

The following alternatives to determine where intra-row weeding has to be performed were taken into consideration (see also figures 2.3 and 2.4):

- **Seed mapping.** During seeding the positions seeds can be recorded by RTK-DGPS. A seed sensor senses the seeds while they are falling from the machine into the soil. Griepentrog et al. (2005) found that the mean deviation between estimated sugar beet seed position and true plant position ranged from 16-43

mm, which means that for targeting weeds close to the crop plants additional sensing would be required.

- **Shape and color.** Plant species can be identified based on characteristic shape, colour and texture features using image analysis. Gerhards and Christensen (2003) report an average identification rate of 80% using image analysis when plant species were grouped into five different herbicide classes. Åstrand and Baerveldt (2002) were able to classify beets with a classification rate of 98% using image analysis. Extraction of individual plants out of a scene was done manually and the colour features used may change due to differences in soils, nutrients and sunlight. Excluding colour features, the classification rate of beets classified as beets was reduced to 80%. Åstrand (2005) reports also the results of a combination of using plant pattern information and the individual plant features derived from image analysis. Crop plant classification rates of 92% and 98% on a dataset are reported using a classifier trained offline. Åstrand (2005) expects that variations in plant appearance within and between fields could easily reduce the performance in a real-time field application.

- **Pattern recognition of plant spacing.** Row crops like sugar beet have approximately equal intra-row distances. Therefore, crop plants can be identified based on this regularity. Bontsema et al. (1998) reconstructed individual positions of crop plants in a row successfully with Fourier transform on a signal made by a low cost infrared light barrier. The quality of detection was decreasing with a decreasing distance between the crop plants, an increasing standard deviation of the distance between the crop plants, an increasing number of weeds per meter and decreasing width of the crop plants. In experiments 80% to 97.5% of the crop plants were detected correctly (Bruggen, 2001; Bontsema et al., 2003). Åstrand and Baerveldt (2004) also present two methods to detect the position of the crop plants in the row based on the planting pattern of the crop. Crop classification rates of 78-99% were achieved.

- **Spectral reflectance.** Reflectance of crop, weeds and soil differ in the visual and near infrared wavelengths, so this spectral information has potential to be used for discrimination (Zwiggelaar, 1998). Vrindts et al. (2002) used the reflectance spectra of sugar beet and weed canopies to evaluate the possibilities of weed detection. In field experiments up to 95% of the sugar beets were classified as sugar beets and up to 84% of the weeds were classified as weeds.

None of the methods in literature reports a sugar beet recognition rate of 100% under all conditions. Finally, pattern recognition was chosen because it is expected to be sufficient and because of its further advantages: the approach is not restricted to one specific crop and only few parameters must be known in advance.

Positioning of weeding

The following alternatives to position the weeding actuator at the location indicated by the plant detection system were taken into consideration:

- **GPS.** The position of the actuator can be measured by mounting a GPS antenna above the actuator position. It is questionable whether the maximum position update frequency of about 10 Hz is sufficient for a precise actuator positioning.
- **Dead reckoning**. With a wheel encoder the position of the actuator relative to the crop plant location can be measured (Bontsema et al., 1998). Accumulation of inaccuracies over the distance between sensors and actuators occurs but is limited if the distance between both is small.
- **Machine vision.** A machine vision system could track both the actuator position and the position at which it should become active. To do this a specially developed image processing algorithm is needed

The choice made is to use dead reckoning. It is sufficient, and an encoder wheel would be already available because it is also needed for the pattern recognition system.

Intra-row weeding

The following alternatives to perform intra-row weeding have been taken into consideration:

- **Mechanical.** Weeds can be cut or removed from the soil by mechanical actuators. Actuators for intra-row weeding are described by several authors (Bontsema et al., 1998; Home, 2003; Åstrand, 2005; Kielhorn et al., 2000; Gobor, 2007; Tillett et al., 2008). Some of them are specially designed for operation in sugar beet (Bontsema et al., 1998; Åstrand, 2005). A disadvantage is the inertia of the mechanics limiting the capacity of the machine.

Determine where intra-row weeding has to be performed	seed mapping	shape & color	pattern	spectral reflectance	seed mapping, shape & color	seed mapping spectral refl.	shape & color pattern
	shape & color spectral refl.	pattern spectral refl.					
Positioning of weeding	GPS	GPS, dead reckoning	dead reckoning	camera			
Intra-row weeding	mechanical	air	flaming	electrical	hot water	freezing	microwaves
	infrared	laser	water jet				
Determine if within field	GPS	GPS, dead reckoning	vision, dead reckoning				
Navigate along the row	GPS	GPS, dead reckoning	vision	vision, dead reckoning	tactile, dead reckoning	ultrasonic, dead reck	optical, dead reckoning
	GPS, tactile	GPS, ultrasonic	GPS, optical				
Determine if on headland	GPS	GPS, dead reckoning	vision	vision, dead reckoning	ultrasonic, dead reck	optical, dead reckoning	

Figure 2.3: Morphologic chart - part 1

Navigate on the headland	GPS	GPS, dead reckoning	dead reckoning	vision, dead reckoning	GPS, vision	GPS, dead reck., vision	
Supplying energy	fill up	power point	sun				
Convert energy into movement	gas engine	diesel engine	electric engine				
Transmission of movement	gearbox	continuous variable	hydrostatic				
Move	3 wheels	4 wheels	2 tracks	4 tracks			
Input of robot settings	boardcomputer	sms	pda	pc	wap	webpage	
Sending user status info at request	boardcomputer	sms	pda	pc	wap	webpage	
Notify status to user	boardcomputer	sms	pda	pc	wap	webpage	
Detect unsafe situations	super canopy front & rear	super canopy around	sub canopy front & rear	sub canopy around	super & sub front & rear	super & sub around	

Figure 2.4: Morphologic chart - part 2

- **Air.** Pressured air can be used to remove weeds from the intra-row area. Lütkemeyer (2000) applied pressured air through two horizontal air nozzles at both sides of the crop row about two centimeters under the soil surface, removing weeds from the intra-row area when moved in row direction.
- **Flaming.** The plants in the field are exposed to flames generated by burning fuel in such a way that the heat injury causes the weeds to die but the crop plants to survive (Ascard, 1995). Recently developments are reported on intra-row flaming with an array of small burners that can be turned on and off rapidly (Poulsen, 2008).
- **Electrical discharge.** Weeds can be killed by producing an electrical discharge. Blasco et al. (2002) applied an electrode producing electrical discharges of 15 kV and 30mA during 200 ms for a single leaf. The system was able to eliminate 100% of the small weeds, but on bigger plants only the affected leaves showed some kind of damage. Safety with these high voltages is also a concern.
- **Hot water.** Weeds are exposed to hot water so that heat injury causes the weeds to die. Hansson and Ascard (2002) conclude that hot water weed control has potential on urban surfaces and railroad embarkements.
- **Freezing.** Weeds can be killed by freezing them.
- **Microwaves.** Weeds can be killed by exposing them to microwave radiation (Kurstjens, 1998).
- **Infrared.** Thermal weed control can be applied using infrared radiation (Ascard, 1998).
- **Laser.** Laser can be used as a weed stem cutting device or for stopping or delaying weed growth by directing a laser towards the apical meristem the weeds (Mathiassen et al., 2006). A laser can not cut below ground surface, and has therefore minor effect on certain weed species. On the other hand, not moving the soil prevents buried seeds from germinating. High power laser is needed to reach reasonable performance, and this involves high costs (Heisel et al., 2002).
- **Water-jet.** Weed stems can be cut with high-pressure water-jets. Warner (1975) investigated water jet cutting as a possible means for thinning of row crops. In a field experiment with seedlings with 1.5 mm thick stems about 60-70% of the seedlings were damaged. But with 3 mm thick stems there was virtually no effect. Water jet cutting for intra-row weeding needs more investigation before it can be applied.

Flaming, hot water, infrared, freezing, microwaves and pressurized air are normally applied non-targeted. The effect of these techniques is based on a difference

between crop plants and weeds in resistance to the applied dosage. Non-targeted application will always harm the crop and will not replace hand weeding totally. Targeting these techniques just to the weeds, without damaging the crop, is expected to be difficult in the intra-row area because the weeds are growing close to the crop plants. From the techniques that can be targeted to the weeds only, mechanical actuators are still the most proven solution despite its limited capacity due to inertia. Therefore, a mechanical actuator was chosen as working principle for intra-row weeding. However, further investigation is needed to segmented weeding where one of the cheaper, less precise approaches are used far from the crop and an expensive, more precise technique is applied nearer to the crop stems.

Determine if within field

The determination whether the weeding robot is located within the field or not, needs to be correct at any time. The following alternatives were taken into consideration:

- **GPS.** Given the coordinates of the field boundary, GPS signals can be used to decide whether the robot is located inside or outside the boundary. The inaccuracy is less or equal to the sum of the inaccuracies of measuring the field boundary and the accuracy of the GPS receiver used on the robot. Dead reckoning could improve the accuracy of position measurement.
- **Machine vision and dead reckoning.** Machine vision combined with dead reckoning can detect the absence of plants at a forward distance and from this it could be concluded whether the robot is still in the area where crop plants are growing or not. Åstrand and Baerveldt (2002), Tillett et al. (1998) and Pilarski et al. (2002) used this technique for detecting the end of rows.

GPS was selected to determine whether the weeding robot is within the field or not, because it is more reliable.

Navigate along the row

The following alternatives are taken into consideration for navigating along the crop rows:

- **GPS.** When the absolute location of the rows are known from sowing (Griepentrog et al., 2005), the robot can follow this predetermined route based on GPS. Commercial RTK GPS automatic tractor guidance systems claim to be capable of steering with precision errors of 25 mm from pass to pass (Trimble, 2008a). O'Connor (1997) tested the accuracy of navigation with CDGPS (Carrier-phase Differential GPS) and found a mean error of 0.83 cm and a standard deviation of 1.22 cm over a driving distance of 50 meters at a speed of 0.33 m/s, while the ordinary GPS measurements over the same distance showed a mean error of 0.38 cm and a standard deviation of 1.32 cm. Major drawbacks of using GPS systems are: the performance can be affected by objects around a field like trees obscuring the radio signals from the satellites; and the difficulty in dealing with the yearly changing row locations and the high costs of high accuracy.

- **Machine vision.** Machine vision algorithms can detect crop rows in real time. The relative position and orientation of the robot to the row can be used as input for tracking the crop row. Although weed density, shadows, missing plants and other conditions degrade the performance of machine vision guidance systems, some researchers have been successful in row detection in sugar beet (Marchant, 1996; Tillett et al., 2002; Åstrand and Baerveldt, 2002; Bakker et al., 2008a).

- **Tactile sensors and dead reckoning.** A tactile sensor guided by the crop row can be used to indicate the relative position and orientation of the crop rows to the robot (Nybrant, 1991). The relative position of the robot to the row can be used as input for tracking the crop row. A drawback is that tactile sensors can harm the crop.

- **Ultrasonic sensors and dead reckoning.** Ultrasonic sensors can measure the distance of the robot to the crop row. From multiple ultrasonic sensors or from combining ultrasonic sensor information with dead reckoning the relative position and orientation of the robot to the crop row can be determined. The relative position of the robot to the row can be used as input for tracking the crop row.

- **Optical sensors and dead reckoning.** Optical sensors can measure the distance of the robot to crop plants in the row. From multiple optical sensors or from combining optical sensor information with dead reckoning the relative position and orientation of the robot to the crop row can be determined. The relative position of the robot to the row can be used as input for tracking the crop row.

With machine vision the weeding robot can work in any field without requiring absolute coordinates of a path to be followed. Absolute positioning by means of GPS, possibly combined with other sensors, requires knowledge of the absolute position of crop rows in a field. Tactile sensors are not going to be used because in case of sugar beet they could harm the crop. Machine vision is preferred over ultrasonic or optical sensors, because of the ability to look forward, which contributes to a more accurate control of the position of the weeding robot relative to the crop row. Though dead reckoning could contribute to the navigation accuracy, exclusive machine vision was selected for navigation along the row, because it was expected to be sufficient.

Determine if on headland

The following alternatives were taken into consideration to decide whether the robot is on headland:

- **GPS.** Given the coordinates of the headland boundary, GPS can measure whether the robot is located inside or outside the headland boundary. Dead reckoning could improve the accuracy of position measurement with GPS.
- **Machine vision.** Machine vision combined with dead reckoning can detect the absence of plants at a forward distance and from this it could be concluded whether the robot is still in the area where crop plants are growing or not (Åstrand and Baerveldt, 2002; Tillett et al., 1998; Pilarski et al., 2002). Pilarski et al. (2002) report a prediction accuracy of 90% during cutting 40 ha of alfalfa and sudan crop, meaning that in 10% of the cases the headland was not detected. False positives also occasionally occurred. Tillett et al. (1998) detected the end of row in transplanted cauliflower with machine vision and dead reckoning. Setting an approximate row length was required to avoid premature turns.
- **Ultrasonic sensors and dead reckoning.** Ultrasonic sensors can measure the distance of the robot to crop plants in the row. Increased distances over a certain driven distance can indicate absence of plants and can indicate that the robot arrived at the headland.
- **Optical sensors and dead reckoning.** Optical sensors can measure the distance of the robot to crop plants in the row. Increased distances over a certain driven distance can indicate absence of plants and can indicate that the robot arrived at the headland.

Tactile, ultrasonic or optical sensors in combination with dead reckoning can not guarantee a correct detection of the end of row when another crop grows on the headland - for instance when seeded to prevent germinating of weeds -, and therefore also can not guarantee a correct headland detection. Machine vision could give more reliable results. But because the headland management is inconsistent in practice, the resulting variety of headland vegetation makes reliable vision perception too difficult. Therefore GPS was selected to determine whether the weeding robot is located on the headland. Using GPS requires some labor for recording the border of the headlands in advance, but will result in correct headland detection. In order to avoid additional software for combination with dead reckoning needed to achieve sufficient accuracy with ordinary GPS, a high accuracy GPS has been selected.

Navigate on headland

On the headland the weeding robot has to make a turn and position itself in front of the next rows to be weeded. The following alternative strategies were taken into consideration:

- **GPS.** The path is planned at the moment the robot arrives at the headland or as soon as the headland is identified. Navigating along this path can be done by GPS. Thuilot et al. (2002) show that it is possible to follow a curved path with a tractor relying on a single GPS receiver. Dead reckoning could improve the accuracy of position measurement with GPS.
- **Dead reckoning.** The headland turn is made by following a planned path as soon as the robot arrives at the headland. This dead reckoning can be performed via a vehicle Kalman filter. Tillett et al. (1998) showed that a maximum error measured as the normal distance between the commanded and measured path was around 60 mm.
- **Machine vision and dead reckoning.** Headland turns performed by dead reckoning could be improved by detecting crop rows with a forward looking camera to align the robot with the crop rows.

Accuracy of dead reckoning will decrease with the length of the turning path and in situations where more slip occurs. Absolute position measurement by GPS does not have this drawback. Therefore, GPS was chosen to navigate on headland.

Locomotion related functions

The following alternatives in terms of locomotion related functions were taken into consideration. All options in each row in the morphological chart are discussed together.

- **Energy supply.** The high energy content of fuel makes a fuel as energy source still very practical for energy consuming treatments that have to be performed in agriculture. Another option is to supply the robot with energy via an electric power point charging batteries mounted on the robot. The robot could also obtain its energy from the sunlight via solar panels
- **Energy conversion.** Energy can be converted into movement by a gas engine, a diesel engine or by an electric engine. A diesel engine is the most common engine used in agriculture. However, gas engines or electrical engines could be used as well.
- **Transmission of movement.** The engine movement could be transferred to the wheels by a standard mechanical transmission like used in conventional tractors, but also by a continuously variable transmission incorporating both mechanical and hydraulic parts like those introduced in recent tractor models. Hydrostatic transmissions have lower energy efficiency than the previous alternatives, but are still a proven concept in agricultural machines that require not so much traction force.
- **Traveling gear.** Three wheels, four wheels, two tracks or four tracks would be alternative travelling gears for a robot. The most important advantages of tracks compared to wheels are the better traction and the lower soil compaction. Disadvantages are the higher costs, less suitability for driving on hard surfaces and damage to the soil in sharp turns due to skid steering. Therefore, tracks are normally applied only for heavy machinery or for special purpose machinery for soft surfaces (Ansorge and Godwin, 2007).

From the alternatives, a diesel engine with a hydraulic transmission was selected for the locomotion related functions, because it is a proven concept in agriculture. A gearbox would limit the choice of driving speed and shuffling would be difficult to automate. A continuously variable transmission was therefore preferred over a gearbox. Hydraulics makes it possible to design a compact wheel construction preventing damage to the crop.

A design with four wheels is preferred over one with three wheels because of stability. Four wheels were also preferred over two or four tracks. It is expected that if four wheels are used for such a light-weight vehicle (not more than 1500 kg) soil

compaction would be acceptable. Traction when using wheels is expected to be good enough because of limited need of traction for intra-row weeding. Four wheel drive and four wheel steering were chosen to have the possibility to investigate all kinds of driving strategies, which best meets the requirement to design a platform suitable for research.

Communication with the user

The communication between robot and user differs in who is taking the initiative for communication, the type of information to be exchanged and in the distance of the user to the robot. The following communication related functions were distinguished:

- **Input of robot settings.** The robot should be put into operation by the user after it was brought to the field. Robot, task and field specific settings must be set.
- **Sending status information at request**. The robot sends information about its operational status at remote user request (e.g. the progress of the execution of its task).
- **User notification**. The robot takes the initiative to inform the remote farmer (e.g. when stopped due to security reasons or when it is ready).

For each of the functions, the following alternatives were taken into consideration:

- **Board computer.** A computer with a user interface mounted on the robot could be used as a means to input data settings like the row distance. It could also display notifications status information on a user request.
- **SMS.** Information between the robot and the user could also be exchanged by Short Message Service (SMS) messages (Jensen and Thysen, 2003; Tseng et al., 2006).
- **PDA.** Dedicated software running on a PDA could be a means to exchange information between robot and user via the internet.
- **PC.** Information between the robot and the user could be exchanged by dedicated software running on a PC.
- **Webpage.** Information between the robot and the user could be exchanged by updating a database on a webserver. A webpage would be accessible via mobile phones, PDA or PC.

If the user is near the robot, the most reliable method for user robot communication is communication via a board computer. Therefore a board computer was selected for input of robot settings. In the Netherlands any place is covered by the GSM

network. Every modern cell phone can use SMS and in practice, most messages arrive fairly quickly. Therefore SMS was selected for user notification. A webpage gives good opportunities to represent information in a well arranged way and it is easily accessible from everywhere. From the alternatives a webpage was selected for sending status information at request.

Detect unsafe situations

The following alternatives were taken into consideration for detection of unsafe situations:

- **Super canopy front & rear.** Unsafe situations can be detected by detecting obstacles above the crop plants at the front and rear side of the robot by e.g. laser scanner, stereovision, millimeter wave radar or ultrasonic sensors (Gray, 2002; Wei et al., 2005). Any obstacle detected is classified as an obstacle causing an unsafe situation. While the robot can move sideways, the prevailing driving direction will be forward, followed by reverse. Objects in between the crop plants would not be detected.
- **Super canopy circumferential.** Unsafe situations can be detected by detecting obstacles above the crop plants at all sides of the robot by e.g. laser scanner, stereovision or ultrasonic sensors. Objects in between the crop plants would not be detected.
- **Sub canopy front & rear.** Unsafe situations could be detected by detecting obstacles in between crop plants at the front and rear side of the robot. However, this requires detection techniques for discrimination between crop and other obstacles, and classifying the latter into obstacles to stop for and obstacles not to stop for. While there is some interesting research in this area, this problem is not yet solved (Manduchi et al., 2005; Stentz et al., 2002).
- **Sub canopy circumferential.** Detecting obstacles in between crop plants at the front and rear side of the robot could be extended to detection at all sides of the robot.

Ideally the weeding robot should detect every unsafe situation, at every level and direction. Even if somebody is lying in between the crop rows below canopy level this should be detected. Because of the costs for such a solution, circumferential super canopy detection was chosen to provide a basic level of safety.

Figure 2.5: The platform

2.3 The vehicle

This section describes how the concept solution is worked out in detail. The resulting versatile platform is shown in figure 2.5.

The size of the vehicle was determined by the standard track width used for mechanical weeding in sugar beet in the Netherlands which is 1.50 m. This track width also makes the design versatile in the sense that it is suitable for crops grown in beds like carrots and onions.

Sugar beets are grown at a row distance of 50 cm so the weeding robot covers three rows. The engine power is chosen so that sufficient capacity is available for driving and steering under field conditions and for operating three weeding actuators. The required power for the actuators was calculated based on an actuator specially designed for intra-row weeding by Bontsema et al. (1998). The engine is a 31.3 kW Kubota V1505-T.

The ground clearance is about 50 cm to prevent the crop from being damaged by the vehicle. The vehicle is 2.5 m. long to have enough space for mounting actuators under the vehicle in the middle between the front and rear wheels. The tire width of 16 cm leaves enough space for steering in-between crop rows while soil compaction is expected to be acceptable. The weight of the vehicle is about 1250 kg.

The engine powers a hydraulic pump. It supplies the oil for steering and driving, while another pump can be mounted for driving the actuators. The oil for driving and steering flows to an electrically controllable valve block with eight sections. Four sections are used for steering and four are used for controlling wheel speed, so wheel speeds and wheel angles can be controlled individually. The wheels are driven by radial piston motors. The driving speed ranges from 0.1 to 1.8 m/s. A maximum travel speed of 3.6 m/s for fast moving of the robot from field to field could be realized by switching to two wheel drive by combining the oil flows of four wheels into two flows.

Each wheel is steered by a hydraulic motor with a planetary reduction gear. The maximum steering speed is 180 degrees per second. The angles of the wheels are measured by angle sensors. The oil for driving the wheels flows via a turnable oil throughput. This makes it possible to turn the wheels in any angle from 0-360 degrees.

The weeding robot electronics consists of 6 units connected by a Controller Area Network (CAN) bus using the ISO 11783 protocol. In figure 2.6 a schematic overview of this system is given with vehicle control related sensors and valves. In every wheel a cogwheel is mounted with 100 cams thus giving 100 pulses per revolution via magneto-resistive sensors. Per wheel two of those sensors are mounted such that their signals are 90 degrees out of phase, thus permitting both speed and direction detection. Per wheel steering unit an analogue angle sensor is mounted with an accuracy of 1 degree and a range of 180 degrees. The sensors are connected to four micro controllers located near the four wheels which transmit the wheel speeds and the wheel angles via the CAN bus. A laptop processes images supplied by the front sight camera and transmits the location of the crop rows in relation to the vehicle position in a CAN bus message. An embedded controller running a real time operating system (National Instruments PXI system) also connected to the CAN bus performs the vehicle control. The GPS receiver and a radio modem are connected with the PXI via RS232. The radio modem interfaces the remote control used for manual control of the weeding robot. The PXI system gathers wheel angles, wheel speeds, crop row location data, GPS data and remote
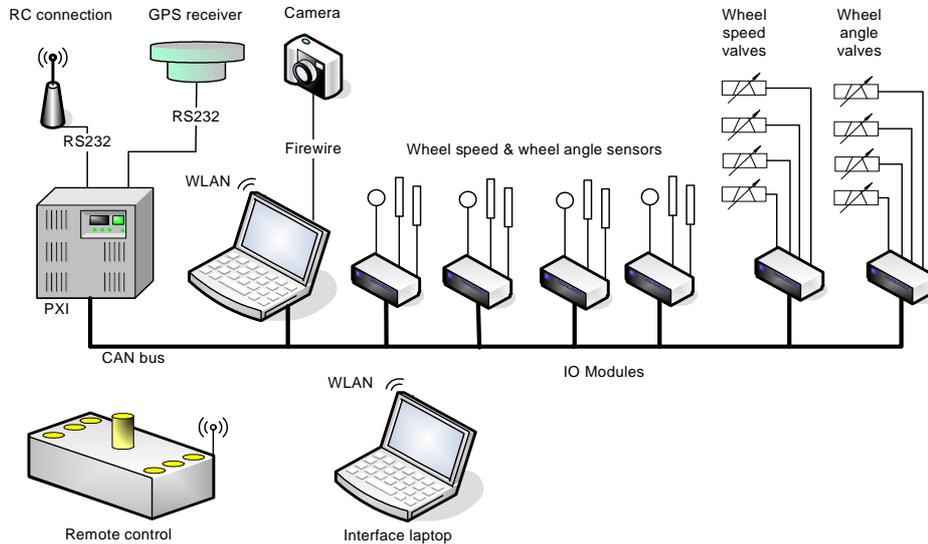
Figure 2.6: Electronics architecture

control data and controls the vehicle by sending messages to two micro controllers connected to the valve block. The user interface of the weeding robot software running on the PXI system can be visualized on a laptop via a wireless connection (Ethernet). Besides the sensors that are directly related to navigation and control, there are some more sensors connected to the modules. These sensors, indicating oil filter status, oil temperature and oil level are also interfaced to the PXI via the micro controllers and the CAN bus. In case a sensor indicates an emergency, the weeding robot will switch off automatically. Devices for the communication related functions and for obstacle detection are projected but not mounted yet.

2.4   Discussion and Conclusion

The research vehicle was designed using a structured design method. The advantage of using this method is that it clearly structures the design process. It provides a good overview of the complete design and because of the structured sequence of design activities, it is easy to keep track of the progress of design. Another advantage of the structured design method is that it forces the designer to look at alternative solutions and this decreases the probability of heuristic bias and increases the quality of the outcome. Although the designer is forced to thoroughly judge the identified alternative solutions when selecting the final concept, the

outcome is still depending on the available knowledge of the designer about the alternative solutions. So, while the method can not guarantee that the absolute best solution possible will be selected, it certainly is superior to a trial and error approach. In a research context it is easy to identify alternative subjects that are worthwhile to investigate further, while in the same time the main line of the research remains clear.

The result of the design is a versatile research vehicle with a diesel engine, hydraulic transmission, four wheel drive and 360 degrees four wheel steering. The robustness of the vehicle and the open software architecture permit the investigation of a wide spectrum of research options regarding solutions for intra-row weed detection and weeding actuators. The result of the design is a reliable concept for an autonomous weeding robot in a research context.

Chapter 3

A vision based row detection system for sugar beet

Abstract

One way of guiding autonomous vehicles through the field is using a vision based row detection system. A new approach for row recognition is presented which is based on grey-scale Hough transform on intelligently merged images resulting in a considerable improvement of the speed of image processing. A color camera was used to obtain images from an experimental sugar beet field in a greenhouse. The color images are transformed into grey scale images resulting in good contrast between plant material and soil background. Three different transformation methods were compared. The grey scale images are divided in three sections that are merged into one image, creating less data while still having information of three rows. It is shown that the algorithm is able to find the row at various growth stages. It does not make a difference which of the three color to grey scale transformation methods is used. The mean error between the estimated and real crop row per measurement series varied from 5 to 198 mm. The median error from the crop row detection was 22 mm. The higher errors are mainly due to factors that do not occur in practice or that can be avoided, such as a limited number and a limited size of crop plants, overexposure of the camera, and the presence of green algae due to the use of a greenhouse. Inaccuracies created by footprints indicate that linear structures in the soil surface in a real field might create problems which should be considered in additional investigations. In two measurement series that did not suffer from these error sources, the algorithm was able to find the row with mean errors of 5 and 11 mm with standard deviations of 6 and 11 mm. The image processing time varied from 0.5 to 1.3 seconds per image.

Keywords: Vision guidance, Sugar beet, Row detection, Hough transform, Machine vision, Crop rows.

3.1   Introduction

In agricultural production weeds are mainly controlled by herbicides. As in organic farming no herbicides are permitted, mechanical weed control methods are developed to control the weeds. For crops growing in rows like sugar beet sufficient equipment is available to control the weeds in between the rows, but weed control within the row (intra-row weeding) still requires a lot of manual labor. This labor involves high cost and is not always available. Autonomous weeding robots might replace manual weeding in the future. A possible approach for the autonomous navigation is GPS-based with predefined route planning. However, for autonomous weeding also the locations of the crop rows should be incorporated in the route planning, but the crop row locations in world coordinates are currently not available. Furthermore, even if e.g. sowing machines could output the row-location information, some effort will still be required for information transfer for GPS-based navigation with a weeding robot. In our approach we want to design a navigation system for an autonomous weeder using a minimum of a-priori information of the field. Navigation along the crop row is based on real-time sensed data. In this paper a real-time vision based row detection system providing steering information is described.

Recent research describes vision based row detection algorithms tested in cauliflowers (Marchant and Brivot, 1995), cotton (Billingsley and Schoenfisch, 1997; Slaughter et al., 1999), tomato and lettuce (Slaughter et al., 1999) and cereals (Hague and Tillett, 2001; Søgaard and Olsen, 2003). Some research has been successful in row detection in sugar beet. Marchant (1996) tracks sugar beet rows using images acquired by a standard CCD monochrome camera. The camera is enhanced in the near infrared by removing the blocking filter and a bandpass filter was used to remove visible wavelengths. The images with crop plants of about 120 mm high were thresholded resulting in binary images. On these images Hough transform was applied. Tillett et al. (2002) describe a vision system for guiding hoes between rows of sugar beet. Image acquisition is done using a camera with near infrared filter. A bandpass filter extracts the lateral crop row location at eight scan bands in the image. The position and orientation of the hoe with respect to the rows is tracked using an extended Kalman filter. Åstrand and Baerveldt (2002) use a grey scale camera with near-infrared filter for vision guidance of an agricultural mobile robot in a sugar beet field. After an operation to make the image intensity independent, a binary image is extracted with a fixed threshold. The crop row position is found by applying Hough transform on the binary image.

Hough Transform was also applied successfully on camera images to detect seed drill marker furrows and seed rows in order to provide driver assistance in seed drill guidance (Leemans and Destain, 2006). For non-agricultural applications grey scale Hough transform was used (Lo and Tsai, 1995). In grey scale Hough transform the accumulator space is increased with the grey scale value of the corresponding pixel in the image. In this way, higher probability of the pixel containing plant information will lead to greater contribution to the Hough accumulator. Also a number of methods to transform color images to grey scale images while maximizing the contrast between green plants and soil background have already been published (Woebbecke et al., 1995; Philipp and Rath, 2002).

The overall objective of our research was to develop a real-time steering system for an autonomous weeding robot with typical forward speeds of about 0.5 - 1 m/s. Although there are different methods for real-time row detection published for different prototypes, there is still need for improvement for applications in agricultural practice in terms of robustness, accuracy and speed. Therefore our detailed objectives have been:

- To assure sufficient speed of data processing.
- To identify an optimal image transformation algorithm.
- To improve the robustness of row detection.

3.2 Materials and method

3.2.1 Experimental setup

A sugar beet field was prepared for image acquisition in a greenhouse. The soil in the greenhouse was hand-plowed. September 29th 2003 the beets were sown manually. A cord was tightened from one side of the field to the other by two people and laid down after that. Every 18 cm a seed was put into the ground just beside the cord. This was repeated for 5 rows at row distances of 50 cm. The length of the rows was about 25 m. Because there was no thermal or chemical sterilization of the soil before sowing, the area became gradually covered by weeds mainly *Stellaria media*. Long intervals of manual weed control have been chosen to investigate the effect of high weed density on the accuracy of row detection.

For image acquisition a Basler 301fc color camera with a resolution of 659 by 494 pixels was mounted on a platform (fig. 3.1). The camera was mounted at 1.74 meters above the ground looking forward and down at an angle of 40° to the

Figure 3.1: Experimental platform.

vertical. The area covered by one image was 2.5 meters long in row direction and 1.5 meters wide at the side closest to the camera (fig. 3.2a). This means that three complete rows are visible in the image. The platform was pulled backwards over the field by a rope. The backward movement was done to prevent the pulling rope to be in view of the camera. While the vehicle was moving, it grabbed images and stored them as 24 bits bitmaps on the hard disk of the computer. This was done in a continuous loop resulting in a speed of circa 9 images per second on a PC with a clock frequency of 1.6 GHz. Eleven series of images were acquired subsequently between October 2003 and January 2004 to have images available at different growth stages (table 3.1). Because of the high image acquisition speed, the images overlapped each other for a large part and the total amount of images was too large to evaluate each of them subsequently. Therefore, per measurement series 10 to 13 images were selected which covered the whole length of the field, with a little overlap of the images remaining. On these subsets of images the algorithm was applied using a PC with a clock frequency of 1.6 Ghz. Labview$^{\circledR}$ was used for both the image acquisition and the algorithm development.

3.2.2 Inverse perspective transformation

Because the camera is looking downward at an angle from the vertical, the images undergo a perspective transformation. The images are corrected for this perspective transformation by an inverse perspective transformation. The parameters for this inverse perspective transformation are calculated for the setup of our experiment by a build-in calibration procedure of Labview$^{®}$. Each image is then rectified by standard Labview$^{®}$ functions using the parameters calculated during calibration to get real world dimensional proportions (fig. 3.2b).

3.2.3 Image transformation

The second step in the row recognition algorithm, is transforming the rectified image to a grey scale image with enhanced contrast between green plants and soil background (fig. 3.2c). The pixel intensity values I are calculated as:

$$I = 2g - r - b \tag{3.1}$$

Calculating r, g and b was done in three different ways to find the optimum in terms of accuracy.
Firstly without normalization:

$$r = R_c \quad g = G_c \quad b = B_c \tag{3.2}$$

where R_c, G_c and B_c are the RGB values of the current pixel.
Secondly r, g and b are calculated with image transformation according to Woebbecke et al. (1995)

$$r = \frac{R_c}{R_c + G_c + B_c} \quad g = \frac{G_c}{R_c + G_c + B_c} \quad b = \frac{B_c}{R_c + G_c + B_c} \tag{3.3}$$

Thirdly with an own algorithm where r, g and b are obtained as:

$$r = \frac{R_c}{R_m} \quad g = \frac{G_c}{G_m} \quad b = \frac{B_c}{B_m} \tag{3.4}$$

where R_m, G_m and B_m are the maximum RGB values of the image.
After this a threshold for I is applied.

$$I = A \qquad if\ I < A \tag{3.5}$$

Pixel values lower than a threshold A, are set to the value of threshold A. The optimal value of threshold A depends on whether equation 3.2, 3.3 or 3.4 is used.
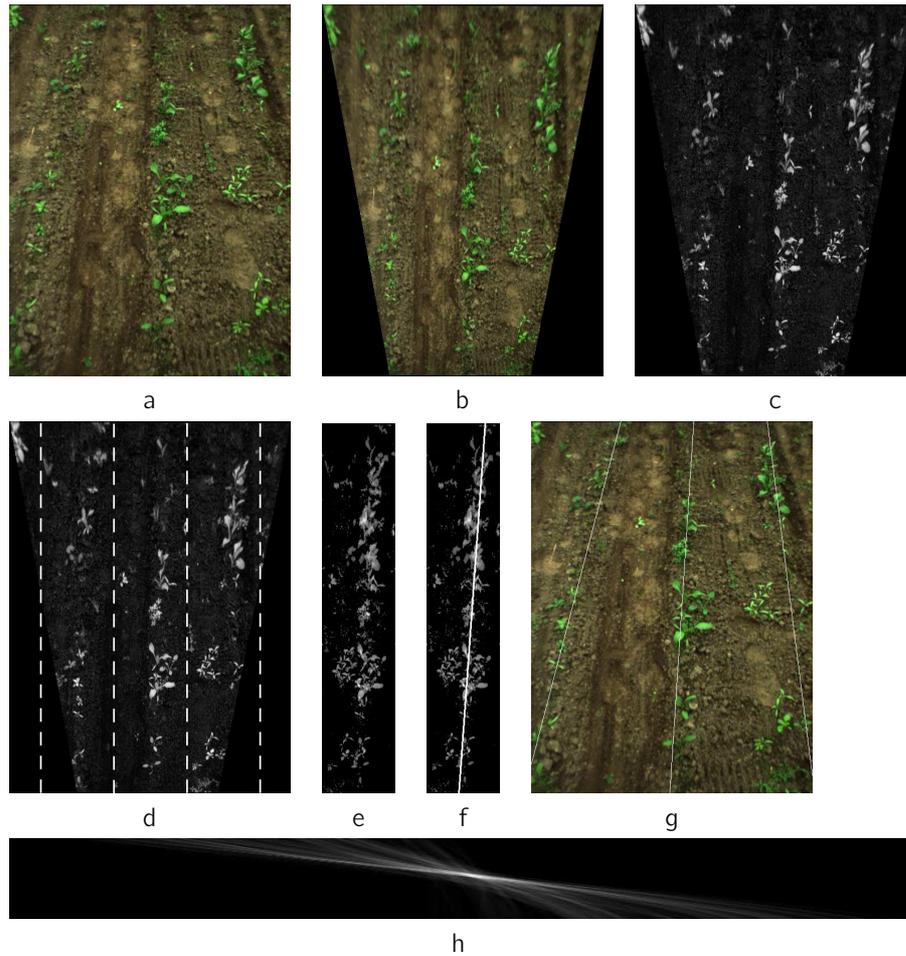
Figure 3.2: Image processing: Original image (a), rectified image (b), thresholded grey scale image calculated with equation 3.2 (c), selection of the segments in c (d), thresholded combined image (e), overlaid combined image (f), overlaid original image (g), Hough accumulator (h).

3.2.4 Summation of image segments

In the grey scale image three rectangular sections of crop row spacing are selected, i.e. a-priori information about the crop row spacing is needed. The length of the section corresponds to the length of the image. The first section is selected in the middle of the image. The other two are selected at both sides of the first section. The sections are combined by summing up the grey values of the sections to a combined image (fig. 3.2d and 3.2e).

$$I_{comb} = I_{sec1} + I_{sec2} + I_{sec3} \tag{3.6}$$

This way a smaller image is generated with a more intensified row signature than with one row alone. The advantage of this summation is that Hough transform on the combined image will be faster because of the reduced size and because we now have to look for one row only.

$$I_{comb,scaled} = \frac{I_{comb}}{I_{comb,max} - I_{comb,min}} * 255 \tag{3.7}$$

The pixel values are scaled to 0-255. After this a threshold B is applied for $I_{comb,scaled}$.

$$I_{comb,scaled} = 0 \qquad if \ I_{comb,scaled} < B \tag{3.8}$$

The value of B is chosen in such a way that no important plant information is lost. Pixel values lower than threshold B, are set to 0. The optimal value of B depends on which of the image transformation methods described in paragraph 3.2.3 is used.

3.2.5 Hough transform

To the resulting combined image, grey scale Hough transform is applied (Lo and Tsai, 1995). The Hough transform is a standard tool in image analysis that allows recognition of among others straight lines in an image space by recognition of local patterns (ideally a point) in a transformed parameter space. We assume the straight line parameterized in the form:

$$\rho = x \cos\theta + y \sin\theta \tag{3.9}$$

where ρ is the perpendicular distance from the origin and θ the angle with the normal. All lines through a location (x, y) can be represented by a curve in the (ρ, θ) plane. Every line through all locations (x, y) in the image with a certain range of values for θ is mapped into the (ρ, θ) space and the greyvalue $I(x, y)$ of the points (x, y) that map into the locations (ρ_m, θ_m) are accumulated in the two dimensional histogram:

$$A(\rho_m, \theta_m) = A(\rho_m, \theta_m) + I(x, y) \tag{3.10}$$

If this is done for every pixel in the image, the best estimate for a line representing the crop row position can be found by searching for the highest peak in the Hough accumulator, which is represented in (fig. 3.2h) with the brightest spot.

It is assumed that the orientation of the weeding robot with respect to the crop rows will never exceed 45°. Therefore the implemented Hough transform calculates the accumulator values only for lines with θ_j between 45° and 135° in steps of 1°. In this way the computational load is reduced. The algorithm of this grey-scale Hough transform is summarized in steps as follows:

1. Initialize the Hough accumulator content $A(\rho, \theta)$ to 0

2. For every pixel with coordinates (x_i, y_i) and value $I(x_i, y_i) > 0$ with i ranging from 1 to the number of pixels in the image and for every θ_j ranging from 45° to 135° in steps of 1°

   (a) Calculate $\rho_{ij} = x_i cos(\theta_j) + y_i sin(\theta_j)$, ρ_{ij} is rounded to the nearest integer

   (b) Set the accumulator value $A(\rho_{ij}, \theta_j) = A(\rho_{ij}, \theta_j) + I(x_i, y_i)$

3. Find $(\rho^*, \theta^*) = \arg\max(A(\rho, \theta))$

The parameters ρ^* and θ^* of the found peak define the crop row position. The line representing the row was modelled as three parallel, adjacent lines, because even young sugar beets had a minimal width of three pixels. Therefore the peak is determined by searching for the maximum of the sum of three adjacent cells in the Hough accumulator space. The estimated crop line in the combined image (fig. 3.2f) can be transformed back into three lines representing the crop rows in the original image (fig. 3.2g).

3.2.6 Evaluation method

The quality of the row position estimation is evaluated by comparing the lines found by the algorithm with lines positioned over the crop rows by visual inspection. To

Table 3.1: Mean error with standard deviation and peak error per measurement series using equation 3.2 for image transformation with threshold $A = 0$ and threshold $B = 60$.

Measurement	Date	Mean error (mm)	Standard deviation (mm)	Peak error (mm)
1	10-10-2003	77	108	328
2	15-10-2003	120	95	463
3	20-10-2003	25	22	159
4	24-10-2003	77	55	195
5	31-10-2003	104	90	316
6	05-11-2003	15	13	82
7	10-11-2003	10	12	62
8	19-11-2003	5	6	31
9	25-11-2003	35	45	245
10	04-12-2003	11	11	81
11	06-01-2004	198	55	289

this end in Labview® a tool was developed, by which the position of three lines in the original image can be positioned by hand interactively so that they match the crop rows. These lines are assumed to represent the real row position. The accuracy of the algorithm is calculated as the error between a line found by the algorithm and a line found manually. The error is calculated as follows:

- The area enclosed by the two lines in the rectified image is calculated.
- The error between the lines is calculated as this area divided by the length of the image. Also the largest distance between the two lines is calculated. All values are expressed in mm in the real world.

3.3 Results

3.3.1 Data processing

In each of the eleven measurement series the crop stage and the series light conditions are different. In figure 3.3 three typical images are shown, together with the estimated row position. These results were obtained using equation 3.2 for image transformation. Threshold A equals 0 and threshold B equals 60.

In figure 3.4 the errors are shown graphically for all images of all measurement series. Per measurement series the mean error, the standard deviation of the error,
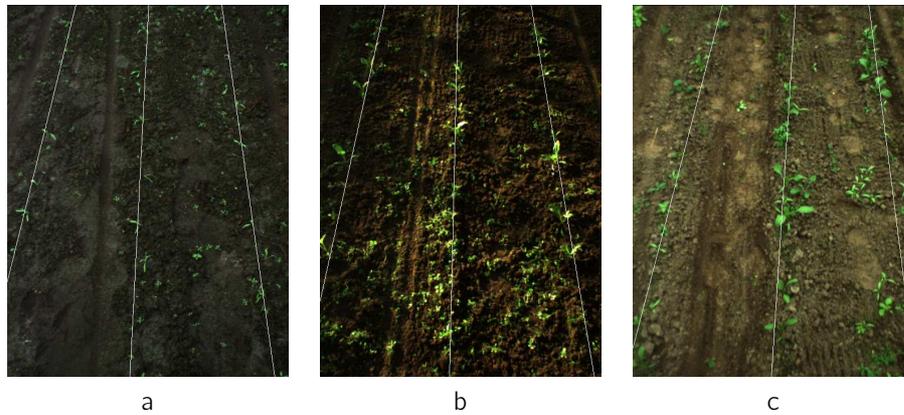
Figure 3.3: Typical images of series 3 (a), 6 (b) and 8 (c) together with estimated row position.

and the peak error are calculated. The peak error is the maximum over all images of the largest distance in each of the 10-13 images of a measurement series. The results are summarized in table 3.1.

3.3.2 Evaluation

There is a large difference in accuracy of crop row position estimation between the different measurement series. The mean error per measurement series varies from 5 to 198 mm and the standard deviation varies from 6 to 108 mm. The median error of all 119 images of the 11 measurement series is 22 mm.

Since the algorithm has to be used for navigation, also the performance of the algorithm in terms of the calculation time per image is an important factor, because it could limit the working speed of the autonomous robot. The performance of this algorithm depends on the amount of weed. The measured processing time varied from 0.5 to 1.3 seconds per image. This variation can be explained by the fact that pixels with a pixel value equal to zero are not processed by the Hough transform.

3.3.3 Effect of transformation and thresholds

As explained before, all results up till here were obtained with equation 3.2 for image transformation and one set of thresholds $[A = 0, B = 60]$. After this, for each image transformation method the mean error of a subset of all series is calculated
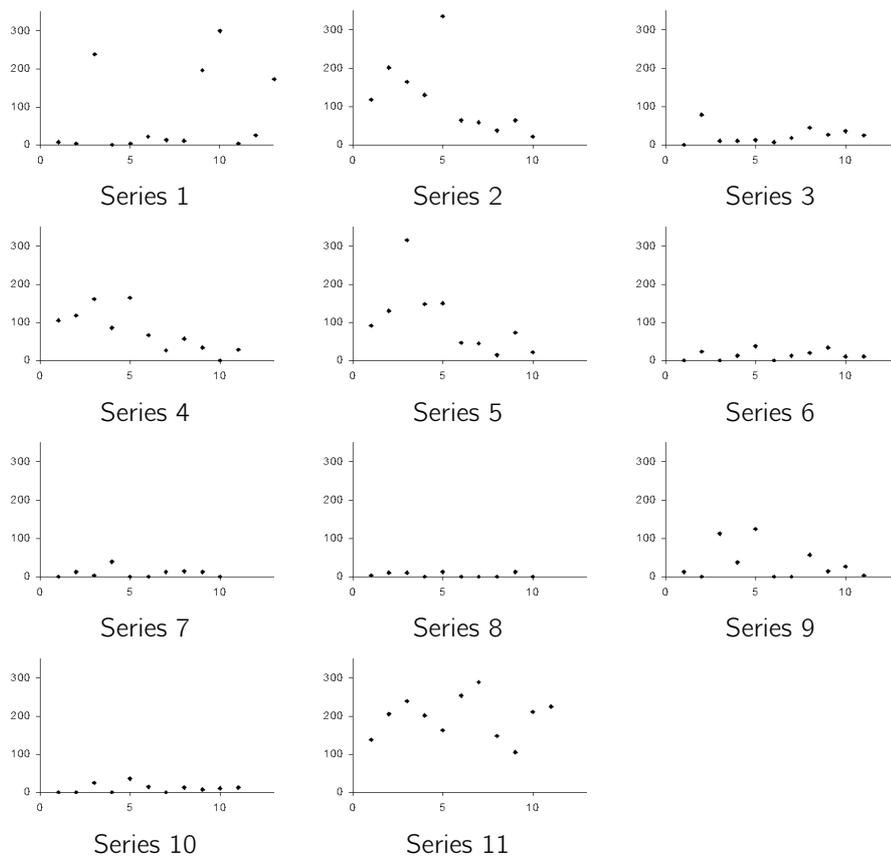
Figure 3.4: Accuracy of the crop row detection algorithm. Vertically the error in mm and horizontally the image number.

at different combinations of thresholds. The subset consists of series 6, 7, 8 and 10 which were selected because they produced the best results. Using equation 3.2 and the original set of thresholds the mean error of these series was 15 mm or less (see table 3.1). Because the pixel value ranges for the image transformation methods are different, optimal values for threshold A and threshold B will also differ. So the mean error per image transformation method is calculated for image transformation specific threshold ranges.

- Image transformation according to equation 3.2: threshold A varies from -240 to 160 with steps of 40 and threshold B from 0 to 200 with steps of 20. The mean error per threshold combination is plotted in figure 3.5. The smallest error found is 10 mm at $A = 0$ and $B = 60$.
- Image transformation according to equation 3.3: threshold A varies from -1 to 0.4 with steps of 0.2 and threshold B from 0 to 200 with steps of 10. The mean error per threshold combination is plotted in figure 3.6. The smallest error found is 9 mm $A = 0.2$ and $B = 0$.
- Image transformation according to equation 3.4: threshold A varies from -1 to 0.4 with steps of 0.2 and threshold B from 0 to 200 with steps of 10. The mean error per threshold combination is plotted in figure 3.7. The smallest error found is 9 mm at $A = 0$ and $B = 10$.

3.4   Discussion

Series 1, 2, 3, 4, 5, 9 and 11 have images with relatively high errors. In these cases the contribution of crop plants to the Hough accumulator is limited compared to the contribution of other parts of the image like unusual high amount of weeds, green algae and footprints.

The images of series 1 were made in an early crop stage and at some places the number of plants was still too low to find the crop row (fig. 3.8b). However, the algorithm can detect crop rows if the plants are small (fig. 3.8a). This is illustrated by the fact that in most images of this measurement series the algorithm gives a good estimation of the row position (fig. 3.4). Because of the low plant emergence in some parts of our experimental field the number of crop plants in some images made at later growth stages is also low. This contributed also to large errors in images of the series 2, 3, 4 and 9. This situation could also occur in real sugar beet fields if plants are missing in a row, however in our method three rows are combined for the final result and the probability of parallel gaps in all three rows is low.
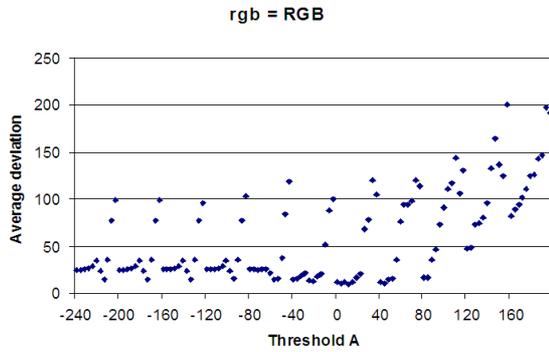
rgb = RGB

Figure 3.5: Mean error of the images of series 6, 7, 8, 10 using the color transformation according to equation 3.2 at different threshold combinations. Threshold *A* varies with steps of 40. For each value of threshold *A*, threshold *B* ranges from 0 to 200 with steps of 20.

r=R/(R+G+B) g=G/(R+G+B) b=B/(R+G+B)

Figure 3.6: Mean error of the images of series 6, 7, 8, 10 using the color transformation according to equation 3.3 at different threshold combinations. Threshold *A* varies with steps of 0.2. For each value of threshold *A*, threshold *B* ranges from 0 to 200 with steps of 10. After image transformation, pixel values higher then 1.99 or lower than -0.99 are removed.

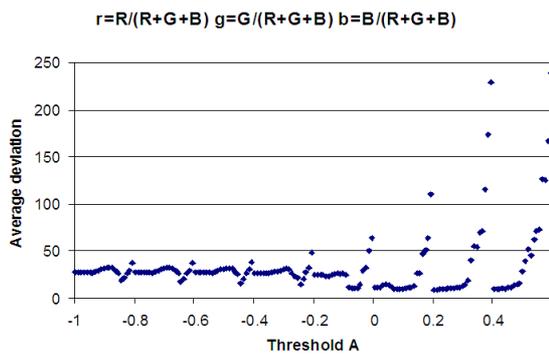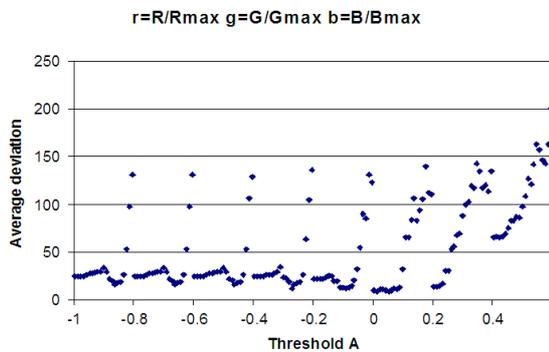**r=R/Rmax g=G/Gmax b=B/Bmax**

Figure 3.7: Mean error of the images of series 6, 7, 8, 10 using the color transformation according to equation 3.4 at different threshold combinations. Threshold *A* varies with steps of 0.2. For each value of threshold *A*, threshold *B* ranges from 0 to 200 with steps of 10.
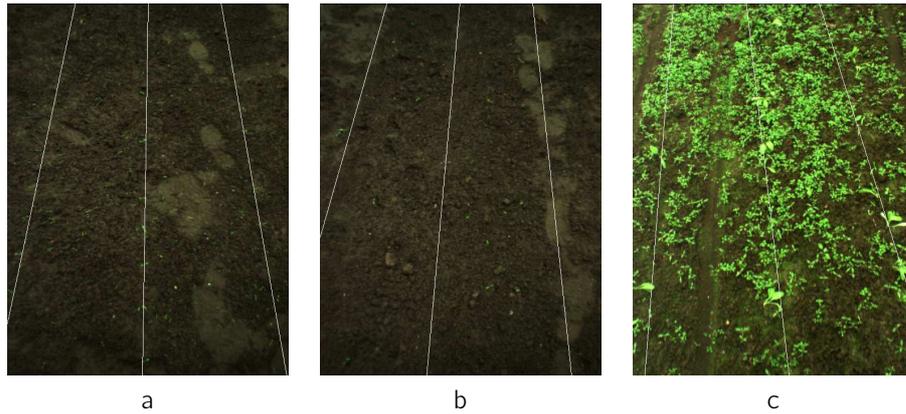
Figure 3.8: Estimated rows in small sugar beets (a successful, b failed) and in an image with high weed density (c).
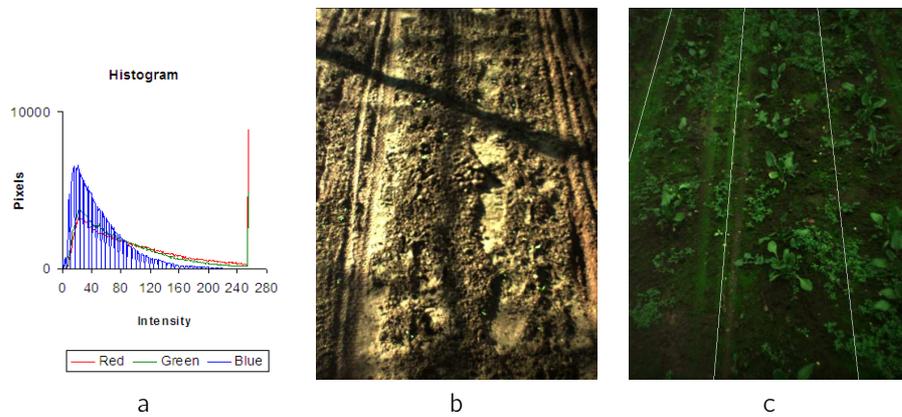

Figure 3.9: Histogram (a) of an overexposured image (b) of series 2. The red and green waveband are truncated at the intensity 255. The peak at 255 indicates pixels with too high exposure. An image with a lot of green algae (c).

In some images of series 2, 4, 5, 6, 9, and 11 the large error is due to the high weed density. However the density applied in these series is much higher than to be found in practice where short weeding intervals are common (fig. 3.8c).

Series 2 and 7 and also to lower extend series 4, 5 and 6 suffer from overexposure (fig. 3.9a, b). Pixels which have too high exposure do not contribute in a right proportion to the Hough accumulator. Also, in an image with overexposure the soil appears lighter and therefore the contribution of soil to the Hough accumulator increases. Overexposure could be prevented by decreasing the aperture or the shutter time. The shutter time of the camera can be controlled by software. If the shutter time is controlled so that the pixels are within the intensity range of the camera, it should be possible to increase the accuracy.

Footprints contribute to large inaccuracies in measurement series 1, 2, 4 and 5. Footprints in the soil cause pixels to appear more light. The contribution of footprints to the Hough accumulator is only disturbing the result, if the footprints are forming a linear pattern in row direction. Similar problems could occur by tracks of farm machinery which was not investigated in our study.

In series 11 and also to a lower degree in series 4 and 5 there were green algae in the field, especially in the tracks left by the vehicle from earlier measurements (fig. 3.9c). These tracks form green stripes, which are identified as crop rows by the algorithm. This is an artefact, which will not appear under practical conditions.

Series 8 and 10 do not suffer from these error sources and have mean errors of 5 and 11 mm respectively and standard deviations of 6 and 11 mm. In general, contributions to the Hough accumulator coming from parts of the images other than crop plants like unusual high weed density, green algae, footprints and overexposure reduced the quality of detection. However, reliable row detection was possible in spite of these artefacts. If applied in a real field without those artefacts the quality even might be better.

3.5 Conclusions

It does not make much difference which of the image transformation methods mentioned in paragraph 3.2.3 is used. If the optimum threshold combination is used, the mean minimum error is similar for the different image transformation methods. Therefore the most simple method i.e. using directly the RGB values from the camera can be recommended.

The merging of three crop rows to limit the image size while keeping the information of three rows was successful in creating an enhanced crop row signature that could be located using grey-scale Hough transform. In images made at different growth stages the median error from the crop row was 22 mm. Large errors were caused by limited number and small size of crop plants, overexposure of the camera, green algae and high weed density. It is expected that these conditions are not a problem in practice or can be compensated by choosing the right camera settings. Two measurement series that did not suffer from these error sources had mean errors of 5 and 11 mm, with standard deviations of 6 and 11 mm. The image processing time varied from 0.5 to 1.3 seconds per image. That means the proposed row detection method now is sufficient for finding row crops at speeds typical for intra-row weeding operations in the range of 0.5-1 m/s. The only a-priori information needed from the field is the row spacing.

Inaccuracies created by footprints indicate that linear structures in the soil surface like tracks of agricultural machinery in a real field might create problems which should be considered in additional investigations. Further research should focus on applying the proposed row detection method for autonomous navigation under practice conditions in a sugar beet field.

Chapter 4

Path following with a robotic platform

Abstract

This paper considers path following control for a robotic platform. The vehicle used for the experiments is a specially designed robotic platform for performing autonomous weed control. The platform is four-wheel steered and four-wheel driven. A diesel engine powers the wheels via a hydraulic transmission. The robot uses RTK-DGPS to determine both position and orientation relative to the path. The deviation of the robot to the desired path is supplied to two high level controllers minimizing the orthogonal distance and orientation to the path. Wheel angle setpoints are determined from inversion of the kinematic model. At low level each wheel angle is controlled by a P controller combined with a Smith predictor. Results show the controller performance following different paths shapes including a step, a ramp, and a typical headland path. A refined tuning method calculates controller settings that let the robot drive as much as possible along the same path to its setpoint, but also limit the gains at higher speeds to prevent the closed loop system to become unstable due to the time delay in the system. Mean, minimum and maximum orthogonal distance errors while following a straight path on a paving at a speed of 0.5 m/s are 0.0, -2.4 and 3.0 cm respectively and the standard deviation is 1.2 cm. The control method for four wheel steered vehicles presented in this paper has the unique feature that it enables control of a user definable position relative to the robot frame and can deal with limitations on the wheel angles. The method is very well practical applicable for a manufacturer: all parameters needed are known by the manufacturer or can be determined easily, user settings have an easy interpretation and the only complex part can be supplied as a generic software module.

Keywords: Robot, Path following, 4WS, RTK-DGPS.

4.1 Introduction

In organic farming there is a need for weeding robots that can replace manual weeding. The required labour for hand weeding is expensive and often difficult to obtain. In 1998 in the Netherlands on average 73 hours of hand weeding were spent on one hectare of sugar beet in organic farming (Van der Weide et al., 2002). In this paper a path following control system for a weeding robot is presented enabling the robot to navigate autonomously along a path.

A common design for a control system for agricultural vehicles is to split up the control system in a low level and a high level controller (Bendtsen et al., 2002; Bak and Jakobsen, 2004). The low level electro-hydraulic system is a system with dead time. A well known method to compensate for time delays is the Smith predictor (Stephanopoulos, 1984). Ge and Ayers (1991) applied this successfully to control an electro-hydraulic system on a hydraulic test bench. We used a Smith Predictor to compensate for time delays in the application of an electro-hydraulic steering system in practice.

The high level control system is partly inspired by work of Hague and Tillett (1996) and Bendtsen et al. (2002). Bendtsen et al. (2002) used a model for a four-wheel steered vehicle derived from Campion et al. (1996) and presented simulation studies applying feedback linearization as a control method. Hague and Tillett (1996) worked out a method for path following for a vehicle with two driven wheels and two free rolling wheels. For a simplified vehicle model they developed a controller. From the output of this controller follow the wheel speed setpoints by inversion of the kinematic vehicle model. In this paper this method is worked out for a four wheel steered robot, using the kinematic model derived from Campion et al. (1996) resulting in wheel angle and wheel speed setpoints for the low level control system. A refined tuning method of the high level controller, adapted from Skogestad (2003), lets the robot drive as much as possible along the same path to its setpoint independent from speed, but also limit the gains at higher speeds to prevent the closed loop system from becoming unstable at higher speeds because of the time delay.

4.2 Robotic platform

4.2.1 Platform

The vehicle used for the experiments is a specially designed robotic platform for performing autonomous weed control (figure 4.1). The design of the platform was described earlier by Bakker et al. (2008b). The platform is four-wheel steered and four-wheel driven. There is no mechanical constraint on the maximum turning angle of a wheel around its vertical axis, but the wheel angles should be constrained to prevent twisting of the cables of the wheel speed sensors. Power is provided by a diesel engine that powers the wheels via an hydraulic transmission. The hydraulic transmission consists of a pump supplying oil to eight proportional valves, each connected to one fixed displacement hydraulic motor. Four hydraulic motors are used to drive the wheels, the other four to steer the wheels. Computer control of the valves is achieved using pulse width modulation via two micro-controllers connected to a CAN bus. The pump/valves combination is a 'load sensing' system: the pressure drop over the valves controls the displacement of the pump via an hydraulic load sensing connection and is limited to a small value, independent of load pressure. The platform is further equipped with a hitch that can be lifted hydraulically. A second hydraulic pump mounted in series with the first, supplies oil to two valves: one for lifting the hitch, one for control of auxiliary implements. Computer control of the valves is achieved also via a micro controller connected to the CAN bus.

4.2.2 Electronics

The weeding robot electronics consists of 9 embedded controllers connected by a CAN bus using the ISO 11783 protocol. In the inside of every wheel rim a cogwheel is mounted for wheel speed measurement. The two magneto resistive sensors per cogwheel are placed in such a way that the direction of rotation can be resolved. The rotation of the wheels is measured by these sensors with a resolution of 100 pulses per wheel revolution. The wheel angle of each wheel is measured by a Kverneland 180 degree sensor with an accuracy of one degree. Per wheel a micro controller is mounted transmitting wheel speed and wheel angles via the CAN bus. Two GPS antennas are used to measure both vehicle position and orientation. Both are connected to a Septentrio PolaRx2eH RTK-DGPS receiver with a specified position accuracy of 1-2 cm and a specified orientation accuracy of 0.3 degrees (1σ). The

Figure 4.1: Robot platform

two GPS antennas are mounted on a metal plate to prevent multipath errors. A base station with a Septentrio PolaRx2e RTK-DGPS supplies the RTK-correction signals via a radio connection to the Septentrio PolaRx2eH receiver. The position of the base station itself can be configured by a correction supplied by the service of a company called 06-GPS via GPRS. One embedded controller running a real time operating system (National Instruments PXI system) also connected to the CAN bus does the vehicle control. The GPS receiver, and a radio modem are connected to the PXI via RS232. The radio modem interfaces the remote control used for manual control of the weeding robot. The manual control is used for guaranteeing safety during field trials and for transportation to and from the field. Different colored lamps of the signal tower can be operated via a micro-controller to indicate the current status of the robot platform. The platform is further equipped with sensors measuring diesel level, hydraulic oil level, engine temperature and hitch height. The PXI system gathers wheel angles, wheel speeds, GPS data, remote control data and hitch height and controls the vehicle by sending messages to the three micro controllers connected to the hydraulic valves. A safety system consisting of four red emergency switches at the corners of the vehicle and a remote switch, controls the valves to neutral position on activation, overruling the computer control.

4.3   Path following structure

The vehicle control consists of two levels. At high level the wheel angle setpoints and wheel speed setpoints are determined in order to decrease the deviation from the path and the error in orientation. At low level, controllers are used to realize the wheel angles and wheel speeds determined by the high level control.

The deviation and the orientation error of the robot from a path are determined by a specially designed orthogonal projection on the path using the measured orientation and the GPS position. The orthogonal projection is designed to calculate the deviation and the orientation error relative to a line of positions $y(x)$.

4.4   Low level control

4.4.1   Wheel angle process model

At low level for each wheel the wheel angle and wheel speed are controlled. The hydraulic valves used for steering the wheels of the weeding robot have a certain reaction time, resulting in a time delay of the steering. Furthermore, if a valve has a commanded open time of less than the dead time, a control does not have any effect. So the wheel angle process can be represented by:

$$\dot{\beta} = 0 \qquad\qquad for\ t_{open}\ < t_{dead} \qquad\qquad (4.1)$$

$$\dot{\beta} = K_p \cdot u(t - t_d) \quad for\ t_{open}\ > \ t_{dead} \qquad (4.2)$$

and:
$u(t) = -1995$ *if* $U < 2500$
$u(t) = U - 4495$ *if* $2500 \leq U \leq 4000$
$u(t) = 0$ *if* $4000 < U < 6000$
$u(t) = U - 5405$ *if* $6000 \leq U \leq 7500$
$u(t) = 2095$ *if* $U > 7500$
where:
$\dot{\beta}$ is the wheel steering angle speed $[°/s]$.
K_p is the gain of the process and equals 0.0712.
u is the control corrected for the dead band.
U is the control $[\%U_{DC} \cdot 100]$.
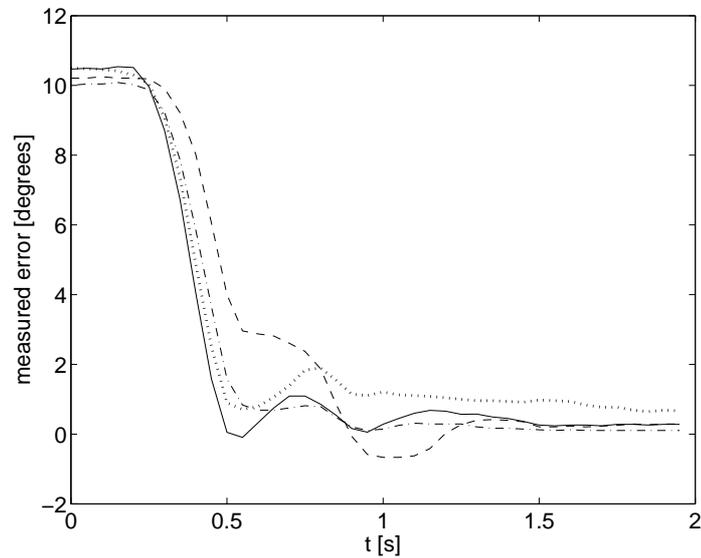U_{DC} is the power supply voltage and equals about 12 [V].

Figure 4.2: Performance of the wheel angle control, average of 96 measurements. The setpoint changes at t = 0 s from 10 to 0 degrees (- - - front left , —— rear left, $\cdot$ - $\cdot$ rear right, $\cdots$ front right)

t_d	is the delay of the system and equals 0.25 [s].
t_{open}	is the time generated by a counter counting the time that the commanded control is in the active band (outside the dead band where $4000 < U < 6000$). It resets when the commanded control returns to the dead band.
t_{dead}	is the dead zone of the system and equals 0.15 [s].

The value of t_{dead} was determined from tests in which the open time of a valve was varied, K_p, t_d and the values that relate u to U followed from step responses of the system.

4.4.2 Wheel angle control

To compensate for the time delay a P controller with Smith predictor is used for the wheel steering control (Stephanopoulos, 1984).

The wheel angle control of the robot was tested by applying setpoint changes to one wheel while the robot was standing still on a flat concrete floor. From some first measurements it appeared that at large setpoint changes the variable pump controlled by the load sensing system could not react fast enough for the change
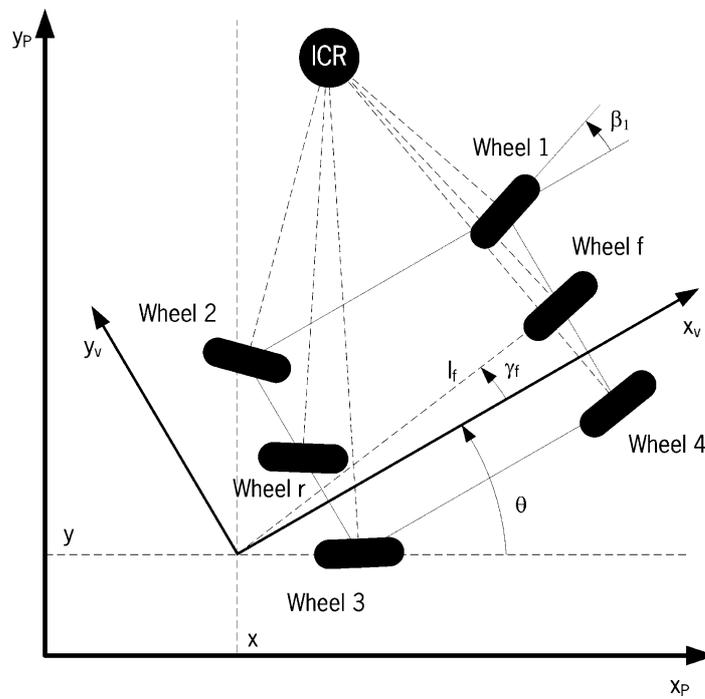
Figure 4.3: Robot with ICR

in the flow required to maintain full pressure in the hydraulic system. Furthermore, if we imagine the robot driving over the field, the flow needed for steering will require only small changes in the flow already present for driving. So to simulate the presence of a continuous oil flow for driving during the wheel angle control test, one wheel was lifted from the floor and a constant control was put on the valve controlling its speed.

The average error of a series of 96 measurements on a wheel angle setpoint change of 10 degrees decreased within one second to zero plus or minus 2 degrees (see fig. 4.2).

4.5 High level control

4.5.1 Vehicle model

The point of the vehicle that should follow the path is the vehicle implement attached to the vehicle at a certain speed v. Consider a path-relative coordinate system (x_P, y_P) as illustrated in figure 4.3. The implement position is then completely described by $\xi = [x\ y\ \theta]^T$ where x denotes the distance along the path, y the perpendicular offset from the path, and θ the heading angle of the platform relative to the path (see figure 4.3).

Consider a coordinate system (x_v, y_v) fixed to the robot frame. The position of a wheel in this vehicle coordinate system is characterized by the angle γ_i and the distance l_i where i is the wheel index. The orientation of a wheel relative to x_v is denoted β_i. The model assumes pure rolling and non-slip conditions and driving in a horizontal plane. Therefore the motion of the robot can always be viewed as an instantaneous rotation around the instantaneous center of rotation (ICR). At each instant, the orientation of any wheel at any point of the robot frame must be orthogonal to the straight line joining its position and the ICR. The two-dimensional location of the ICR is specified by the angles of two wheels. For convenience a virtual front wheel β_f and a virtual rear wheel β_r is introduced with corresponding γ_f, l_f, γ_r and l_f, respectively located right in between the front wheels and right in between the rear wheels. The motion of the vehicle implement is described by the following state-space model derived from earlier work from Campion et al. (1996) and Bendtsen et al. (2002):

$$\dot{\xi} = R^T(\theta)\Sigma(\beta_i)\eta \tag{4.3}$$

where $R(\theta)$ is the orthogonal rotation matrix:

$$R(\theta) = \begin{bmatrix} \cos(\theta) & \sin(\theta) & 0 \\ -\sin(\theta) & \cos(\theta) & 0 \\ 0 & 0 & 1 \end{bmatrix} \tag{4.4}$$

and:

$$\Sigma(\beta_i) \quad = \quad \begin{bmatrix} l_f \cos(\beta_r) \cos(\beta_f - \gamma_f) - l_r \cos(\beta_f) \cos(\beta_r - \gamma_r) \\ l_f \sin(\beta_r) \cos(\beta_f - \gamma_f) - l_r \sin(\beta_f) \cos(\beta_r - \gamma_r) \\ \sin(\beta_f - \beta_r) \end{bmatrix} \quad (4.5)$$

The scalar η is a velocity input. The wheel orientation β_3 and β_4 follow from β_f and β_r as described by Bendtsen et al. (2002) and Sørensen (2002) and β_1 and β_2 can be found in a similar way:

$$\beta_1 = \arctan\left(\frac{L \sin(\beta_f) \cos(\beta_r)}{L \cos(\beta_f) \cos(\beta_r) - \frac{1}{2} W \sin(\beta_f - \beta_r)} \right)$$

$$\beta_2 = \arctan\left(\frac{L \cos(\beta_f) \sin(\beta_r)}{L \cos(\beta_f) \cos(\beta_r) - \frac{1}{2} W \sin(\beta_f - \beta_r)} \right)$$

$$\quad (4.6)$$

$$\beta_3 = \arctan\left(\frac{L \cos(\beta_f) \sin(\beta_r)}{L \cos(\beta_f) \cos(\beta_r) + \frac{1}{2} W \sin(\beta_f - \beta_r)} \right)$$

$$\beta_4 = \arctan\left(\frac{L \sin(\beta_f) \cos(\beta_r)}{L \cos(\beta_f) \cos(\beta_r) + \frac{1}{2} W \sin(\beta_f - \beta_r)} \right)$$

where L is the distance between the front and rear wheels and W the distance between the left and right wheels.

The wheel angular speeds $\dot{\phi} = [\dot{\phi}_1, \dot{\phi}_2, \dot{\phi}_3, \dot{\phi}_4]^T$ are controlled at low level, and follow from the vehicle model:

$$\dot{\phi} = J_2^{-1} J_1(\beta_i) \Sigma(\beta_i) \eta(t) \quad (4.7)$$

where:

$$J_1(\beta_i) = \begin{bmatrix} \cos(\beta_1) & \sin(\beta_1) & l_1 \sin(\beta_1 - \gamma_1) \\ \cos(\beta_2) & \sin(\beta_2) & l_2 \sin(\beta_2 - \gamma_2) \\ \cos(\beta_3) & \sin(\beta_3) & l_3 \sin(\beta_3 - \gamma_3) \\ \cos(\beta_4) & \sin(\beta_4) & l_4 \sin(\beta_4 - \gamma_4) \end{bmatrix}$$

$$\quad (4.8)$$

$$J_2 = \begin{bmatrix} r_1 & 0 & 0 & 0 \\ 0 & r_2 & 0 & 0 \\ 0 & 0 & r_3 & 0 \\ 0 & 0 & 0 & r_4 \end{bmatrix}$$

and r_1, r_2, r_3, r_4 are the radii of the four wheels.

According to Campion et al. (1996), η is an artificial variable without a physical meaning that can be interpreted as a velocity input. The unit of η is s^{-1}. However, in our system η has to be related to v. For this we have to bear in mind that v is defined by $\dot{x}$ and $\dot{y}$:

$$v = \sqrt{\dot{x}^2 + \dot{y}^2} \tag{4.9}$$

If the robot is exactly following the path, $\dot{x} = v$. If the robot is moving perpendicular to the path $\dot{y} = v$.

From 4.3 and 4.9 then follows:

$$\eta = \frac{v}{\sqrt{([R^T(\theta)\Sigma(\beta_i)]_{11})^2 + [R^T(\theta)\Sigma(\beta_i)]_{21})^2}} \tag{4.10}$$

For convenience let:

$$a = \sqrt{([R^T(\theta)\Sigma(\beta_i)]_{11})^2 + [R^T(\theta)\Sigma(\beta_i)]_{21})^2} \tag{4.11}$$

and

$$\Sigma(\beta_i) = \begin{bmatrix} \sigma_1 \\ \sigma_2 \\ \sigma_3 \end{bmatrix} \tag{4.12}$$

From 4.3 and 4.12 then follows

$$R^T(\theta)\Sigma(\beta_i) = \begin{bmatrix} \cos(\theta) & -\sin(\theta) & 0 \\ \sin(\theta) & \cos(\theta) & 0 \\ 0 & 0 & 1 \end{bmatrix} \begin{bmatrix} \sigma_1 \\ \sigma_2 \\ \sigma_3 \end{bmatrix} = \begin{bmatrix} \sigma_1 \cos(\theta) - \sigma_2 \sin(\theta) & 0 \\ \sigma_1 \sin(\theta) + \sigma_2 \cos(\theta) & 0 \\ \sigma_3 \end{bmatrix} \tag{4.13}$$

From 4.11 and 4.13 then follows:

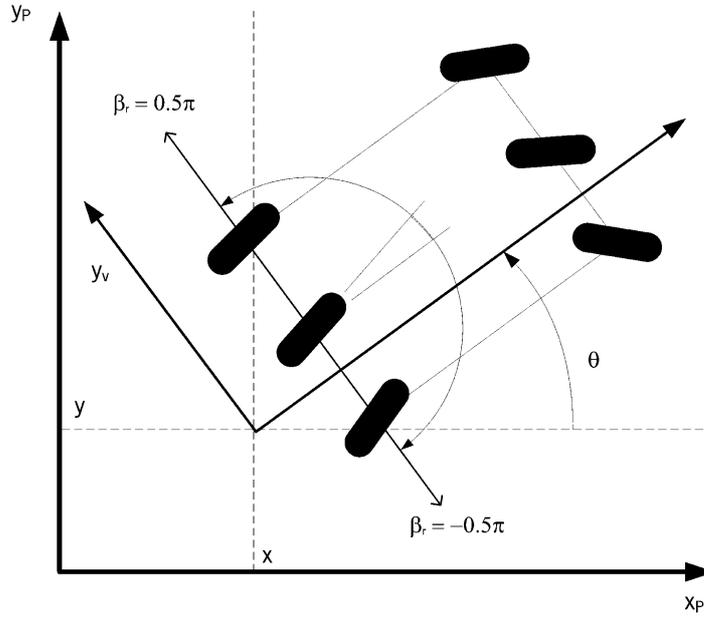$$a = \sqrt{\sigma_1^2 + \sigma_2^2} \tag{4.14}$$

and from 4.10, 4.11 and 4.14:

Figure 4.4: Robot with wheel angle constraints: $-0.5\pi < \beta_i < 0.5\pi$.

$$\eta = \frac{v}{a} = \frac{v}{\sqrt{\sigma_1^2 + \sigma_2^2}} \tag{4.15}$$

Substitution of 4.15 in 4.3 results in the following vehicle model:

$$\dot{\xi} = R^T(\theta)\Sigma(\beta_i)\frac{v}{\sqrt{\sigma_1^2 + \sigma_2^2}} \tag{4.16}$$

4.5.2   Controller design approach

In our application the actuator determines the maximum robot speed possible. This is very common in agriculture operations: in some cases the soil and crop conditions limit the actuator velocity (e.g. when hoeing) and in other cases the actuator itself has properties limiting the maximum speed (e.g. mowers). So the robot should perform path following at a certain constant speed v. Therefore v is not regarded as a control variable, but as a parameter. Since v is fixed it follows from 4.9 only two differential equations remain, for y and θ.

The vehicle model given in 4.16 is a non-linear system which makes it hard to define and tune a simple controller. However, taking the inverse kinematic model, the non-linear system can be described by:

$$\dot{\theta} = u_1$$
$$\dot{y} = u_2 \tag{4.17}$$

by simply defining:

$$u_1 = \frac{v \sin(\beta_f - \beta_r)}{\sqrt{\sigma_1^2 + \sigma_2^2}} \tag{4.18}$$

$$u_2 = \frac{v[R^T(\theta)\Sigma(\beta_i)]_{21}}{\sqrt{\sigma_1^2 + \sigma_2^2}} \tag{4.19}$$

Although there is no mechanical constraint on the wheel angles we introduce the following constraint (see figure 4.4) to prevent twisting of the cables from the wheel speed sensors:

$$-0.5\pi < \beta_i < 0.5\pi \tag{4.20}$$

The path following control consists of two controllers that calculate u_1 and u_2, and a method that inverts the kinematic model in 4.16 to calculate the low level setpoints $\beta_{i,sp}$. The inversion should result in one unique solution for the actual control that satisfies the constraints in 4.20.

4.5.3 Model inversion algorithm

The low level setpoints β_f and β_r can be found from solving the system of the two non-linear equations 4.18 and 4.19, constrained by 4.20. Figures 4.5 and 4.6 show how u_1 and u_2 relate to β_f and β_r at $\theta = 0$ rad and $v = 1$ m/s.

The algorithm to solve β_f and β_r includes the following steps:

1. For every given β_f satisfying 4.20, where β_r is also satisfying 4.20 and $|\beta_f - \beta_r| \leq 0.5\pi$, the allowed range for β_r is calculated by incrementing β_r with 0.01π and checking if $\beta_{1..4}$ calculated with 4.6 meet 4.20. Define $\beta^*_{r,max} = \mathrm{argmin}(\frac{u_1}{v}(\beta_r))$ and $\beta^*_{r,min} = \mathrm{argmax}(\frac{u_1}{v}(\beta_r))$, where $\frac{u_1}{v}$ is defined by 4.18, and calculate $\beta^*_{r,max}$ and $\beta^*_{r,min}$ for the allowed range of β_r. The calculation can be done independent of v, since $\frac{u_1}{v}$ is not depending on v. β_f is incremented with 0.01π resulting in a table with for every β_f a $\beta^*_{r,min}$ and a $\beta^*_{r,max}$. The overall maximum and minimum feasible $u^*_{1,max,feas} = \mathrm{max}(\frac{u_1}{v})$ and $u^*_{1,min,feas} = \mathrm{min}(\frac{u_1}{v})$ is calculated by taking the maximum and minimum over the resulting table.

2. The robot has always to return to the path in the direction of the path even if the angle θ of the robot to the path is larger than 0.5π. If the measured angle θ of the robot to the path is larger than 0.5π it turned out that the robot will make a turn in the opposite direction to return to the path. To avoid this the θ used in the algorithm is constrained.
$\theta = 0.5\pi$ for $\theta > 0.5\pi$
$\theta = -0.5\pi$ for $\theta < -0.5\pi$

3. Constrain u_1 to feasible values:
$u_1 = u^*_{1,max,feas} v$ for $\frac{u_1}{v} > u^*_{1,max,feas}$
$u_1 = u^*_{1,min,feas} v$ for $\frac{u_1}{v} < u^*_{1,min,feas}$

4. Because u_1 is feasible, there exists at least one β_r that solves 4.18 for at least one β_f. For each β_f in the table developed under step 1, a β_r is searched that solves 4.18 by finding the zero of:

$$f_y(\beta_f) = u_1 - \frac{v \sin(\beta_f - \beta_r)}{\sqrt{\sigma_1^2 + \sigma_2^2}} \tag{4.21}$$

where β_r is bounded by $\beta^*_{r,min}$ and $\beta^*_{r,max}$. A solution (β_f, β_r) is valid if $\beta_{1..4}$ calculated with 4.6 fulfills the constraint in 4.20 and if $|\beta_f - \beta_r| \leq 0.5\pi$.

5. For this set of valid solutions (β_f, β_r) the corresponding u^*_2 is calculated with 4.19 where $\xi_1 > 0$. The solution with u^*_2 closest to the controller output u_2 is found by interpolation.

Step 1 has to be done only once for a robot configuration, e.g. at initialization of the system or the resulting table could even just be coded in the software. The reason is that step 1 is not depending on v. The results in the table are only dependent from the system parameters. Steps 2-4 are performed in realtime, because those
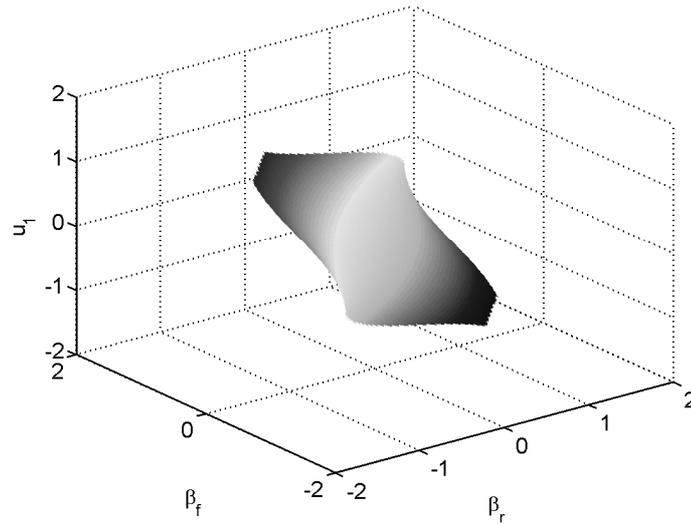
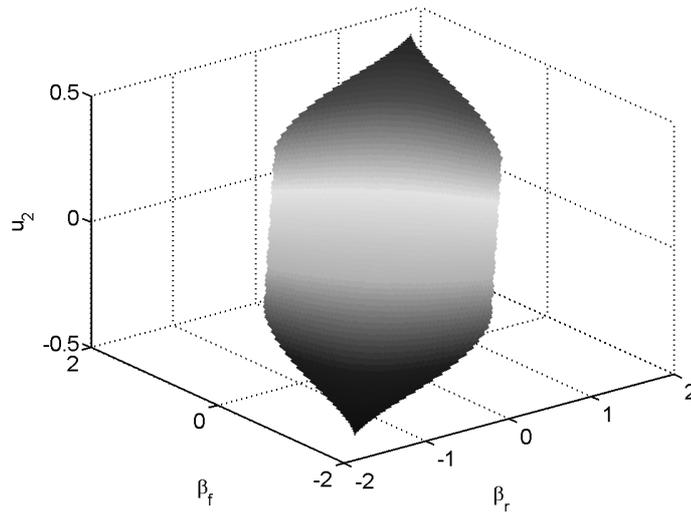Figure 4.5: Relation between β_f and β_r to u_1 at $\theta = 0$ rad and $v = 1$ m/s.

Figure 4.6: Relation between β_f and β_r to u_2 at $\theta = 0$ rad and $v = 1$ m/s.

depend from v and θ. The velocity v can be set by the user and θ is measured by the GPS, so these parameters change after robot startup.

The wheel speed setpoints $\dot{\phi}$ follow from 4.7, but are constrained by the minimum and maximum wheel speeds of the robot $\dot{\phi}_{min}$ = -6.9 rad/s and $\dot{\phi}_{max}$ = 6.9 rad/s. Therefore $\dot{\phi}$ is finally corrected for $\dot{\phi}_{min}$ and $\dot{\phi}_{max}$:

$$\begin{aligned}
\dot{\phi}_i &= \frac{\dot{\phi}_i}{min(\dot{\phi}_i)}\dot{\phi}_{min} \qquad & if \ min(\dot{\phi}_i) < \dot{\phi}_{min} \\
\dot{\phi}_i &= \frac{\dot{\phi}_i}{max(\dot{\phi}_i)}\dot{\phi}_{max} \qquad & if \ max(\dot{\phi}_i) > \dot{\phi}_{max}
\end{aligned} \tag{4.22}$$

4.5.4 Controller design

The path tracking controller must thus compute u_1 and u_2 (and consequently $\beta_{f,sp}$ and $\beta_{r,sp}$) in order to minimize the orientation error to the path θ and the orthogonal distance to the path y.

Using 4.18 and 4.19 it follows that the dynamics for both θ and y are described by pure integrators. Therefore proportional (P) control for both θ and y was expected to be sufficient. Since we use a path-relative coordinate system, from a control point of view the setpoints are equal to zero. A controller is designed which computes u_1 and u_2:

$$u_1 = -K_\theta\theta \tag{4.23}$$

$$u_2 = -K_y y \tag{4.24}$$

In first instance for both K_y and K_θ constant values were used chosen by simulation to give the desired response and both were chosen equal to -1.

P control is not sufficient when there is a disturbance d on the input channel. The disturbance for a pure integrator with process gain K will result in a constant offset when using P control (with controller gain K_c):

$$y = \frac{K}{s + KK_c}d + \frac{KK_c}{s + KK_c}y_{sp} \tag{4.25}$$

and for a constant disturbance d:

$$y(t \to \infty) = \lim_{s \to 0} s\frac{K}{s + KK_c}\frac{d}{s} = \frac{d}{K_c} \tag{4.26}$$

So for reducing this offset, high K_c is needed, but a high K_c gives stability problems because of the delay in the loop.

The constant offset can be reduced by a PI controller, the transfer function is then:

$$y = \frac{Ks}{s^2 + KK_cs + KK_I}d + \frac{KK_cs + KK_I}{s^2 + KK_cs + KK_I}y_{sp}$$

(4.27)

and for a constant disturbance d:

$$y(t \to \infty) = \lim_{s \to 0} s\frac{Ks}{s^2 + KK_cs + KK_I}\frac{d}{s} = 0$$

(4.28)

In simulation the influence of the controller gain K_c and the integration gain K_I was studied. For increasing K_I at constant K_c the overshoot resulting from a setpoint change increases, while the influence of the disturbance is reduced in a shorter time. However, at higher K_I, at a certain moment the transfer of the disturbance is overdamped, resulting in a worse overall response. If K_I is constant and K_c increases the overshoot is reduced. The K_c is further limited by the maximum controller output and the performance of the low-level control. Skogestad (2003) specifies the following PI settings for a pure integrator with time delay:

$$K_c = \frac{1}{K}\frac{1}{\tau_c + t_{d,hl}}$$

(4.29)

and:

$$\tau_I = 4(\tau_c + t_{d,hl})$$

(4.30)

where K is the process gain, $t_{d,hl}$ is the time delay of the high level system, τ_I is the integral time of the controller and τ_c is the desired time constant of the controlled system. In our case the gains depend on speed because we want to let the robot drive independent of its speed as much as possible along the same path to its setpoint. The desired path can be viewed as a reference path or response curve in space, with a characteristic distance τ_c^* that plays the same role as a time constant in a response curve in time. Hence τ_c^* is the distance over which 63% of the ultimate response is realized. That means that:

$$\tau_c = \frac{\tau_c^*}{v}$$

(4.31)

So at low speeds mainly the speed v limits the controller gain K_c, while at higher speeds mainly the time delay $t_{d,hl}$ limits the controller gain K_c.

The manufacturer can choose to leave the setting of τ_c to the farmer, or give it a default value. For this default value he can use the suggestion of Skogestad (2003) of choosing $\tau_c = t_{d,hl}$. In our case the time delay in the high level control response $t_{d,hl}$ as determined from a hardware in the loop step response is 0.5 s (see section 4.5.5). This can be explained from the sum of the low level control t_{dead} and t_d of 0.4 s (see section 4.4.1) and another 0.1 s from both wheel angle measurement and control loop running at 50 ms interval at different nodes connected to the CAN bus. Choosing $\tau_c = t_{d,hl} = 0.5$ s at $v = 0.5$ m/s it follows then K_c = -0.67 and τ_I = 6.0.

4.5.5   Evaluation methods

The performance of the path following control was tested in four different settings: Step responses with hardware in the loop simulation, step responses on pavement, a ramp on pavement and a typical headland path on pavement.

For hardware-in-the-loop tests the robot was mounted on trestles and the robot dynamics of the low level control were included in a closed loop. The robot motion in the x,y-plane was calculated by 4.16. A path with a step at 15 meters from the start was supplied. This distance was chosen to enable the robot to accelerate to its speed setpoint before arriving at the step. The robot was located at the start of the path with the same orientation as the path, was then set to autonomous control and followed the path autonomously. The orthogonal offset from the line was logged at a time interval of 50 ms.

The performance of the control was evaluated also with step responses on a paving. Four path coordinates that form a step were indicated on the pavement by chalk, measured out relative to a straight seam between the concrete plates of the paving. Again the step was located about 15 meters from the start of the path to enable the robot to accelerate to its speed setpoint before arriving at the step. The GPS coordinates of the chalk crosses were then measured by locating a robot GPS antenna pole equipped with a plumb line above the chalk cross by manual control (see figure 4.1). The robot was then positioned on the step path consisting of the surveyed points by manual control, some meters before the step and approximately in the same direction as the path. The robot was then set to autonomous control and followed the path autonomously. Evaluation
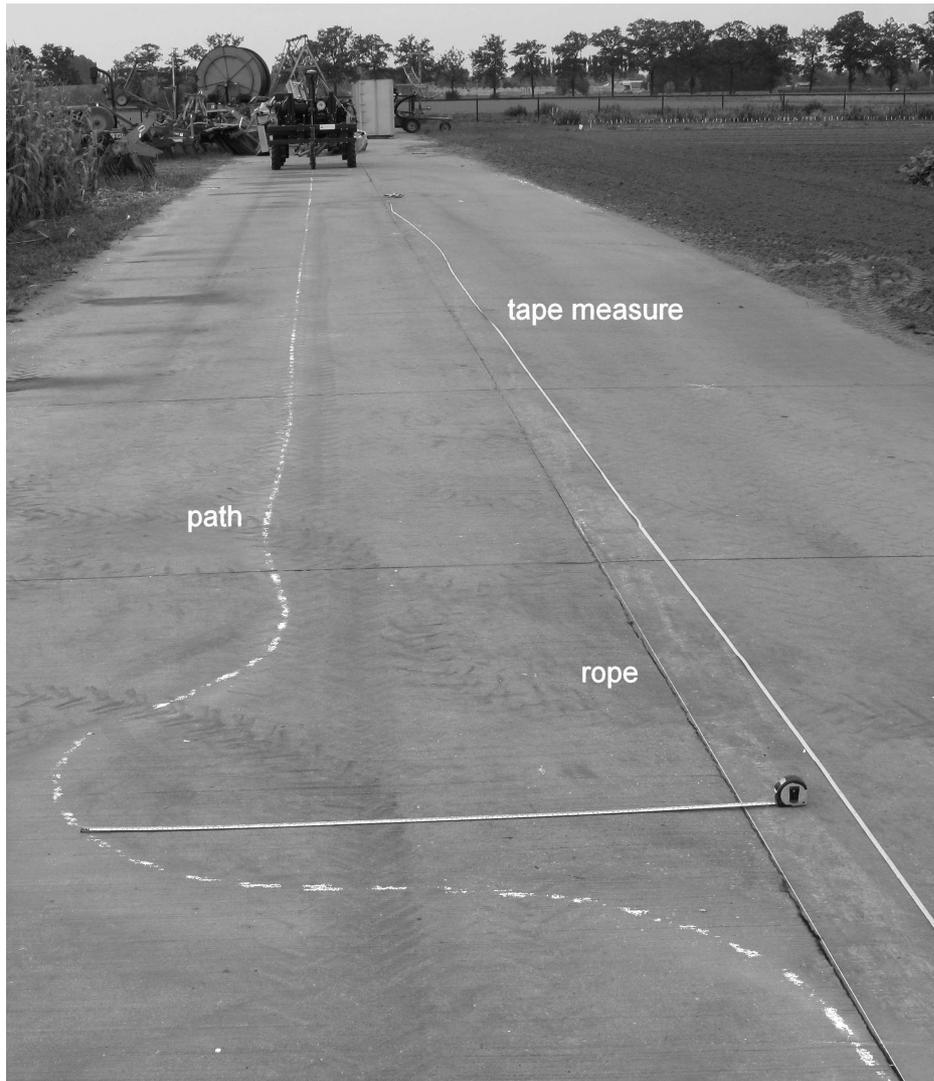
Figure 4.7: Real path drawn on the paving by a weeding unit with a chalk holder attached to the robot. To the right of the the the robot the rope indicating the path is visible.

of the performance of path following was done in two ways: by logging the GPS coordinates, orthogonal distances and orientation errors during path following with a time interval of 50 ms and by measuring the real path drawn on the paving by a weeding unit with a chalk holder attached to the robot, holding about 2 cm wide chalks (see figure 4.7). To measure the chalk line, a rope was tightly stretched between two pins fixed in the seam between the concrete plates over the distance of the the full path length and at regular distances of 25 cm along the rope the orthogonal distances from the rope to the middle of the chalk line were measured manually (see figure 4.7). At the step in the chalk line some more orthogonal distances were measured at distances of 5 and 10 cm from each other.

The performance of the control was evaluated further with a ramp response on a paving. Ramp following evaluates the response to orientation errors. The ramp was marked off as the diagonal of a square of 1 by 1 meter. Surveying the coordinates of the ramp was done in the same way as surveying the step. The robot position following the ramp is the actuator position at the back. Evaluation of the performance of ramp following was done by logging GPS coordinates, orthogonal distances and orientation errors during path following with a time interval of 50 ms.

Finally the performance of the control was evaluated with a typical headland path. The working width of the robot is 1.5 meters, so the paths that are connected by the headland path are only 1.5 meter apart, which results in a turn to the left resulting the left wheel entering the formerly left track before the turn again. The headland path is supplied as a sequence of 159 points, describing about half a circle with a radius of 0.75 meter. For step and ramp responses the position of the implement is following the path, but on the headland the robot middle position is following the headland path. The robot middle position is located exactly in between the four wheels. Evaluation of the performance of headland path following was done by logging GPS coordinates, orthogonal distances and orientation errors during path following with a time interval of 50 ms.

4.6 Experimental results

4.6.1 Hardware in the loop simulation with a P controller

The performance of the P controller with gain $K_c = $ -1 was evaluated in an hardware-in-the-loop test. Results are visualized in figure 4.8. The controller lets the robot
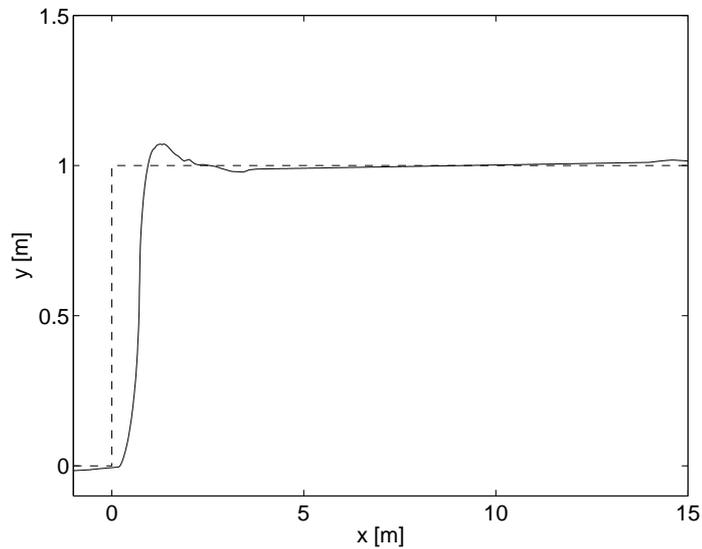
Figure 4.8: Hardware in the loop performance of path following with P control with K_c = -1 at v = 0.5 m/s (- - - step (desired path), — resulting path)

follow the path nicely. The mean orthogonal distance error between 8 and 15 m is 0.1 cm.

4.6.2   Step response on paving with a P controller

The performance of the P controller is tested on paving and both the GPS measurements and chalk line measurements are visualized in figure 4.9. Because of the step was marked off manually and there is a small error in the GPS measurement of the marked off corners of the step, the first and second part of the step are not exactly in parallel, so, for plotting the second part is aligned with the direction of the x-axis. The shape of the graph of the hand-measurement is very similar to the graph of the GPS-measurements: variations that are measured by hand are similar to variations that are measured by GPS. The offset between GPS and hand-made measurements at the start of the plot can be explained from the errors in surveying the marked-off corners of the step. The results in figure 4.9 show that there remains a static offset in the error that is not reduced by the controller: After the initial settling distance of x = 8 m, the mean error determined by GPS measurements over the distance 8 to 30 m is -1.6 cm and the minimum and maximum are -3.3 cm and 0.0 cm respectively and the standard deviation is 0.8 cm. The error in θ shows a
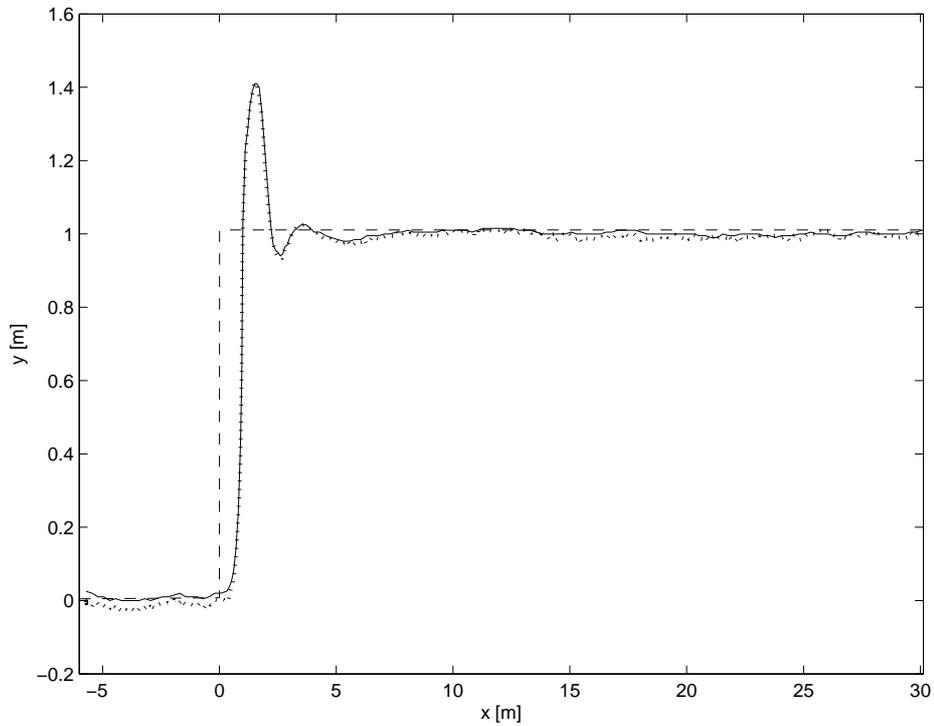
Figure 4.9: Path following with P control with K_c = -1 at v=0.5 m/s. The mean stationary offset between 8 and 30 m is 1.6 cm (--- step, $\cdots$ resulting path measured by GPS, — resulting path by hand-measuring the chalk line).
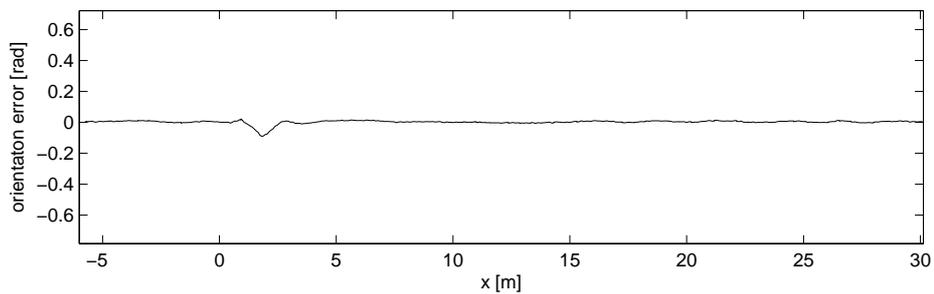

Figure 4.10: Orientation error during path following with P control with K_c = -1 at v = 0.5 m/s. The mean offset between 8 and 30 m is 0.003 rad (0.2°).
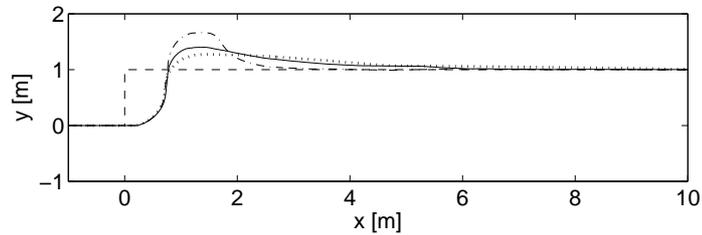
Figure 4.11: Step response of y with PI control at $\tau_c^* = 0.3$ ($\cdot\,\text{-}\,\cdot$), $\tau_c^* = 0.4$ (—) and $\tau_c^* = 0.5$ ($\cdots$) obtained with hardware in the loop simulation at v=0.5 m/s.
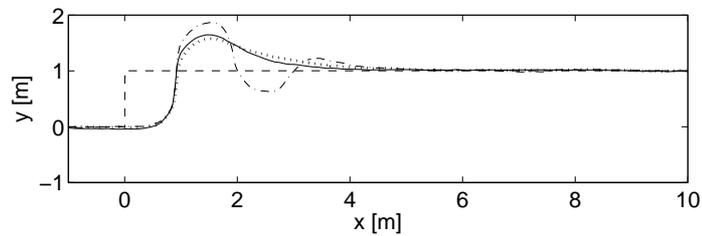
Figure 4.12: Step response of y with PI control at $\tau_c^* = 0.3$ ($\cdot\,\text{-}\,\cdot$), $\tau_c^* = 0.4$ (—) and $\tau_c^* = 0.5$ ($\cdots$) obtained with tests on paving at v=0.5 m/s.

very small static offset over this distance of $0.2\,^\circ$, see figure 4.10. The static offsets can be explained from a disturbance caused by the inaccuracy of the low-level wheel angle control. This inaccuracy of the wheel angle control can be explained from two main factors:

- Calibration errors of the zero position of the wheels. It appeared to be difficult to define the zero position of the wheels exactly.
- The accuracy of the control of the wheel angles is 2 degrees.

4.6.3   Step response with PI controller

Table 4.1 lists values for K_I and K_c corresponding with three values of τ_c^* at v=0.5 m/s for which the performance of the PI controllers is tested. Figure 4.11 shows hardware in the loop step responses with these settings and figure 4.12 shows the step responses on pavement. In the test on paving it takes a longer distance before the system responds to the step than in the hardware in the loop test. This can be explained from an extra time delay of the position measurement in the paving test of maximal 0.2 seconds from the GPS receiver outputting data at 5 Hz. This

73
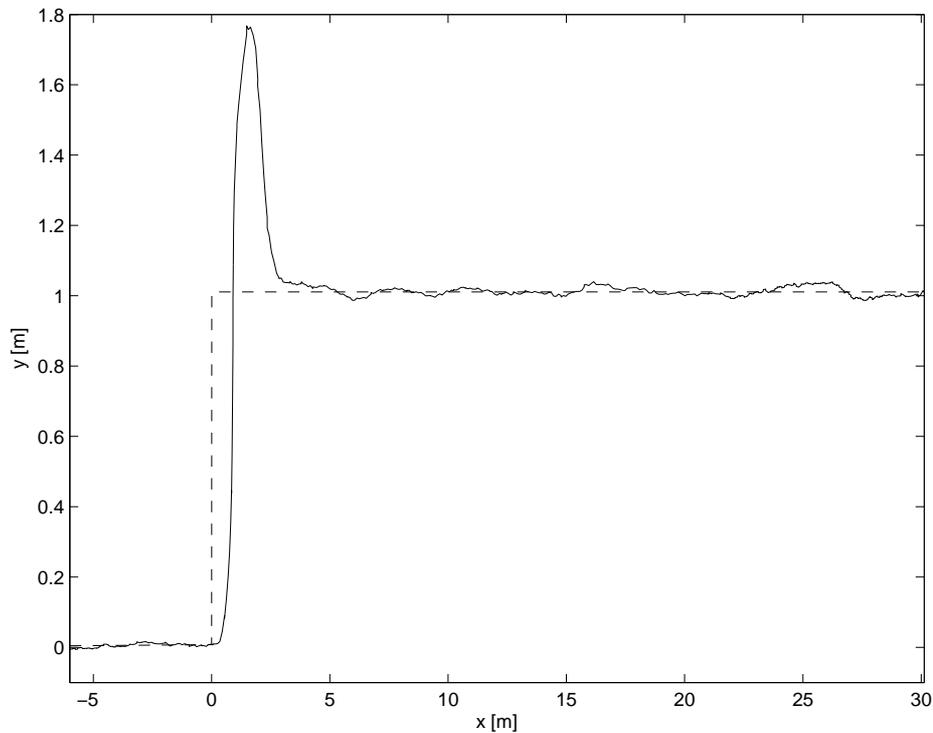
Figure 4.13: Path following with PI control at τ_c^*=0.4 and v = 0.5 m/s. The mean stationary offset between 8 and 30 m is 0.0 cm

extra time delay can also explain the higher overshoot in the step responses on pavement compared to the hardware in the loop step responses. A possible solution for better simulating the real situation is to include this GPS time delay also in the hardware in the loop simulation.

To be able to compare the orthogonal distance error after the settling distance with the experiment with P control, the step on pavement was repeated with the finally chosen control setting τ_c^*=0.4, which means after 40 cm the robot is at 63% of its setpoint (see figure 4.13). The mean orthogonal distance error between 8 and 30 m is now 0.0 cm, the minimum and maximum are -2.4 cm and 3.0 cm respectively, and the standard deviation is 1.2 cm.

The controller settings were also tested at higher speeds: figure 4.14 shows results from hardware in the loop tests and figure 4.15 shows results from a test on paving. Again the effect of the extra time delay from of the GPS receiver in the paving test results in a longer reaction distance and a higher overshoot. A raise in speed from

Table 4.1: PI controller settings tested in a hardware in the loop setting.

τ_c^*	0.3	0.4	0.5
τ_c	0.6	0.8	1
K_c	-0.91	-0.77	-0.67
τ_I	4.4	5.2	6.0
K_I	0.21	0.15	0.11

Figure 4.14: Step response with the chosen controller setting $\tau_c^* = 0.4$ at $v = 0.25$ m/s ($\cdot\!-\!\cdot$), $v = 1.0$ m/s (—) and $v = 1.5$ m/s ($\cdots$) obtained with hardware in the loop simulation.
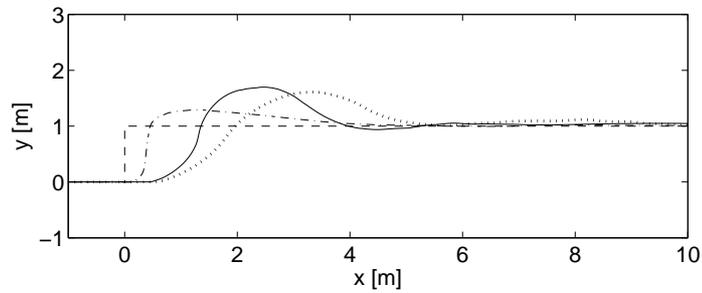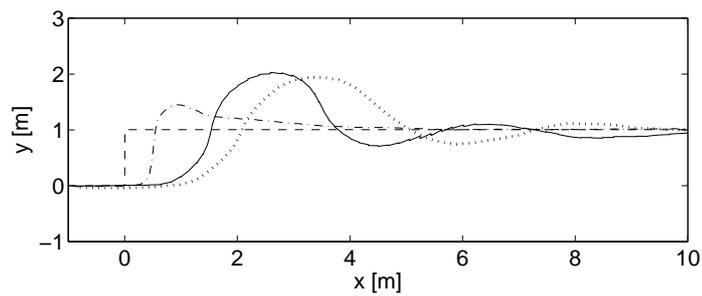

Figure 4.15: Step response with the chosen controller setting τ_c=0.4 at $v = 0.25$ m/s ($\cdot\!-\!\cdot$), $v = 1.0$ m/s (—) and $v = 1.5$ m/s ($\cdots$) obtained with tests on a paving.
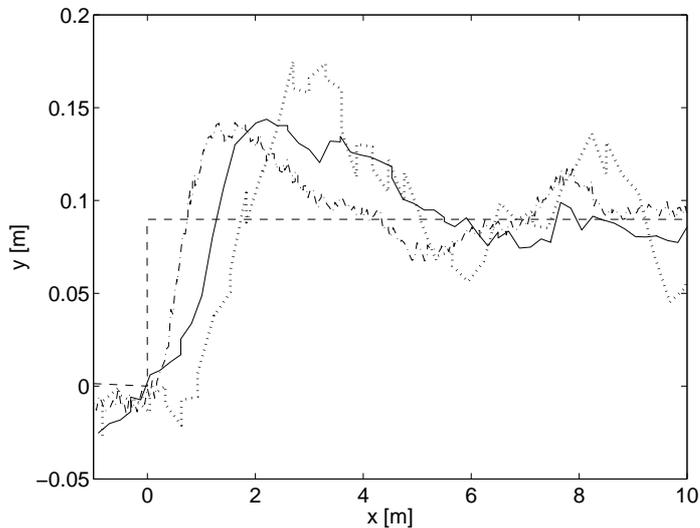
Figure 4.16: Response at step of 0.1 m with the chosen controller setting $\tau_c^* = 0.4$ at $v = 0.25$ m/s $(\cdot - \cdot)$, $v = 1.0$ m/s (—) and $v = 1.5$ m/s $(\cdots)$ obtained with tests on a paving. Notice the scale.

v=0.25 m/s to 1.0 m/s increases the overshoot, but the overshoot does not further increase when the speed is further raised to 1.5 m/s. At higher speed equation 4.29 nicely reduces the τ_c but K_c and τ_c go to fixed values resulting from $t_{d,hl}$, resulting in a stable response.

During path following on a field while performing weed control large step changes in the path will not occur and also large deviations from the path will not occur. Maximum error will only be around 0.1 m. Also under these circumstances the controller should perform well. Therefore a path following trial with a step of 0.1 meter was performed at several speeds on a paving. Results in figure 4.16 show besides the noise at this small scale including the noise of the GPS receiver a return to the path plus and minus 3 cm after a distance of 5 m for v=0.25 m/s and v =1 m/s which is satisfying.

4.6.4   Ramp response

A step in orientation was tested by performing a ramp response on a paving with PI controller settings $\tau_c^* = 0.4$ at $v = 0.2$ m/s (see figure 4.17). The maximum orthogonal error is 50 *cm* and the maximum orientation error is 1.13 rad.
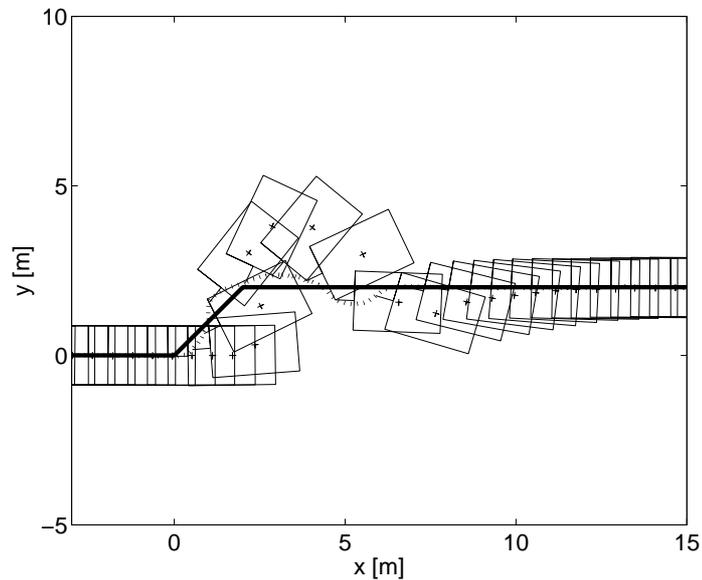
Figure 4.17: Ramp setpoint (—) and resulting response ($\cdots$) with the chosen controller setting $\tau_c = 0.4$ at v =0.2 m/s obtained with a test on paving

4.6.5   Headland path following

During turning the errors are increasing quite rapidly because of the sharp turn (turning radius of the path is 0.75 m) and the constraints on the wheel angles. To avoid overshoot due to the integrating action and because fast response during turning is much more important then high accuracy, P controllers are used. The possible offset at the end of the turn is then removed by the PI controller along the new straight path. The P controller gains for both the orthogonal distance controller and the orientation error controller are K_c = -0.77. Figure 4.18 shows the headland path, the driven route and the robot driving the path at v = 0.5 m/s plotted at a time interval of 3 seconds. Figures 4.19 and 4.20 show the orthogonal distance to the headland path and the orientation error while following the headland path. The maximum orthogonal distance and the maximum orientation error during the turn are respectively 69 cm and -0.93 rad. This headland path with such a limited radius can not be realized by the robot controller due to the constraints on the wheel angles. However, on the headland it is less important to follow the headland path exactly than arriving in front of the next path again. After the sharp turn in the headland path, the errors are reduced very soon, the turning itself takes only about 15 seconds (from t = 11 s to t = 26 s). The orientation error and
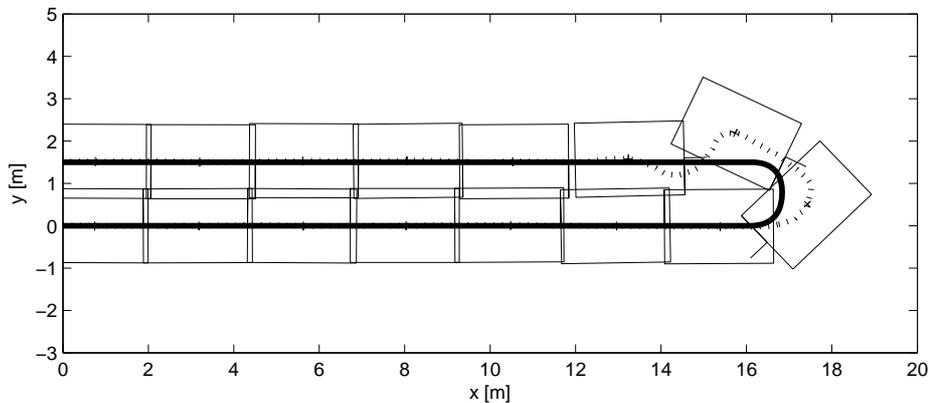
Figure 4.18: Driven route ($\cdots$) at headland path (—) following with P controller gain K_c = -0.77 at v = 0.5 m/s obtained with a test on paving

orthogonal distance error at the end of headland path following are 0.01 rad (<1°) and 1.4 cm respectively.

4.7   Discussion

The difference in step responses of the hardware in the loop tests and tests on paving can be explained from the fact that the GPS time delay is not included in the hardware in the loop simulation.

The smaller time delay in hardware in the loop did also affect the chosen controller setting $\tau_c^* = 0.4$. While the performance is very good when following a straight line, the overshoot in the step responses is rather large: at normal working speeds for weeding from 0.25 m/s to 1 m/s and taking a small step of 10 cm the overshoot is about 5 cm. A higher τ_c^* chosen about equal to a total time delay including the GPS receivers' time delay should result in less overshoot and an even better result.

Although the path following performance is satisfying for the application of weeding, the results point out that if further improvements would be required for some other application these improvements should focus on reducing time delays in the system. Ways to do this could be increasing the GPS receiver frequency, introduce Kalman filtering by using also wheel angle, wheel speed and gyro data, and by changing the flow compensated hydraulic valves to faster standard proportional valves.
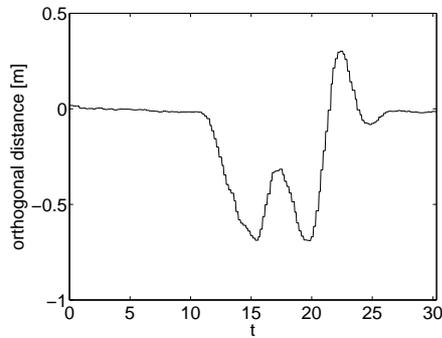
Figure 4.19: Orthogonal distance error at headland path following with P controller gain K_c = -0.77 at v = 0.5 m/s obtained with a test on paving
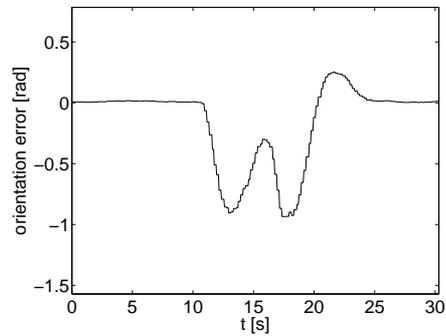
Figure 4.20: Orientation error at headland path following with P controller gain K_c = -0.77 at v = 0.5 m/s obtained with a test on paving

Another improvement of path following accuracy would be to improve the low level wheel angle control. The limited steering accuracy of 2 degrees is due to the frequency of the electronic control units (20 Hz), hydraulic valve gain and the minimal required wheel angle controller output. The accuracy could be improved by changing the hydraulic valves to valves with a lower gain, but will be limited then again by the current angle sensor with an accuracy of one degree. So to obtain higher accuracies than one degree, both hydraulic valves and angle sensors should be changed.

The GPS-made measurements correspond very well with the hand-made measurements of the chalk line. Even small variations in the driven path are visible in both measurements. The largest error source causing the two measurements not to correspond exactly is the error in measuring the GPS coordinates of the corners of the step. The inaccuracy of a few centimeters in measuring these positions result from GPS accuracy, the GPS antenna height of about 2 meters above the paving surface, small not measured roll and pitch and the accuracy of about 1 cm by which the lead line connected to the GPS antenna pole could be positioned above the mark indicating the position to be measured. But it is very clear that the GPS measurements are perfectly usable for controller development, even handmade measurements are difficult to be made more precise than the RTK-DGPS ones.

To handle high errors that arise during headland path following due to robot constraints and path shape, P control was used to avoid overshoot due to the integrating action and because fast response during turning is much more important

then high accuracy. To handle small errors while following a straight path with high accuracy, PI control was needed to overcome small errors from the low level control. This suggests a more generic approach that uses P control for large errors and PI control when the error is below a certain limit.

The high level control parameter τ_c^* can just be set by the user and controller tuning parameters follow then from the method adapted from Skogestad (2003). In contrary to a feedback linearization-based approach like Bendtsen et al. (2002), this approach gives the possibility to deal with limitations on the wheel-angles as they exist on almost every four-wheel steered vehicle in practice.

4.8 Conclusion

The Smith predictor compensates well for time-delays in electro-hydraulic steering systems in practice.

The control method for four wheel steered vehicles presented in this paper has a number of attractive features:
- Enables control of a user definable position relative to the robot frame which usually is the position of the implement.
- Can deal with limitations on the wheel angles.
- Has a good performance as shown in step responses made in a hardware in the loop fashion, on a paving and by following a typical headland path.

The method is very well practical applicable for a manufacturer:
- The time delay can be determined from a step response at the factory, possibly to increase with the time delay of the GPS.
- The model inversion requires only some dimensions of the robot and its wheels. These are all parameters that are known by the manufacturer. The inversion of the vehicle model (the only complex part) could be supplied as a generic software module.
- The user supplies v and τ_c^*, where τ_c^* has an easy interpretable meaning: it is the driven distance along the path where 63% of the setpoint is reached. The method adapted from Skogestad (2003) determines then the controller settings and even suggests a default value for τ_c^*.

In contrast of the expected sufficiency of P control because of the dynamics of the processes for both θ and y act as pure integrators, PI control is needed to overcome small errors caused by inaccuracies of the low level wheel control.

The refined tuning method adapted from Skogestad (2003) calculates controller settings that let the robot drive as much as possible along the same path to its setpoint, but also limit the gains at higher speeds to prevent the closed loop system to become unstable because of the time delay.

Mean, minimum and maximum orthogonal distance errors while following a straight path on a paving at a speed of 0.5 m/s are 0.0 -2.4 and 3.0 cm respectively and the standard deviation is 1.2 cm. Further improvements in accuracy of path following of a straight path are not to be expected, because of the standard deviation of 1.2 cm is about equal to the RTK-DGPS accuracy.

Additional research should show if the performance of the control will also be sufficient on a field with uneven soil surface. Combining the path following with automatic headland detection and automatic headland path generation should enable the robot to navigate autonomously over a whole field.

Chapter 5

Autonomous navigation in a field with a robot platform

Abstract

This paper presents autonomous navigation with a robotic platform for weed control in a sugar beet field combining both absolute and relative navigation. Two trials are performed at the same time: navigating along crop rows based on RTK-DGPS and crop row mapping by combining vision based row detection with RTK-DGPS information. Standard deviation, mean, minimum and maximum orthogonal distance of the actuator to the path while following a straight crop row on the field with RTK-DGPS at a speed of 0.3 m/s are respectively 1.6, 0.1, -4.5 and 3.4 cm. The point-in-polygon algorithm proved to be a suitable method for detection in which part of the field the actuator position coordinates or the field of view of the camera are located. A smooth headland path that nicely connects to the subsequent path along the crop is generated in realtime with a spline based algorithm. The hybrid deliberate software architecture with a behavior based reactive layer allows a convenient evaluation of the robot performance. Results from the field experiments show that the implement can be guided along a defined path with cm precision by an autonomous robot navigating in a field.

Keywords: Robot, Weed Control, RTK-DGPS, Vision, SLAM.

5.1 Introduction

Autonomous navigation in an agricultural field with a robotic platform has been done by absolute navigation with GPS (Bak and Jakobsen, 2004; Noguchi et al., 2001a; Nagasaka et al., 2004) and by relative navigation with machine vision (Tillett et al., 1998; Jørgensen et al., 2006; Åstrand and Baerveldt, 2002). The crop row mapping with a mobile robot navigating with GPS as presented in this paper can be seen as a first step to integrate both GPS based absolute navigation and machine vision based relative navigation. With the robot platform two trials are performed at the same time in a sugar beet field: navigate along crop rows based on RTK-DGPS and crop row mapping by combining vision based row detection with RTK-DGPS information.

Autonomous navigation in a field requires automatic headland turning to the next path to be followed. One approach is feed forward headland turning: the wheel angles are controlled to an angle corresponding to the desired turning radius. Some researchers combined this method with feedback on the orientation obtained from compass or gyroscope to determine when to switch to path following of the new path to be followed (Darr et al., 2005; Nagasaka et al., 2004). This method is comparable to approaches often adopted by field robots competing at the Field Robot Event (Van Straten, 2004; Van Henten and Müller, 2007) like by the Wurking (Hofstee et al., 2007). It works fairly well only when the distance to travel over the headland is not too long. For longer distances this method is less suitable because the accuracy of the position deteriorates with the distance traveled. Using feedback during the headland turn can avert that the deviation from the subsequent path to be followed after the turn becomes large. Approaches that use feedback start with the generation of a headland trajectory. The computation of the headland trajectory considers constraints like steering wheel speed, maximum steering angle and headland dimensions (Noguchi et al., 2001b; Kise et al., 2002; Bell, 1999). Some approaches calculate trajectories that let trailed implements return in front of the next path to be followed (Oksanen, 2007; Rekow and Ohlemeyer, 2007). Some trajectory calculation methods can also avoid obstacles (Vougioukas et al., 2006; Linker and Blass, 2008). In our case we do not have a trailed implement, there are no obstacles in the field and the feasible pathes are not so much limited by platform constraints because the platform is four-wheel steered and the maximum wheel steering angle is 111 degrees. For this reason we chose to implement a straightforward headland trajectory generating method.

Design of software is of crucial importance for the functioning of mobile robots. The hybrid deliberate software architecture, like for example adopted by Bak and Jakobsen (2004) for an agricultural robotic platform for weed detection, is widely recognized to be the most common architecture for robot software (Orebäck and Christensen, 2003). Blackmore et al. (2007) showed that this architecture is very well suited for automation of agricultural operations because the agricultural environment is usually semi-structured. Deterministic tasks can be optimized based on known structures within the field, while reactive tasks are carried out in real-time in reaction to local conditions that were not known before the operation started.

The reactive layer in the hybrid deliberate architecture is often behavior based (Orebäck and Christensen, 2003). In a behavior perception is coupled to action, where mechanisms like subsumption coordinate the interaction of the active individual behaviors resulting in the consequential 'emergent' robot behavior (Arkin, 1998). The navigation system presented in this paper also has a hybrid deliberate software architecture with a reactive layer. Subsumption is used as a coordination mechanism for reactive behaviors like path following, crop row following and stop on emergency thus leading to autonomous behavior in the field.

The objective of this research is to:
- develop a RTK-DGPS based autonomous field navigation system including automated headland turns.
- develop a method for crop row mapping combining machine vision and RTK-DGPS.
- evaluate the benefits of a behavior based reactive layer in a hybrid deliberate systems architecture.

5.2 Platform description

5.2.1 Design approach

The robotic platform is specially designed for performing autonomous weed control. During the design process, a methodological approach to engineering design was used to ensure the quality of the result of the design process and to facilitate the communication and decision making. This design methodology is reported in Bakker et al. (2008b).

Figure 5.1: Robot platform.

5.2.2   Robotic platform

The platform (see figure 5.1) has a ground clearance of 0.5 m, 16 cm wide wheels and 1.5 m wheel distance for in-row driving in both 0.5 and 0.75 m rows. The wheelbase is 1.91 m and the length and width of the platform chassis including a hitch are 1.75 by 2.80 m. A hinged support of the front part of the chassis to which both the front wheel modules are connected guarantees that all wheels are always in contact with the ground. Implements may be mounted at the center of the platform underneath the chassis, at the front bar or at a rear hitch. Currently only one hoe holder is connected right in the middle of the rear hitch. The platform is four-wheel steered and four-wheel driven. Each of the four wheel modules includes a fixed displacement hydraulic motor for propulsion that provides direct drive without gearing. Another fixed displacement hydraulic motor mounted on top of the wheel module steers the wheel via a planetary reduction with a ratio of 1 to 73.56. Although there are no mechanical constraints on maximum and minimum turning angle of a wheel around its vertical axis, maximum and minimum wheel angles are constraint by the control to plus and minus 111 degrees to prevent twisting of the cables from the wheel speed sensors. Power is provided by a 31 kW Kubota diesel engine that powers two hydraulic pumps mounted in series. The hydraulic

transmission to the wheels consists of a variable displacement pump supplying oil to eight electric proportional valves, four connected to the steering motors and four connected to the drive motors. The pump/valves combination is a 'load sensing' system: the pressure drop over the valves controls the displacement of the pump via an hydraulic load sensing connection and is limited to a small value, independent of load pressure. The second hydraulic pump is connected to two valves, one feeding 3 parallel auxiliary connections for implements, and one connected to a cylinder controlling the hitch height.

5.2.3   Hardware and sensors

The weeding robot electronics consists of 9 embedded controllers connected by a CAN bus using the ISO 11783 protocol. In the inside of every wheel rim a cogwheel is mounted for wheel speed measurement. The two magneto resistive sensors per cogwheel are placed in such a way that the direction of rotation can be resolved. The rotation of the wheels is measured by these sensors with a resolution of 100 pulses per wheel revolution. The wheel angle of each wheel is measured by a Kverneland 180 degree sensor with an accuracy of one degree. Per wheel a micro controller is mounted transmitting wheel speed and wheel angle via the CAN bus. Two GPS antennas are used to measure both vehicle position and orientation. Both are connected to a Septentrio PolaRx2eH RTK-DGPS receiver with a specified position accuracy of 1-2 cm and a specified orientation accuracy of 0.3 degrees (1 σ). The two GPS antennas are mounted on a metal disc to prevent multipath errors. A base station with a Septentrio PolaRx2e RTK-DGPS supplies the RTK-correction signals via a radio connection to the Septentrio PolaRx2eH receiver. The position of the base station itself can be configured by a correction supplied by the service of a company called 06-GPS via GPRS. For image acquisition a Basler 301fc colour camera with a resolution of 659 by 494 pixels is mounted on a platform. The camera is mounted at 0.9 meters above the ground looking forward and down with an angle of 37° to the vertical. The area covered by one image is 2.4 meters long in row direction and 1.5 meters wide at the image border closest to the camera. Sugar beet is grown at a row distance of 50 cm, so this means that three rows are visible in the image. This camera is connected via Firewire to a laptop on which the image processing algorithm is implemented. The laptop is connected to the CAN bus. One embedded controller running a real time operating system (National Instruments PXI system) also connected to the CAN bus performs the general vehicle control. The GPS receiver, and a radio modem are connected to the PXI via RS232. The radio modem interfaces the remote control used for manual

control of the weeding robot. Remote manual control is used for transportation to and from the field. The ability to switch remotely to manual control is also required for guaranteeing safety during field trials. Colored lamps of the signal tower can be operated via a micro-controller to indicate the current status of the robot platform. The platform is further equipped with sensors measuring diesel level, hydraulic oil level, engine temperature and hitch height. The PXI system gathers wheel angles, wheel speeds, GPS data, remote control data and hitch height and controls the vehicle by sending messages to the three micro controllers connected to the hydraulic valves. A safety system consisting of four red emergency switches at the corners of the vehicle and a remote switch, sets the valves to the neutral position on activation, overruling the computer control. A laptop connected via ethernet to the PXI system functions as the user interface of the robot platform.

5.2.4   Software architecture

The three layers of the hybrid deliberate architecture are a deliberate layer, a reactive layer and one middle layer. The top deliberate layer handles planning and interaction with the operator. The middle layer is the supervisory layer: it bridges the gap between the deliberate and the reactive layer. The reactive layer performs repetitive time critical calculations. The reactive layer of the robot platform software is behavior based, so the subsystem consists of separate behaviors, where each behavior has one specified task (Murphy, 2000): CheckActuatorIn-MidField, CheckRowsInViewOfCam, FollowPath, FollowHeadlandPath, FollowRow, Listen2RemoteControl, StopOutsideField and StopOnEmergency, OperateHitch, OperateLamp, WheelSpeedControl and WheelAngleControl, that will be explained more extensively in section 5.3. Each behavior can be released and suppressed. For coordination of behaviors two mechanisms are used: releasing and suppression. As long as a behavior is released it is active (Murphy, 2000). Suppression prevents the current signal from being transmitted, and replaces that signal with the suppressing signal (Arkin, 1998). In every behavior perception is coupled to action, except for the behaviors CheckActuatorInMidField, CheckRowsInViewOfCam, these do not result in actuator commands, but just perceive if the implement is in the main field area and if the area of view of the camera is in the main field area, respectively. Depending on the perception of these last two behaviors and information from the deliberate layer, the supervisory layer determines if behaviors are released or suppressed as will be explained more extensively in paragraph 5.3.2. If different behaviors act on the same outputs, one behavior suppresses another behavior. In our case the behaviors StopOutsideField and StopOnEmergency always have the

possibility to suppress other behaviors that act on the wheel speed and wheel angle setpoints.

5.3 Navigation system

5.3.1 Initial parameters

In the autonomous field navigation trial on a sugar beet field the navigation along crop rows is done based on RTK-DGPS. In order to check the camera system, at the same time crop row mapping is performed by combining vision based row detection with RTK-DGPS information. The experimental field was a sugar beet field sown in the autumn 2007 to perform field tests with the robot. Due to the autumn and winter time the crop plants remained small and when the experiment was done on 14 January 2008 the crop was still in about four true leaves stage. The headland width was 18 meters. The prior information needed before navigating on the field are the field and headland boundaries, the row locations and the first turning direction of the robot on the first headland to arrive at. The field and headland boundaries were determined by surveying the eight defining corner positions and the row locations were determined by measuring begin and end positions of two rows 1.5 meter apart (see figure 5.2). Surveying is done by driving the robot by manual control to the different locations so that the GPS antenna is located above the location to be surveyed. A lead line is attached to the GPS antenna to simplify visual determination of the correct robot position. With the surveyed GPS coordinates four files are made, two headland files and a path file, each of them just containing a sequence of GPS coordinates (WGS84 coordinates). At the start of the autonomous navigation the field and headland boundary files are loaded and the minimum values found are chosen as the origin of a local field coordinate system. Next the field and headland boundaries and path files are calculated to meter scale in this field coordinate system. The speed setpoint for all tests was set to 0.3 m/s. The user indicates also the first turning direction (left or right) for the first headland. This turning direction stays the same for this headland during navigating over the field, and the turning direction at the other headland is then opposite to the first turning direction.
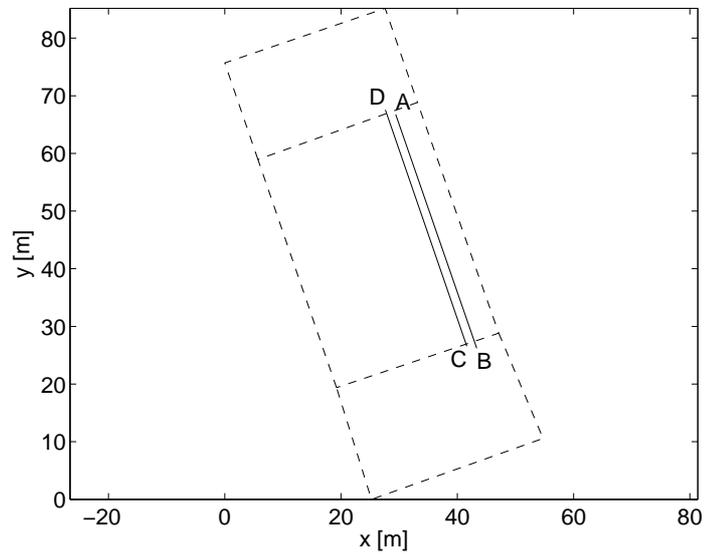
Figure 5.2: Field with a priori information for experiments. Eight surveyed positions define the borders of the two headlands and the main field area. The positions A and B are the surveyed begin and end position of a first row respectively, C and D are begin and end positions of a second row 1.5 m apart from the first one.

5.3.2 Supervisory layer

The supervisory layer decides which behavior is released and which is suppressed depending on information from the deliberate layer and the following perceived conditions:

- Autonomous: whether the robot is in autonomous mode, which is set by the user with the remote control.
- ActInMidField: whether the actuator is in the main field area, which is set by the behavior CheckActuatorInMidField.
- RowsInViewOfCam: whether the rows are in view of the camera, which is set by the behavior CheckRowsInViewOfCam.

The following behaviors are always released: StopOnEmergency, WheelSpeedControl, WheelAngleControl, OperateHitch and OperateLamp. From the deliberate layer the supervisory layer knows the robot's mission: Navigate autonomously over the field while mapping crop rows. If the supervisory layer perceives autonomous mode, it stops releasing Listen2RemoteControl and it releases the following behaviors to accomplish the mission: FollowPath, FollowHeadlandPath, FollowRow,

StopOutsideField, CheckIplementOnMidField, CheckRowsInViewOfCam. The behaviors FollowPath, FollowHeadlandPath, FollowRow and StopOutsideField have the same outputs: wheel angle setpoints and wheel speed setpoints. Depending on the perceived conditions the supervisory layer determines by suppression which behaviors' setpoints are transmitted to the WheelAngleControl and WheelSpeed-Control behaviors as shown in table 5.1. StopOutsideField and StopOnEmergency can always suppress the setpoints generated by other behaviors and transmit their setpoints (with zero values) to the WheelAngleControl and WheelSpeedControl behaviors. Because in this study the FollowRow behavior is only used for crop row mapping, the outputs from the FollowRow behavior are always suppressed. The robot behavior for the mission navigation on the field by GPS while mapping crop rows can simply be visualized by table 5.1. This table shows under which perceived conditions the different behaviors are released and suppressed.

5.3.3 FollowPath

The path following behavior controls a user specified position relative to the robot frame. The coordinates of this position in the robot frame to follow the path are set to the position of the hoe in the middle of the rear hitch, because this hoe has to follow the path. The hoe position is calculated from its position in the vehicle frame and from the GPS position and orientation. The path is just a sequence of waypoints in field coordinates generated as described under section 5.3.1. The orthogonal distance and orientation to the path are calculated by a specially designed orthogonal projection. At initialization this orthogonal projection calculates the shortest orthogonal distance and the corresponding orientation error from a path segment to the current position. If no orthogonal projection is possible to any path segment the path segment with the shortest distance between its starting position and the current position is extended and the orthogonal distance and orientation error to this vector is calculated. After initialization the orthogonal distance and orientation to the path is calculated by first trying to project on the last segment used and if not possible to successive segments, extended at the side connecting to the last segment used, until a projection is possible. The orthogonal distance and orientation to the path are controlled by two PI controllers (high level control), resulting in low level control setpoints for wheel angles and wheel speeds as described by Bakker et al. (2007a). An improved controller can be found in Bakker et al. (2008c). The high level PI controller settings are chosen to be K_c = -2 and K_I = 0.5, for both orthogonal distance and orientation error. If the quality of the

Table 5.1: Perception conditions under which the supervisory layer releases behavior with corresponding suppression status during manual control and during autonomous navigation on a field while mapping crop rows (1=yes, 0=no).

Perception			Behavior		
Autonomous	ActInMidField	RowsInViewOfCam	Name	Released	Suppressed
1	0	0	FollowPath	1	1
1	0	1		1	0
1	1	0		1	0
1	1	1		1	0
1	0	0	FollowHeadlandPath	1	0
1	0	1		1	1
1	1	0		1	1
1	1	1		1	1
1			FollowRow	1	1
1			StopOutsideField	1	0
1			CheckActuatorInMidField	1	0
1			CheckRowsInViewOfCam	1	0
0			Listen2RemoteControl	1	0
			StopOnEmergency	1	0
			WheelSpeedControl	1	0
			WheelAngleControl	1	0
			OperateHitch	1	0
			OperateLamp	1	0

GPS signal is decreasing, large orthogonal and orientation errors occur. Therefore in that case the orthogonal distance and orientation errors are set to zero.

5.3.4 FollowHeadlandPath

The headland path following is quite similar to path following except that the headland path following is generating a headland path by itself. A headland path must be available well before the robot enters the headland. Therefore FollowHeadlandPath initializes when its suppression status changes to suppressed due to entering the midfield. While of course being suppressed from that moment on, the headland path following behavior continually determines its distance to the headland from its position and orientation, where the robot orientation is calculated from the measured robot positions during the last 3 driven meters. If the distance of the robot middle position to the headland is less than 3 meters, the robot generates a path to the start of the next row to be followed. To create this path first the coordinates of the following positions are determined (see figure 5.3).

a the current robot middle position.

b position at the end of a vector starting at the robot position extended in forward direction with an orientation equal to the robot orientation, to a length so that it crosses the main field/headland boundary by a distance of 6.5 m.

c position at the end of a vector $\vec{ab}$ made by extending in the direction of b with 1.5 m.

d position at the start of a vector parallel to vector $\vec{ab}$ at an offset of plus or minus the working width. The sign of the offset of the third headland path vector to the first headland path vector is known from the first turning direction indicated by the user. For the other headland the turning direction is opposite to the first one.

e position at the end of a vector starting in d, parallel to $\vec{ab}$, extended to a length so that it crosses the headland boundary by a distance of 6.5 meters.

f position at the end of a vector made by extending $\vec{de}$ in the direction of e with 1.5 m.

The polygon $\{b, c, f, e\}$ (see figure 5.3) is used as the control polygon to define a quadratic uniform B-spline curve consisting of 157 positions. Positions a and d are added to respectively the start and end of these positions and so form the generated headland path. The robot middle position is set to follow the headland path because the function of headland path following is to turn the platform and not
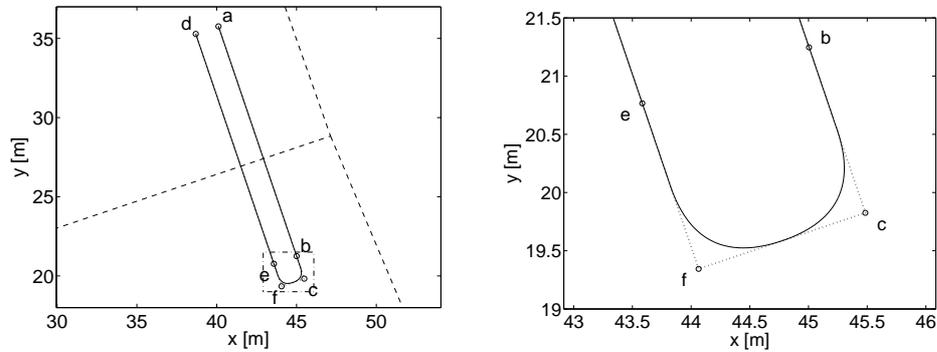
Figure 5.3: Headland path (——) generated from polyline $\{a, b, c, f, e, d\}$ ($\cdots$). Part of the left figure indicated by the box ($\cdot$-$\cdot$) in the left figure is displayed enlarged in the right figure.

to perform an operation with the implement. The robot middle position is located exactly in between the four wheels. The robot follows the generated headland path if the headland path following is released and if it is not suppressed. The orthogonal projection and control during following the headland path is the same as described in paragraph 5.3.3, except that two P controllers are used. During turning the errors are increasing quite rapidly because of the constraints on the wheel angles. To avoid overshoot due to the integrating action and because fast response during turning is much more important then high accuracy, P controllers are used. The P controller settings for both the orthogonal distance controller and the orientation error controller are K_c = -2.

5.3.5 FollowRow

The FollowRow behavior controls a position relative to the robot frame to follow a crop row. The coordinates of this position in the robot frame to follow the crop row is set to the position of the hoe in the middle of the rear hitch. Thus, in the future, the FollowRow behavior can replace the FollowPath behavior when in between the rows. The crop row is a path in field coordinates reconstructed from combining absolute RTK-DGPS positioning with crop row detection by machine vision. The machine vision algorithm for crop row detection is described in Bakker et al. (2008a). If the rows are in view of the camera as indicated with RowsInViewOfCam and the quality of GPS signal is good the image processing determines for every image:

$\epsilon\delta_{img}$	the distance to the row in the image at the image border nearest to the robot frame [m].
$\epsilon\theta_{img}$	the orientation of the row in the image [rad].
$\Delta t_{image\ proc}$	the duration of the image processing for row detection of an image [ms]. Figure 5.4 shows the robot near a crop row in the field coordinate system (x_{field}, y_{field}).

Let:

$\xi = [x\ y\ \theta]^T$	the implement position x, y [m] and orientation θ [rad] in the field coordinate system.
ξ_{image}	is $\xi(t - \Delta t_{imageproc})$ and is calculated from the latest logged $\xi(t)$ by linear interpolation.
l_{image}	the length of an image in direction of the length of x_v [m].
c_1	front position of the row in the latest image in field coordinates.
c_2	rear position of the row in the latest image in field coordinates.
$\epsilon\delta$	the orthogonal distance of the robot to the row [m].
$\epsilon\theta$	the orientation of the robot to the row [rad].

If the rows are in view of the camera and if the difference between the last implement position ξ measured is bigger than 2 cm (so the robot is moving) for every new image the coordinates of c_1 and c_2 are calculated. The coordinates of c_1 and c_2 follow from ξ_{image}, l_{image}, $\epsilon\delta_{img}$ and $\epsilon\theta_{img}$ and from the position of the image relative to the vehicle frame x_v, y_v. The coordinates of c_1 and c_2 are added to an array C, indicated by the crosses in figure 5.4. The array C is cleared if RowsInViewOfCam changes from 0 to 1 or on a release of the FollowRow behaviour. C_{reg} is a subset of C including only the positions c_i that are located within an certain distance r from the current robot position ξ. The distance r is equal to the radius of the circle in figure 5.4 and is equal to 1.5 m. Through the positions C_{reg} a line m is fitted using least squares linear regression. The orthogonal distance $\epsilon\delta$ and the orientation error $\epsilon\theta$ of the actuator position to the crop row is now calculated to this line m. These errors are used in the same way for control as in the method described in paragraph 5.3.3.

5.3.6 StopOutsideField

StopOutsideField calculates if one of the positions of the robot contour is outside the main field area polygon and outside both headland polygons with the point-in-polygon algorithm (Burrough and MacDonnell, 1998). The robot contour in field coordinates is calculated from the robot position and orientation and from the robot
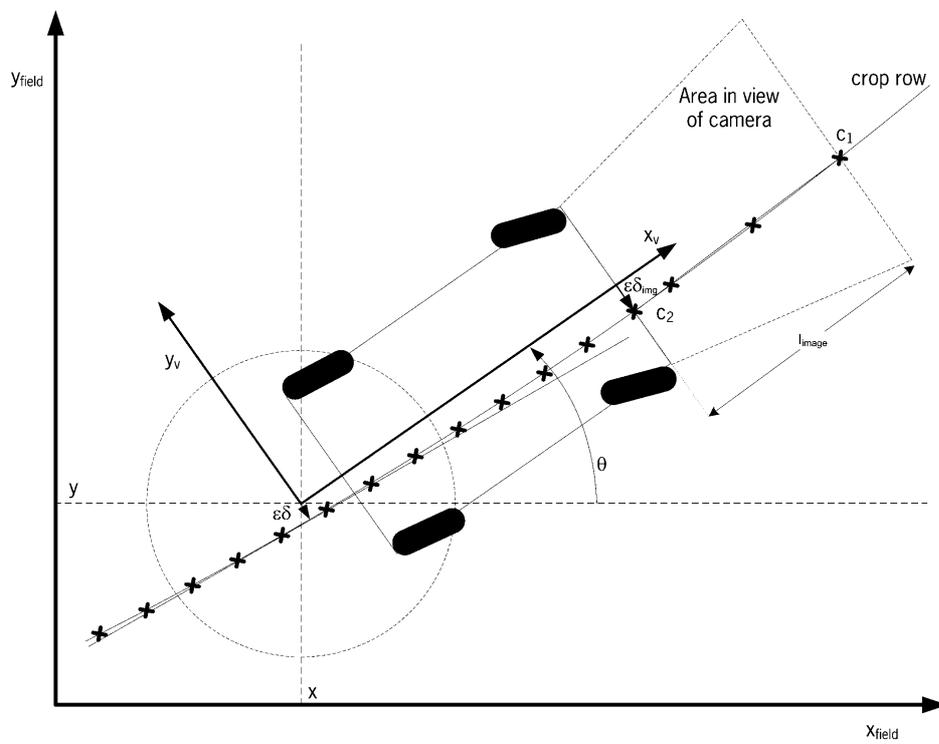
Figure 5.4: Robot driving along a crop row in the field coordinate system.

dimensions. If a robot contour coordinate is located outside the polygons, the wheel angle setpoints and wheel speed setpoints are set to zero.

5.3.7   CheckActuatorInMidField

CheckActuatorInMidField checks if the robot's actuator position is inside the main field area polygon with the point-in-polygon algorithm and then sets ActInMidField accordingly. The actuator position in field coordinates is calculated from the robot position and orientation and from the actuator position within the robot coordinate system.

5.3.8   CheckRowsInViewOfCam

CheckRowsInViewOfCam checks if the contour of the area covered by the camera performing row recognition is inside the main field area polygon with the point-in-polygon algorithm and then sets RowsInViewOfCam accordingly. The contour of the area covered by the camera in field coordinates is calculated from its coordinates in the robot coordinate system and from the robot position and orientation.

5.3.9   Listen2RemoteControl

Listen2RemoteControl converts the remote control joystick position to wheel angle and wheel speed setpoints depending on the selected steering mode resulting in setpoints for wheel angles and speeds of two virtual wheels, one between the front wheels and one between the rear wheels. Possible steering modes are: front wheel, rear wheel, four-wheel opposite and four-wheel parallel steering. The setpoints for each of the four individual wheels follow from the vehicle model (Bakker et al., 2008c).

5.3.10   StopOnEmergency

StopOnEmergency makes the wheel setpoints zero if one of the following conditions apply:
- there is an emergency indicated by the remote control
- there is an emergency indicated by the remote switch held by a safety officer.
- the remote control is out of range

- a communication error exists in the CAN communication. This happens when not all modules are communicating.

5.3.11   WheelSpeedControl and WheelAngleControl

Wheel speed control is done by one PI controller per wheel. Wheel angle control is done by a P controller combined with a Smith predictor to compensate for time delays. This is described more extensively in Bakker et al. (2008c).

5.3.12   OperateHitch

OperateHitch switches the hitch position between a minimum hitch height if the ActInMidField indicates that the actuator is in the main field area and maximum hitch height if the actuator is not in the main field area. Controlling the hitch height is done with a simple on/off control.

5.3.13   OperateLamp

OperateLamp switches the different lamps of the lampstack on and off. The five different lamps show if FollowHeadlandPath is suppressed, if the remote control Emergency button is pressed, if the GPS receiver has an accurate position, and if the robot is in manual control mode or in autonomous mode.

5.4   Results

5.4.1   Initial parameters

Figure 5.2 shows the a priori information of the field as measured before the experiment, consisting of the corners of the field and headland boundaries and the begin and endpoints of some row locations.
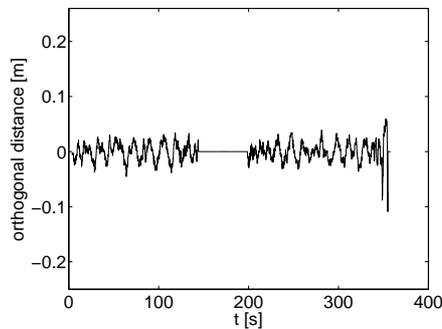
Figure 5.5: Orthogonal distance of the actuator position to the path during path following over AB from t = 4 s to t = 144 s and CD from t =199 s to t = 355 s.
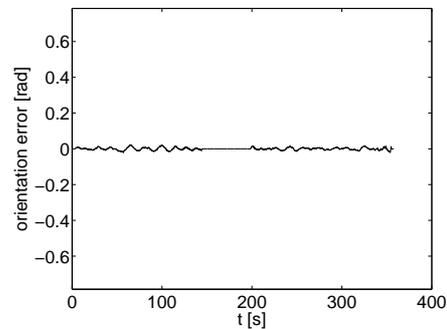
Figure 5.6: Actuator orientation error during path following over AB from t = 4 s to t =144 s and CD from t = 199 s to t = 355 s.

5.4.2 Path following along crop rows

Figures 5.5 and 5.6 show the performance of the path following along the first and the second path. From t=4 s to t=144 s the robot drives along the line A-B. The standard deviation, mean, minimum and maximum orthogonal distance of the actuator to the path are 1.6, 0.1, -4.5 and 3.4 cm respectively. Between t=144 s and t=199 s the robot is turning at the headland, so the FollowPath behavior is not released. From t=199 s to 355 s the robot drives along the line CD. The standard deviation, mean, minimum and maximum orthogonal distance of the actuator to the path are 1.8, 0.00, -10.9, and 6.0 cm respectively. The figure shows relatively large orthogonal offset when the actuator is near the end of the path CD. This is possibly due to roll caused by the bumpier headland, because here the actuator is near the end of the path and the robot wheels are already on the headland. If these last measurements are excluded the standard deviation, mean, minimum and maximum orthogonal distance over t=199 to t=340 are 1.4, 0, -3.6 and 3.9 cm respectively, which is comparable to the values from the first path. Figure 5.6 shows the orientation of the actuator relative to the path. The standard deviation, mean, minimum and maximum of the orientation error are 0.008, 0.000, -0.022 and 0.023 rad from t=4 s to t=144 s and 0.007, 0.000, -0.021 and 0.017 from t=199 to t=355 s. The accuracy is very good and RTK-DGPS based path following is very suitable for situations in which the crop rows are known from previous treatments like sowing.
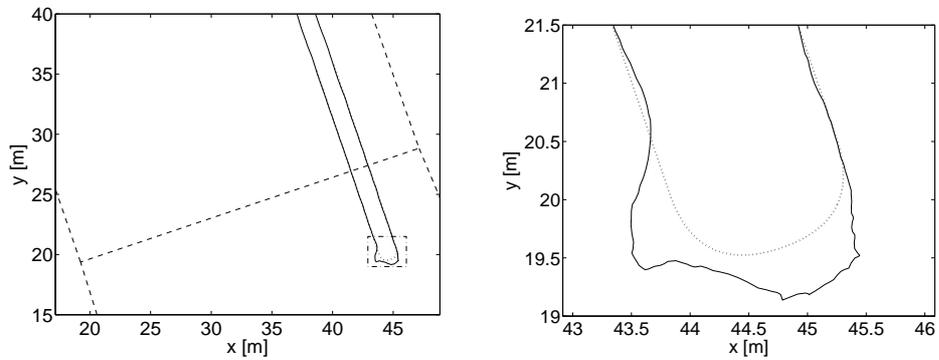
Figure 5.7: Actuator route (—) and path (···) during headland path following over BC. Part of the left figure indicated by the box (·-·) in the left figure is displayed enlarged in the right figure.
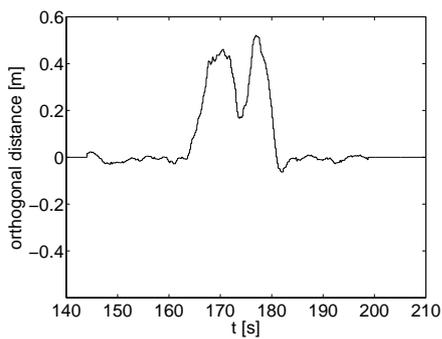
Figure 5.8: Orthogonal distance of the actuator position to the headland path during headland path following over BC
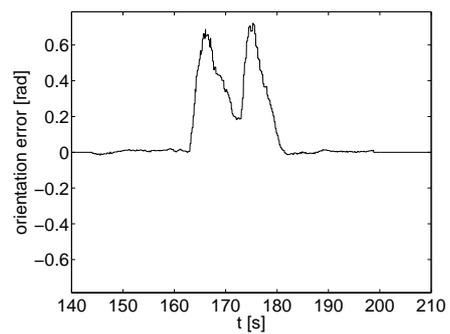
Figure 5.9: Actuator orientation error during headland path following over BC.

5.4.3   Path following on the headland

Figure 5.7 shows the headland path generated while following the path and the driven route. The realtime generated headland path is in line with the position of the crop row and also with the driven route.

Figures 5.8 and 5.9 show the orthogonal distance to the headland path and the orientation error while following the headland path. At the start of the headland path following at t=144.1 the orthogonal distance is 1.7 cm and the orientation error is 0.00 rad while the last orthogonal distance of the actuator from the path AB at that time was 2.1 cm and the orientation error -0.01 rad, thus indicating
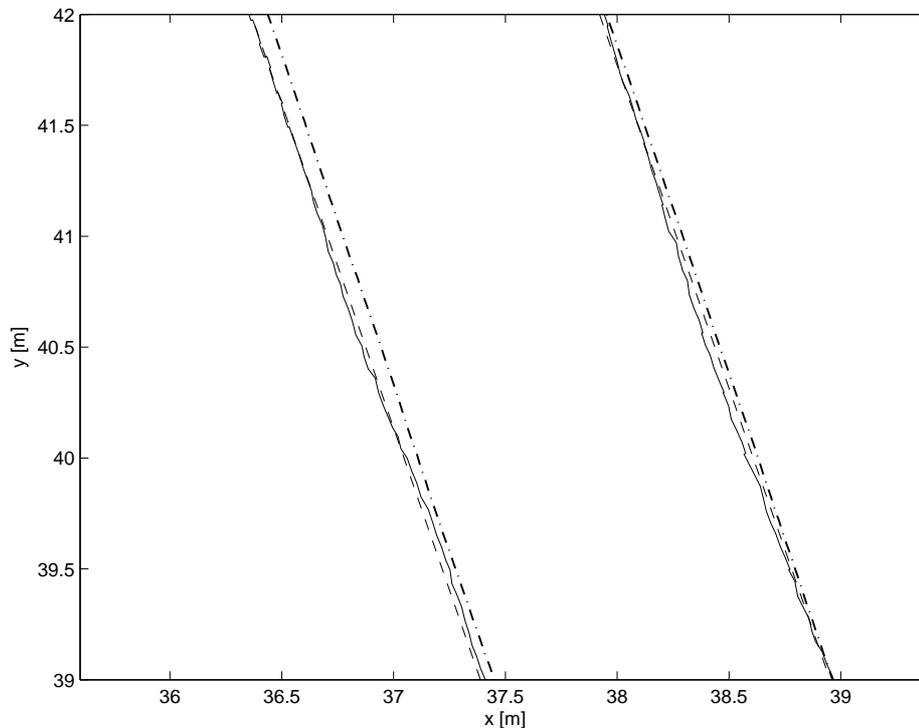
Figure 5.10: Path (- - -), driven route measured with GPS (—) and mapped rows (· - ·) in the field.

that the transition from path following to headland path following goes smoothly. The maximum orthogonal distance and the maximum orientation error during the turn are respectively 52 cm and 0.72 rad. This headland path with such a limited radius can not be realized by the robot controller due to the constraints on the wheel angles. However, on the headland it is less important to follow the headland path exactly than to arrive in front of the proper crop rows again. After the sharp turn in the headland path, the errors are reduced very soon and when the actuator leaves the headland at t=209 seconds, the orthogonal distance and the orientation error of the actuator to the crop row path are only 0.1 cm and 0.00 rad respectively.

5.4.4 Crop row mapping

Currently in most situations in practice no accurate absolute crop row location information is available to be used for guidance of a weeding robot like demonstrated
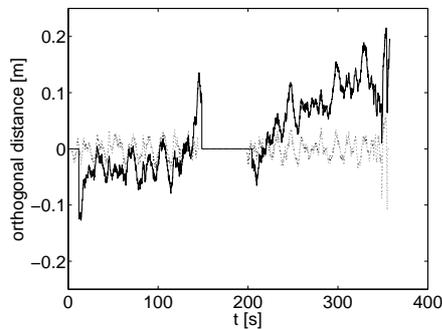
Figure 5.11: Orthogonal distance of the actuator position to the crop row as measured by the vision system (—) and to the path ($\cdots$) during path following over AB from $t = 4$ s to $t = 144$ s and CD from t=199 s to t=355 s.
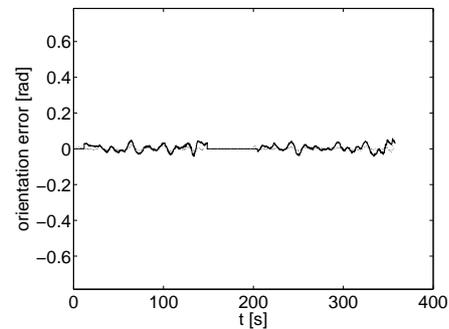
Figure 5.12: Actuator orientation error to the crop row as measured by the vision system (—) and to the path ($\cdots$) during path following over AB from $t = 4$ s to t=144 s and CD from $t = 199$ s to $t = 355$ s.

in the previous sections. So our original idea was to follow crop rows by camera alone, and to combine this with the headland path following as described in paragraph 5.4.3. However, currently the robot can follow the crop rows based on camera alone, but only with a constant offset of about 25 cm that has not been explained thus far. Therefore it was decided to first just map the crop rows with the camera and GPS, and compare the orthogonal distances and orientation errors with those from path following, which is done in this section. The hybrid deliberate software architecture permits this comparison by a mission that releases the behaviors FollowPath, FollowHeadlandPath and FollowRow, but that suppresses permanently the outputs of FollowRow. Figure 5.10 shows the surveyed crop rows, the driven route and the mapped crop rows on the field. In figures 5.11 and 5.12 the orthogonal distance and the orientation error of the actuator to both path and the crop rows as reconstructed by the vision system are shown. The error to the path and the errors to the crop rows do not match exactly, this could be explained by the fact that the path and the crop rows are not located at exactly the same position. The used path is a straight line in between two surveyed positions, but in agriculture a row is never an exact straight line. In case a RTK-DGPS-based steered tractor is used during sowing the rows can be quite straight, but in our case the tractor was steered manually. During following path AB, path and mapped row are quite close. During following path CD the error to the crop row increases. This is probably caused by not exactly positioning point D above the crop row. The orthogonal distances measured by the crop row following at the start and end of each crop row

103

are larger than in the middle part. As described in paragraph 5.3.5, all row positions within a distance of 1.5 meter from the actuator position are used for estimating the row position, but at the start the number of row positions used will be limited and the average distance of the actuator to the positions used will be larger until the actuator passes the front of the first image taken by a distance larger than 1.5 meter. This could explain the larger orthogonal distance. After this the orthogonal error is reduced because the number of measured row positions being used for row location estimation has increased and stays more or less constant because of the constant driving speed and also the average distance of the row positions from the actuator position will be about constant. At the end of the row, if the actuator is closer than 1.5 meter from the rear border of the last image taken before entering the headland, the quality of the row location estimation reduces again. This is because the number of positions used for crop row estimation reduces and the average distance of these positions to the actuator position increases from here. This possibly results in a less accurate row location estimation and by that in a larger orthogonal distance. So while there are differences when comparing the orthogonal distances of path following and crop row following, those could still be explained. The row detection works quite well and shows good perspective for guidance.

5.5   Discussion

The standard deviation, mean, minimum and maximum orthogonal distance of the actuator to the path while following a straight crop row on the field with RTK-DGPS of 1.6, 0.1, -4.5 and 3.4 cm respectively are very good results. But it should be kept in mind that the position of the actuator is calculated from the antenna positions that are located about 2 m above the soil surface, and is not corrected for roll. In this case the even soil surface did not cause any problems, but to be able to navigate so precise under bumpier conditions, roll compensation will be required.

The results showed that at the moment the actuator left the headland path, it was located almost exactly in line with the new row. However, there could be a bigger offset in practice when the seeder tramlines are not exactly one working width apart. But even if there is a small mismatch between the end of the headland path and the new crop row, the actuator is expected to arrive very well in line with the new row, because the actuator position starts to be controlled based on feedback from the camera vision system starting already when the field of view of the camera has left the headland. It then takes about the robot length to drive forward before the

actuator leaves the headland, which will be enough time to control the actuator position very well in line with the crop row.

The hybrid deliberate approach is very helpful, especially because this clear architecture helps in neatly organizing the software, but even more because it enables separate testing of the different behaviors: the path following behavior controlled the vehicle while the suppressed crop row following behavior was tested. The constellation of behavior to get a total behavior for the application of a weeding robot can be described easily with a simple table. With this architecture the functionality of the robot is easily extendible by just adding new behaviors and some small changes to the deliberate and sequencer layer.

More complexity is in the perception of the orthogonal distance and orientation error of the implement to the row. Crop row location data filtering is needed to handle variability of the output of the crop row detection when we want to guide the implement position along the crop row.

5.6 Conclusion

The autonomous field navigation system is a practical method for RTK-DGPS based autonomous navigation in a field requiring limited a priori information: the field boundary, the headland boundaries, the row locations and the turning direction at the first headland to arrive at.

The autonomous navigation system enabled the robot to navigate autonomously on a field based on RTK-DGPS. Standard deviation, mean, minimum and maximum orthogonal distance of the actuator to the path while following a straight crop row on the field with RTK-DGPS at a speed of 0.3 m/s are respectively 1.6, 0.1, -4.5 and 3.4 cm. Standard deviation, mean, minimum and maximum of the orientation error over the same distance are 0.008, 0.000, -0.022 and 0.023 rad.

Further improvements in accuracy of path following of a straight path are not to be expected, because of the standard deviation of 1.6 cm is about equal to the RTK-DGPS accuracy. The point-in-polygon algorithm proved to be a suitable method for detection in which part of the field given coordinates like the actuator position or the field of view of the camera are located. With the spline based algorithm a smooth headland path is generated in realtime that nicely connects the subsequent paths along the crop.

The crop row mapping shows results with good perspective for guidance of the robot.

It has been shown that it is possible to apply the hybrid deliberate architecture with a behavior based reactive layer for the case of autonomous weeding. The experienced benefits are that behaviors can be tested separately, that the architecture of the software is very transparent and that the software is easily extendible.

Further research should focus on roll compensation of the position measurement for navigation under bumpier conditions, on equipping the robot with hoes to demonstrate autonomous hoeing of a field and on further developing the crop row following using vision to enable autonomous navigation independent of the availability of a priori information of the crop rows.

Chapter 6

Conclusions and Perspectives

6.1 Conclusions

The autonomous weeder robot platform was designed using a structured design method. The advantage of using this method is that it clearly structures the design process. It provides a good overview of the complete design and because of the structured sequence of design activities, it is easy to keep track of the progress of design. Another advantage of the structured design method is that it forces the designer to look at alternative solutions and this decreases the probability of heuristic bias and increases the quality of the outcome. Although the designer is forced to thoroughly judge the identified alternative solutions when selecting the final concept, the outcome is still depending on the available knowledge of the designer about the alternative solutions. So, while the method can not guarantee that the absolute best solution possible will be selected, it certainly limits trial and error. In a research context it is easy to identify alternative subjects that are worthwhile to investigate further, while at the same time the main line of the research remains clear.

The chosen design concept identifies working principles for the required functionality to obtain the original objective: to replace hand weeding on a field. A number of these working principles are worked out based on existing knowledge of proven technology: It resulted in a versatile research platform with a diesel engine, hydraulic transmission, four wheel drive and 360 degrees four wheel steering.

The identified navigation related principle solutions were worked out by means of research to:

- A method for row detection for navigation along the row (Chapter 3).
- A control design for path following with the four-wheel steered robot platform (Chapter 4).
- A system that integrated the navigation related principle solutions in a navigation system that enabled the robot to navigate autonomously in a field (Chapter 5).

The vision based row detection method was able to detect crop rows in images made at different growth stages with a median error of 22 mm. Errors at the high end of the distribution corresponded to situations with limited number of crop plants and small size of crop plants, overexposure of the camera, green algae and high weed density. It is expected that these conditions are not a problem in practice or can be compensated for by choosing the right camera settings. Two measurement series that did not suffer from these error sources had mean errors of 5 and 11 mm, with standard deviations of 6 and 11 mm.

It does not make much difference which of the investigated methods is used to transform the RGB images to grey-scale images. If the optimum threshold combination is used, the mean minimum error is similar for the different image transformation methods. Therefore the most simple method i.e. using directly the RGB values from the camera, can be recommended. The merging of three crop rows to limit the image size while keeping the information of three rows was successful in creating an enhanced crop row signature that could be located using grey-scale Hough transform. The only a-priori information needed from the field is the row spacing. The image processing time varied from 0.5 to 1.3 seconds per image. That means the proposed row detection method now is sufficient for finding row crops at speeds typical for intra-row weeding operations, i.e. in the range of 0.5-1 m/s. Inaccuracies created by footprints indicate that linear structures in the soil surface like tracks of agricultural machinery in a real field might create problems which should be considered in additional investigations.

The developed path following control of the four-wheel steered robot platform consists of two levels. At high level the wheel angle setpoints and wheel speed setpoints are determined in order to decrease the deviation from the path and to decrease the error in orientation. At low level, controllers are used to realize the wheel angles and wheel speeds determined by the high level control. The proportional controller combined with a Smith predictor used for low level wheel angle control compensates well for time-delays in the electro-hydraulic steering system in practice.

The high level control method for four wheel steered vehicles presented in this thesis has a number of attractive features:
- Enables control of a user definable position relative to the robot frame which usually is the position of the implement.
- Can deal with limitations on the wheel angles.
- Has a good performance as shown in step responses made in a hardware in the loop fashion, on a paving and by following a typical headland path.

The method is very well practically applicable for a manufacturer:
- The estimation of the delay time that is needed for both the design of the low and high level control can be determined from a step response at the factory, for the high level control possibly to increase with the time delay of the GPS.
- The model inversion is very generic. It requires only some dimensions of the robot and its wheels. These are all parameters that are known by the manufacturer. The inversion of the vehicle model (the only complex part) could therefore be supplied as a generic software module.

109

- The user supplies the desired forward speed v and the desired parameter τ_c^*, where τ_c^* has an easy interpretable meaning: it is the driven distance along the path where the deviation, caused by a step shaped disturbance from the path, has decreased by 63%. The method adapted from Skogestad (2003) determines then the controller settings and even suggests a default value for τ_c^*.

In contrast to expectations based on theory that P control should be sufficient, as both the processes for the orientation θ and the orthogonal distance y act as pure integrators, proportional-integral (PI) control is needed to overcome small inaccuracies of the low level system.

The refined tuning method adapted from Skogestad (2003) calculates controller settings that let the robot drive indpendent of the speed v as much as possible along the same path to its setpoint, but also limit the gains at higher speeds to prevent the closed loop system to become unstable due to the time delay in the process.

Mean, minimum and maximum orthogonal distance errors while following a straight path on a paving at a speed of 0.5 m/s are 0.0 -2.4 and 3.0 cm respectively and the standard deviation is 1.2 cm. Further improvements in accuracy of path following of a straight path are not to be expected, because of the standard deviation of 1.2 cm is about equal to the RTK-DGPS accuracy. The mean orientation error is 0.000 rad, the minimum and maximum are -0.017 and 0.014 rad respectively, and the standard deviation is 0.006 rad.

A guidance system was proposed and tested that enables the robot to navigate autonomously on a field based on RTK-DGPS using the field boundary, the headland boundaries, the row locations and the turning direction at the first headland as preliminary information. The point in polygon algorithm proved to be a suitable method for detection in which part of the field given coordinates like the actuator position or the field of view of the camera are located. With the spline based algorithm a smooth headland path is generated in realtime that nicely connects the subsequent paths along the crop.

Standard deviation, mean, minimum and maximum orthogonal distance of the actuator to the path while following a straight crop row on the field with RTK-DGPS at a speed of 0.3 m/s are respectively 1.6, 0.1, -4.5 and 3.4 cm. Further improvements in accuracy of path following of a straight path are not to be expected, because of the standard deviation of 1.6 cm is about equal to the RTK-DGPS accuracy. The standard deviation, mean, minimum and maximum of the

orientation error were 0.008, 0.000, -0.022 and 0.023 rad. The found values are slightly bigger then the values obtained at the more even pavement. The influence of the evenness of the soil surface becomes even more clear from the larger orthogonal distances (minimum and maximum of -10.9 cm and 6.0 cm respectively) when the robot wheels have arrived at the bumpier headland. This unevenness is not yet compensated for like could be done by measuring the roll.

The crop row mapping from the camera shows results with good perspective for guidance of the robot.

It has been shown that it is possible to apply the hybrid deliberate architecture with a behavior based reactive layer for the case of autonomous weeding. The experienced benefits are that behaviors can be tested separately, that the architecture of the software is very clear and that the software is easily extendable.

6.2 Perspectives

To finally obtain the objective of replacing manual weeding in organic farming by a device operating autonomously at field level the open issues in the concept design need to be worked out further. That means that the robotic platform needs to integrate the working principles for functions like automatic weed detection and weed removal, information exchange with a remote user and for detection of unsafe situations. Recently, more detailed studies of the performance of potential weeding mechanisms have been performed already and resulted in a patent (Bakker, 2007b). That the robotic platform can operate with an implement has been shown in a separate study, commissioned by the Dutch road agency (Rijkswaterstaat). In that study it was demonstrated in practice that it is possible to clear the edges of a parking place along a highway, with a brush, where the coordinates of the edges were provided from a GIS database of the Rijkswaterstaat (Bakker et al., 2007c). Also status information exchange with a remote user and detection of unsafe situations are open issues in the concept design needing a further workout. The proposed system for detection of obstacles is a non-contact detection system detecting above canopy level. This is expected to be implementable with sensors currently on the market like e.g. ultrasonic sensors and laser scanners. A concept of the detection system has already been designed (Martinet, 2005).

In this research autonomous field navigation keeping into account field boundaries is performed by using GPS. The fact that GPS calculates its own measure of accuracy, makes it the preferred choice to use for autonomous navigation considering the

current status of machine vision. However, a disadvantage of using GPS based guidance compared to a machine vision approach is still the need for known row locations in terms of absolute positions. Future work should consider robustly estimating the current quality of the image processing result. Integrating other sensors in a state estimation approach might be required to gain acceptable robustness for autonomous camera based crop row following under a broad set of conditions.

In order to gain the obtained accuracy for RTK-DGPS based navigation of the field experiments also under bumpier conditions, roll compensation of the position measurement would be required. This could be done by measuring the height difference of two GPS antenna's or by integrating sensor information of e.g. accelerometers and gyroscopes (Trimble, 2008b) in a Kalman Filter. RTK-DGPS based navigation can also be improved in terms of robustness: obstruction of the GPS signal over a limited time could be overcome by integrating information of other sensors for reliable estimation of the vehicle's state. Kalman filtering is an appealing method to apply (Van Bergeijk et al., 1998; Stentz et al., 2002).

Reliable functioning of the actuator is barely examined. If full autonomy replaces the driver completely, also his 'looking back over the shoulder' should be automated. This means some way of feedback on the quality of the work or on the left behind status of the crop is needed.

Another function of the driver - maintaining safety - is maybe the technical most challenging issue on the way to full autonomy. However, for practical application of fully autonomous robotic weeders one could also argue for a non-technical solution: just equipping the system with simple security systems like bumper switches that are available now, and accepting the system is unsafe to some extent. While this may feel uncomfortable, one should keep in mind that situations that are unsafe to a certain extend are accepted in a lot of occasions. Also with manually driven vehicles safety is not hundred percent due to for example blind spots, obstacles outside view or inattention of a driver. Also for example in greenhouse horticulture automatic guided vehicles with limited safety measures like ultrasonic sensors and bumper switches at the front following a buried cable are used (Brinkman, 2008; Bogaerts, 2008). Looking from a technical perspective, there are currently no solutions that just guarantee safety of autonomous machinery. The most practical trajectory to full autonomy, not neglecting safety, is probably explained by Stentz et al. (2002). They sketch a scenario in which the autonomous machine is supervised by a human operator, where the autonomous machine is not in view of the operator. The machine itself notifies the operator if it detects a possible unsafe situation, and the

operator can inform the machine if this is really the case or not by checking the situation with remote vision. This concept can be seen as a form of teleoperation, meaning that in contrast to remote controlled systems, the operator can not see directly what the autonomous machine is doing (Murphy, 2000). The extent to which the system can guarantee that every unsafe situation is detected and the relative number of faulty calls upon the operator, will determine the performance and therewith the success of such a system. Improving this performance is an important issue for further research.

References

Ansorge, D., Godwin, R. J., 2007. The effect of tyres and a rubber track at high axle loads on soil compaction, part 1: Single axle-studies. Biosystems Engineering 98 (1), 115–126.

Arkin, R., 1998. Behavior-Based Robotics. The MIT Press, Cambridge, USA.

Ascard, J., 1995. Effects of flame weeding on weed species at different developmental stages. Weed Research 35 (5), 397–411.

Ascard, J., 1998. Comparison of flaming and infrared radiation techniques for thermal weed control. Weed Research 38 (1), 69–76.

Åstrand, B., 2005. Vision based perception for mechatronic weed control. Ph.D. thesis, Chalmers University of Technology, Göteborg, Sweden.

Åstrand, B., Baerveldt, A. J., 2002. An agricultural mobile robot with vision-based perception for mechanical weed control. Autonomous Robots 13 (1), 21–35.

Åstrand, B., Baerveldt, A. J., 2004. Plant recognition and localization using context information. In: IEEE Conference Mechatronics and Robotics 2004. Aachen, Germany, pp. 1191–1196.

Bak, T., Jakobsen, H., 2004. Agricultural robotic platform with four wheel steering for weed detection. Biosystems Engineering 87 (2), 125–136.

Bakker, T., 2007b. Wiedinrichting. Patent application number: NL2001003, Submitted: 2007-11-13. Assingee: Wageningen University.

Bakker, T., Van Asselt, C. J., Bontsema, J., Müller, J., Van Straten, G., 2007a. Path following with a robotic platform. In: Agricontrol 2007. 2nd IFAC International Conference on Modeling and Design of Control Systems in Agriculture. Osijek Croatia, pp. 153–158.

Bakker, T., Van Asselt, C. J., Bontsema, J., Müller, J., Van Straten, G., 2008b. Systematic design of an autonomous platform for robotic weeding. Journal of Terramechanics. Accepted for publication. Chapter 2 of this thesis.

Bakker, T., Van Asselt, C. J., Bontsema, J., Müller, J., Van Straten, G., 2008c. Path following with a robotic platform. Autonomous Robots. Submitted for publication. Chapter 4 of this thesis.

Bakker, T., Van Asselt, C. J., Van Straten, G., 2007c. Robotiseren van het dagelijks onderhoud aan wegen via geo-informatie. SCO Report 07-01, Wageningen.

Bakker, T., Van Bergeijk, J., Biesenbeek, S., Van der Bijl, M., Dhaene, M., Govers, M., Jansen, R., Knol, J., Kroon, B., Speetjens, B., 2006. First universal wheel unit for field robots - poster. In: Field Robot Event 2006. Hohenheim, Germany.

Bakker, T., Wouters, H., Van Asselt, K., Bontsema, J., Tang, L., Müller, J., Van Straten, G., 2008a. A vision based row detection system for sugar beet. Computers and Electronics in Agriculture. 60 (1), 87–95, chapter 3 of this thesis.

Bell, T., 1999. Precision robotic control of agricultural vehicles on realistic farm trajectories. Ph.D. thesis, Stanford University.

Bendtsen, J., Andersen, P., Pedersen, S., 2002. Robust feedback linearisation-based control design for a wheeled mobile robot. In: 6th International Symposium on Advanced Vehicle Control (AVEC '02). Hiroshima, Japan.

Billingsley, J., Schoenfisch, M., 1997. The successful development of a vision guidance system for agriculture. Computers and Electronics in Agriculture 16 (2), 147–163.

Blackmore, S., Fountas, S., Vougioukas, S., Tang, L., Sorensen, C., Jorgensen, R., 2007. Decomposition of agricultural tasks into robotic behaviors. Agricultural Engineering International: the CIGR Ejournal. Manuscript PM 07 006. Vol. IX.

Blackmore, S., Stout, B., Wang, M., Runov, B., 2005. Robotics agriculture - the future of agricultural mechanization? In: Stafford, J. (Ed.), 5th European Conference on Precision Agriculture. Wageningen Academic Publishers, Uppsala, Sweden, pp. 621–628.

Blasco, J., Aleixos, N., Roger, J. M., Rabatel, G., Molto, E., 2002. Robotic weed control using machine vision. Biosystems Engineering 83 (2), 149–157.

Bogaerts, 2008. Electrotrekker "Powerbee". Retrieved 2008-11-5, from: http://www.bogaertsgl.nl/powerbeefolder.pdf.

Bontsema, J., Asselt, C., Lempens, P., Straten, G. v., 1998. Intra-row weed control: a mechatronics approach. In: 1st IFAC Workshop on Control Applications and Ergonomics in Agriculture. Athens, Greece, pp. 93–97.

Bontsema, J., Asselt, C., Vermeulen, G., 2003. Intrarijwieden bij geplante bieslook. evaluatie van het plantherkenningssysteem. Report 016, Wageningen, The Netherlands.

Brinkman, 2008. Robocar. Retrieved 2008-11-5, from: http://www.brinkman.nl/pdf/Transportmiddelen/Robocar.pdf.

116

Bruggen, H. P., 2001. Mechanische onkruidbestrijding in de rij bij uien; veldmetingen en ontwikkeling van een simulatieprogramma. MSc thesis, Wageningen University, Wageningen.

Burrough, P., MacDonnell, R., 1998. Principles of Geographical Information Systems. Oxford University Press.

Campion, G., Bastin, G., D'Andréa-Novel, B., 1996. Structural properties and classification of kinematic and dynamic models of wheeled mobile robots. IEEE Transactions on Robotics and Automation 12 (1), 47–62.

Darr, M. J., Stombaugh, T. S., Shearer, S. A., 2005. Controller area network based distributed control for autonomous vehicles. Transactions of the American Society of Agricultural Engineers 48 (2), 479–490.

Garford, 2008. Robocrop inrow - the revolutionary robotic weeder! Retrieved 2008-11-05, from: http://www.garford.com/inrow.html.

Ge, J., Ayers, P. D., 1991. Design of controllers for nonlinear electrohydraulic systems with time delays. Transactions of the ASAE 34 (3), 1016–1022.

Gerhards, R., Christensen, S., 2003. Real-time weed detection, decision making and patch spraying in maize, sugarbeet, winter wheat and winter barley. Weed Research 43 (6), 385–392.

Gerhards, R., Sökefeld, M., 2001. Sensor systems for automatic weed detection. In: The BCPC Conference - Weeds 2001.

Gerrish, J. B., Fehr, B. W., Van Ee, G. R., Welch, D. P., 1997. Self-steering tractor guided by computer-vision. Applied Engineering in Agriculture 13 (5), 559–563.

Gobor, Z., 2007. Development of a novel mechatronic system for mechanical weed control of the intra-row area in row crops based on detection of single plants and adequate controlling of the hoeing tool in real-time. Ph.D. thesis, Rheinischen Firedrich-Wilhelms-Universität Bonn, Bonn, Germany.

Gobor, Z., Schulze Lammers, P., 2006. Concept and virtual prototype of a rotary hoe for intra-row weed control in row crops. In: XVI CIGR World Congress - Agricultural Engineering for a Better World. Bonn, Germany, pp. 323–324.

Gray, K., 2002. Obstacle detection technology. In: Zhang, Q. (Ed.), 2002 ASAE Conference. Automation technology for off-road equipment. ASAE, Chicago, Illinois, pp. 405–411.

Griepentrog, H. W., Nørremark, M., Nielsen, H., Blackmore, B. S., 2005. Seed mapping of sugar beet. Precision Agriculture 6 (2), 157–165.

Grovum, M. A., Zoerb, G. C., 1970. Automatic guidance system for farm tractors. Transactions of the American Society of Agricultural Engineers 13 (5).

Hague, T., Tillett, N. D., 1996. Navigation and control of an autonomous horticultural robot. Mechatronics 6 (2), 165–180.

Hague, T., Tillett, N. D., 2001. A bandpass filter-based approach to crop row location and tracking. Mechatronics 11 (1), 1–12.

Hansson, D., Ascard, J., 2002. Influence of developmental stage and time of assessment on hot water weed control. Weed Research 42 (4), 307–316.

Harries, G. O., Ambler, B., 1981. Automatic ploughing: A tractor guidance system using opto-electronic remote sensing techniques and a microprocessor based controller. Journal of Agricultural Engineering Research 26 (1), 33–53.

Heisel, T., Schou, J., Andreasen, C., Christensen, S., 2002. Using laser to measure stem thickness and cut weed stems. Weed Research 42 (3), 242–248.

Hofstee, J. W., Jansen, R., Nieuwenhuizen, A., Govers, M. H. A. M., Blaauw, S. K., Van Willigenburg, L. G., Stigter, J. D., Bakker, T., Van Asselt, C. J., Van Straten, G., Speetjens, S. L., 2007. WURking - an autonomous robot for agriculture applications. In: Proceedings of the 5th Field Robot Event 2007. Farm Technology Group, Wageningen, The Netherlands.

Home, M., 2003. An investigation into the design of cultivation systems for inter- and intra-row weed control. Ph.D. thesis, Cranfield University, United Kingdom.

Jensen, L., Thysen, I., 2003. Agricultural information and decision support by SMS. In: EFITA 2003 Conference. Debrecen, Hungary, pp. 286–292.

Jørgensen, R., Sørensen, C., Pedersen, J., Havn, I., Jensen, K., Søgaard, H., Sørensen, L., 2006. Hortibot: a system design of a robotic tool carrier for high-tech plant nursing. In: Rothmund, M., Ehrl, M., Auernhammer, H. (Eds.), Automation technology for Off-Road Equipment 2006. Landtechnik Weihenstephan, Bonn, Germany, pp. 13–21.

Kielhorn, A., Dzinaj, T., Gelze, F., Grimm, J., Kleine-hartlage, H., Kleine-Horstkamp, S., Kuntze, W., Linz, A., Naescher, J., Nardmann, M., Ruckelshausen, A., Trautz, D., Wisserodt, E., 2000. Beikrautregulierung in reihenkulturen - sensorgesteurte querhacke im mais. Zeitschrift für Pflanzenkrankheiten und Pflanzenschutz, Sonderheft XX.

Kirk, T. G., Zoerb, G. C., Wilson, J. N., 1976. Furrow - following tractor guidance system. Paper 76-001. American Society of Agricultural Engineers, St. Joseph, MI.

Kise, M., Noguchi, N., Ishii, K., Terao, H., 2002. Enhancement of turning accuracy by path planning of robot tractor. In: Zhang, Q. (Ed.), Automation Technology for Off-Road Equipment. Chicago, Illinois, USA, pp. 398–404.

Kok, J. P. B., Bakker, T., Lokhorst, C., 2003. Programma van eisen voor een intelligente autonome wieder. Report, Instituut voor Milieu- en Agritechniek (IMAG), Wageningen, The Netherlands.

Kurstjens, D. A. G., 1998. Overzicht van mechanische en fysische technologie voor onkruidbestrijding. Rapport 98-03, Instituut voor Milieu- en Agritechniek (IMAG), Wageningen, The Netherlands.

Lamm, R. D., Slaughter, D. C., Giles, D. K., 2002. Precision weed control system for cotton. Transactions of the ASAE 45 (1), 231–238.

Leemans, V., Destain, M. F., 2006. Application of the Hough transform for seed row localisation using machine vision. Biosystems Engineering 94 (3), 325–336.

Linker, R., Blass, T., 2008. Path-planning algorithm for vehicles operating in orchards. Biosystems Engineering 101 (2), 152–160.

Lo, R. C., Tsai, W. H., 1995. Gray-scale hough transform for thick line detection in gray-scale images. Pattern Recognition 28 (5), 647–661.

Lütkemeyer, L., 2000. Hydropneumatical weedkilling in crop rows. Zeitschrift Für Pflanzenkrankheiten Und Pflanzenschutz-Journal of Plant Diseases and Protection, 661–666Sp. Iss. 17.

Manduchi, R., Castano, A., Talukder, A., Matthies, L., 2005. Obstacle detection and terrain classification for autonomous off-road navigation. Autonomous Robots 18 (1), 81–102.

Manor, G., 1995. Automatic field machine technology. Journal of Terramechanics 32 (2), 79–90.

Marchant, J., Brivot, R., 1995. Real-time tracking of plant rows using a Hough transform. Real-Time Imaging 1 (5), 363–371.

Marchant, J. A., 1996. Tracking of row structure in three crops using image analysis. Computers and Electronics in Agriculture 15 (2), 161–179.

Martinet, A. E. B., 2005. Detection of unsafe situations using an autonomous vehicle. MSc thesis, Wageningen University, Wageningen, The Netherlands.

Mathiassen, S. K., Bak, T., Christensen, S., Kudsk, P., 2006. The effect of laser treatment as a weed control method. Biosystems Engineering 95 (4), 497–505.

Murphy, R., 2000. Introduction to AI Robotics. The MIT Press, Cambridge, USA.

Nagasaka, Y., Umeda, N., Kanetai, Y., Taniwaki, K., Sasaki, Y., 2004. Autonomous guidance for rice transplanting using global positioning and gyroscopes. Computers and Electronics in Agriculture 43 (3), 223–234.

Nieuwenhuizen, A. T., Tang, L., Hofstee, J., Müller, J., Van Henten, E., 2007. Colour based detection of volunteer potatoes as weeds in sugar beet fields using machine vision. Precision agriculture 8 (6), 267–278.

Noguchi, N., Reid, J., Zhang, Q., Will, J., Ishii, K., 2001a. Development of robot tractor based on RTK-GPS and gyroscope. In: Proceedings of the 2001 ASAE Annual International Meeting. ASAE paper 01-1195.

Noguchi, N., Reid, J. F., Zhang, Q., Will, J., 2001b. Turning function for robot tractor based on spline function. In: Proceedings of the 2001 ASAE Annual International Meeting. Sacramento, California, USA.

Nybrant, T., 1991. Automatic guidance of farm vehicles. In: IFAC Mathemetical and Control Applications in Agriculture and Horticulture, Matsuyama, Japan 1991. pp. 219–223.

O'Connor, M., 1997. Carrier-phase differential GPS for automatic control of land vehicles. Ph.D. thesis, Stanford University.

O'Dogherty, M. J., Godwin, R. J., Dedousis, A. P., Brighton, J. L., Tillett, N. D., 2007. A mathematical model of the kinematics of a rotating disc for inter- and intra-row hoeing. Biosystems Engineering 96 (2), 169–179.

Oksanen, T., 2007. Path planning algorithms for agricultural field machines. Ph.D. thesis, Helsinki University of Technology, Helsinki, Finland.

Orebäck, A., Christensen, H. I., 2003. Evaluation of architectures for mobile robotics. Autonomous Robots 14 (1), 33–49.

Parish, R. L., Goering, C. E., 1970. Developing an automatic steering system for hydrostatic vehicle. Transactions of the American Society of Agricultural Engineers 13 (4), 523–527.

Philipp, I., Rath, T., 2002. Improving plant discrimination in image processing by use of different colour space transformations. Computers and Electronics in Agriculture 35 (1), 1–15.

Pilarski, T., Happold, M., Pangels, H., Ollis, M., Fitzpatrick, K., Stentz, A., 2002. The Demeter system for automated harvesting (Reprinted from Proceedings of the American Nuclear Society: 8th international topical meeting on robotics remote systems, Pittsburgh, PA, April 25-29, 1999.). Autonomous Robots 13 (1), 9–20.

Poulsen, F., 2008. Robotic intra-row weeding. Retrieved 2008-11-7, from: www.fp-engin.dk.

Reid, J. F., Searcy, S. W., 1988. Algorithm for separating guidance information from row crop images. Transactions of the American Society of Agricultural Engineers 31 (6), 1624–1632.

Reid, J. F., Zhang, Q., Noguchi, N., Dickson, M., 2000. Agricultural automatic guidance research in North America. Computers and Electronics in Agriculture 25 (1-2), 155–167.

Rekow, A. K. W., Ohlemeyer, H., 2007. Automated headland turns the next step in automated agricultural machines. In: Landtechnik - AgEng 2007. Vol. 2007. Hannover, Germany, pp. 199–209.

Roozenburg, N., Eekels, J., 2003. Productontwerpen, structuur en methoden, 2nd Edition. Lemma BV, Utrecht, The Netherlands.

SBG-Innovatie, 2008. SBGuidance - automatische besturing voor trekkers, zelfrijdende machines en werktuigen (automatic control for tractors, self-propelled machines and implements). Retrieved 2008-11-05, from: http://www.sbg.nl/folders/sbguidance-2006-11.pdf.

Searcy, S. W., Schueller, J. K., Bae, Y. H., Stout, B. A., 1990. Measurement of agricultural field location using microwave frequency triangulation. Computers and Electronics in Agriculture 4 (3), 209–223.

Skogestad, S., 2003. Simple analytic rules for model reduction and PID controller tuning. Journal of Process Control 13 (4), 291–309.

Slaughter, D. C., Chen, P., Curley, R., 1999. Vision guided precision cultivation. Precision Agriculture 1 (2), 199–216.

Slaughter, D. C., Giles, D. K., Downey, D., 2008. Autonomous robotic weed control systems: A review. Computers and Electronics in Agriculture 61 (1), 63–78.

Søgaard, H. T., Olsen, H. J., 2003. Determination of crop rows by image analysis without segmentation. Computers and Electronics in Agriculture 38 (2), 141–158.

Sørensen, C. G., Madsen, N. A., Jacobsen, B. H., 2005. Organic farming scenarios: Operational analysis and costs of implementing innovative technologies. Biosystems Engineering 91 (2), 127–137.

Sørensen, M., 2002. Modelling and control of wheeled farming robot. MSc thesis, Aalborg University, Aalborg, Denmark.

Stentz, A., Dima, C., Wellington, C., Herman, H., Stager, D., 2002. A system for semi-autonomous tractor operations. Autonomous Robots 13 (1), 87–104.

Stephanopoulos, G., 1984. Chemical process control. An Introduction to Theory and Practice. Prentice/Hall International, Inc., London.

Telle, M. G., Perdok, U. D., 1979. Field experiments with a leader cable tactor guidance. American Society of Agricultural Engineers.Paper no. 79-1069 Winnipeg, Canada.

Thoma, 2005. Dit is Automaatje (This is the "Automaatje" robot). Retrieved 2008-11-5, from: http://www.joz.nl/brochures/files/JOZ0005_def.pdf.

Thuilot, B., Cariou, C., Martinet, P., Berducat, M., 2002. Automatic guidance of a farm tractor relying on a single CP-DGPS. Autonomous Robots 13 (1), 53–71.

Tillett, N. D., 1991. Automatic guidance sensors for agricultural field machines:a review. Journal of Agricultural Engineering Research 50, 167–187.

Tillett, N. D., Hague, T., 1999. Computer-vision-based hoe guidance for cereals - an initial trial. Journal of Agricultural Engineering Research 74 (3), 225–236, article.

Tillett, N. D., Hague, T., 2006. Increasing work rate in vision guided precision banded operations. Biosystems Engineering 94 (4), 487–494.

Tillett, N. D., Hague, T., Grundy, A. C., Dedousis, A. P., 2008. Mechanical within-row weed control for transplanted crops using computer vision. Biosystems Engineering 99 (2), 171–178.

Tillett, N. D., Hague, T., Marchant, J. A., 1998. A robotic system for plant-scale husbandry. Journal of Agricultural Engineering Research 69 (2), 169–178.

Tillett, N. D., Hague, T., Miles, S. J., 2002. Inter-row vision guidance for mechanical weed control in sugar beet. Computers and Electronics in Agriculture 33 (3), 163–177.

Torrie, M., Cripps, D., Swensen, J., 2002. Joint architecture for unmanned ground systems (JAUGS) applied to autonomous agricultural vehicles. In: Zhang, Q. (Ed.), Automation Technology for Off-Road Equipment. Proceedings of the 2002 ASAE Conference. Chicago, Illinois, pp. 1–12.

Trimble, 2008a. Trimble precision agriculture. precision solutions for all seasons, all crops, all terrain, all vehicles - a growing investment. Retrieved 2008-11-8, from: http://trl.trimble.com/docushare/dsweb/Get/Document-376567/022503-078C-UK_Ag_Portfolio_BRO_0108_lr.pdf.

Trimble, 2008b. Trimble t2 and t3 technology. Retrieved 2008-11-5, from: http://trl.trimble.com/docushare/dsweb/Get/Document-264990/022503-104_T2_T3_FS_0905_AG_lr.pdf.

Tseng, C. L., Jiang, J. A., Lee, R. G., Lu, F. M., Ouyang, C. S., Chen, Y. S., Chang, C. H., 2006. Feasibility study on application of gsm-sms technology to field data acquisition. Computers and Electronics in Agriculture 53 (1), 45–59.

Van Bergeijk, J., Goense, D., Keesman, K. J., Speelman, L., 1998. Digital filters to integrate global positioning system and dead reckoning. Journal of Agricultural Engineering Research 70 (2), 135–143.

Van den Kroonenberg, H. H., Siers, F. J., 1998. Methodisch ontwerpen. Ontwerpmethoden, voorbeelden, cases, oefeningen, 2nd Edition. Educatieve Partners Nederland BV, Houten, The Netherlands.

Van der Schans, D., Bleeker, P., Molendijk, L., Plentinger, M., Van der Weide, R., Lotz, B., Bauermeister, R., Total, R., Baumann, D. T., 2006. Practical weed control in arable farming and outdoor vegetable cultivation without chemicals. Ppo publication no. 352, Wageningen UR, Applied Plant Research, Lelystad, The Netherlands.

Van der Weide, R., Lotz, L. A. P., Bleeker, P., Groeneveld, R. M. W., 2002. Het spanningsveld tussen beheren en beheersen van onkruiden op biologische bedrijven. In: Wijnands, F., Schroder, J., Sukkel, W., Booij, R. (Eds.), Themaboek 303. Biologisch bedrijf onder de loep. Wageningen Universiteit, Wageningen, pp. 129–138.

Van der Weide, R. Y., Bleeker, P. O., Achten, V. T. J. M., Lotz, L. A. P., Fogelberg, F., Melander, B., 2008. Innovation in mechanical weed control in crop rows. Weed Research 48 (3), 215–224.

Van Evert, F. K., Van Der Heijden, G. W. A. M., Lotz, L. A. P., Polder, G., Lamaker, A., De Jong, A., Kuyper, M. C., Groendijk, E. J. K., Neeteson, J. J., Van Der Zalm, T., 2006. A mobile field robot with vision-based detection of volunteer potato plants in a corn crop. Weed Technology 20 (4), 853–861.

Van Henten, E. J., Müller, J., 2007. The field robot event; an international design contest in agricultural engineering. In: Landtechnik - AgEng 2007. Vol. 2007. Hannover, Germany, pp. 169–174.

Van Henten, E. J., Tuijl, B. A. J., Hemming, J., Achten, V. T. J., Balendonck, J., Wattimena, M. R., 2004. Cropscout - a mini field robot for research on precision agriculture. In: Proceedings of the 2nd Field Robot Event. Farm Technology Group, Wageningen, The Netherlands, pp. 47–60.

Van Straten, G., 2004. Field robot event, Wageningen, 5-6 June 2003. Computers and Electronics in Agriculture 42 (1), 51–58.

Van Zuydam, R. P., 1999. A driver's steering aid for an agricultural implement, based on an electronic map and real time kinematic DGPS. Computers and Electronics in Agriculture 24 (3), 153–163.

Van Zuydam, R. P., Achten, V. T. J. M., 2002. Automaatje, uw beste maatje in het veld! Autonoom voertuig vult ontbrekende arbeidskracht aan. (Automate, your best mate in the field! Autonomous vehicle to compensate a shortage of labor). Landbouwmechanisatie 53 (1), 22–23.

Vestlund, K., Hellstrom, T., 2006. Requirements and system design for a robot performing selective cleaning in young forest stands. Journal of Terramechanics 43 (4), 505–525.

Vougioukas, S., Blackmore, S., Nielsen, J., Fountas, S., 2006. A two-stage optimal motion planner for autonomous agricultural vehicles. Precision Agriculture 7 (5), 361–377.

Vrindts, E., De Baerdemaeker, J., Ramon, H., 2002. Weed detection using canopy reflection. Precision Agriculture 3 (1), 63–80.

Warner, M. R. G., 1975. High speed thinning of rowcrops using water jet hoeing. Report 60/1608, National institute of agricultural engineering, Silsoe, United Kingdom.

Wei, J., Rovira-Mas, F., Reid, J. F., Han, S., 2005. Obstacle detection using stereo vision to enhance safety of autonomous machines. Transactions of the ASAE 48 (6), 2389–2397.

Wilson, J. N., 2000. Guidance of agricultural vehicles - a historical perspective. Computers and Electronics in Agriculture 25 (1-2), 3–9.

Woebbecke, D. M., Meyer, G. E., Bargen, K. v., Mortensen, D., 1995. Shape features for identifying young weeds using image analysis. Transactions of the ASAE 38 (1), 271–281.

Zwiggelaar, R., 1998. A review of spectral properties of plants and their potential use for crop/weed discrimination in row-crops. Crop Protection 17 (3), 189–206.

Summary

The systematic design of an autonomous platform for robotic weeding research in arable farming is described. The objective of this research is to replace manual weeding in organic farming by a device working autonomously at field level. Developing such a device is considered as a design problem. The device is designed using a structured design approach, which forces the designer to systematically review and compare alternative solution options, thus preventing the selection of solutions based on prejudice or belief. The result of the design is a versatile research vehicle with a diesel engine, hydraulic transmission, four-wheel drive and four-wheel steering. The robustness of the vehicle and the open software architecture permit the investigation of a wide spectrum of research options for intra-row weed detection and weeding actuators. The concept design regarding navigation consists of both vision based crop row following and GPS based navigation in a field.

The resulting concept design identified the issues that required further investigation. This research focussed then on answering the research questions related to autonomous navigation:

- How to detect crop rows by machine vision.
- How to perform path-following control with a four-wheel steered robotic vehicle.
- How to navigate autonomously in a field given crop row locations and field and headland boundaries.

To detect crop rows in sugar beet with machine vision a new approach is presented which is based on a grey-scale Hough transform on intelligently merged images resulting in a considerable improvement of the speed of image processing. A color camera was used to obtain images from an experimental sugar beet field in a greenhouse. The color images are transformed into grey scale images resulting in good contrast between plant material and soil background. Three different methods were compared to transform color images into grey scale images. The

grey scale images are divided in three sections that are merged into one image, creating less data while still having information of three rows. It is shown that the algorithm is able to find the row at various growth stages. It does not make a difference which of the three color to grey scale transformation methods is used. The mean error between the estimated and real crop row per measurement series varied from 5 to 198 mm. The median error from the crop row detection was 22 mm. The higher errors are mainly due to factors that do not occur in practice or that can be avoided, such as a limited number and a limited size of crop plants, overexposure of the camera, and the presence of green algae due to the use of a greenhouse. Inaccuracies created by footprints indicate that linear structures in the soil surface in a real field might create problems which should be considered in additional investigations. In two measurement series that did not suffer from these sources of error, the algorithm was able to find the row with mean errors of 5 and 11 mm with standard deviations of 6 and 11 mm. The image processing time varied from 0.5 to 1.3 seconds per image.

To perform path-following control a new method for four-wheel steered vehicles is developed. For testing the control, the deviation of the robot from the path is measured with RTK-DGPS in terms of position and orientation. The deviation of the robot to the desired path is supplied to two high level controllers minimizing the orthogonal distance and orientation to the path. Wheel angle setpoints are determined from inversion of the kinematic model of the vehicle. At low level each wheel angle is controlled by a P controller combined with a Smith predictor. The Smith predictor was introduced to overcome the problems with time delay in the system. A refined tuning method calculates high level controller settings that let the robot drive as much as possible along the same path to its setpoint, but also limits the gains at higher speeds to prevent the closed loop system to become unstable due to the time delay in the system. Results show good controller performance following different path shapes including a step, a ramp, and a typical headland path. Mean, minimum and maximum orthogonal distance errors while following a straight path on a paving at a speed of 0.5 m/s are 0.0, -2.4 and 3.0 cm respectively and the standard deviation is 1.2 cm. The control method for four wheel steered vehicles presented has the unique feature that it enables control of a user definable position relative to the robot frame and can deal with limitations on the wheel angles. The method is very well practical applicable for a manufacturer: all parameters needed are known by the manufacturer or can be determined easily, user settings have an easy interpretation and the only complex part, the model inversion, can be supplied as a generic software module.

Finally a navigation system is developed for autonomous navigation in a field requiring field boundaries and headland boundaries as prior information. In the performed field trial also the robot paths along the sugar beet crop rows were available in absolute coordinates. The field navigation method is developed to enable both absolute navigation using known crop row locations with RTK-DGPS and relative navigation using machine vision based crop row detection. The field navigation further includes field boundary crossing detection, headland detection and automated headland turns by following an automatically generated headland path by RTK-DGPS. Simultaneously two trials were performed in the field with the robot platform: navigating along crop rows based on RTK-DGPS and crop row mapping by combining vision based row detection with RTK-DGPS information. Standard deviation, mean, minimum and maximum orthogonal distance of the actuator to the path while following a straight crop row on the field with RTK-DGPS at a speed of 0.3 m/s are respectively 1.6, 0.1, -4.5 and 3.4 cm. For detection in which part of the field given coordinates like the actuator position or the field of view of the camera are located, the point in polygon algorithm proved to be a suitable method. A smooth headland path is generated in realtime with a spline based algorithm, that nicely connects the subsequent paths along the crop. The hybrid deliberate software architecture with a behavior based reactive layer allows a convenient evaluation of the robot performance. Results from field experiments show that the robot can navigate autonomously in a field.

Samenvatting

Dit proefschrift beschrijft het systematisch ontwerp van een autonoom platform voor onderzoek naar een robot voor onkruidbestrijding in de akkerbouw. Het doel van dit onderzoek is het vervangen van handmatig wieden in de biologische landbouw door een apparaat dat binnen een perceel autonooom zijn werk doet. Het ontwikkelen van zo'n apparaat is beschouwd als een ontwerp probleem. Het apparaat is ontworpen met een gestructureerde ontwerp methode, die de ontwerper dwingt om systematisch alternatieve oplossingen te beoordelen en te vergelijken, en de selectie van oplossingen gebaseerd op vooroordelen of overtuiging voorkomt. Het resultaat van het ontwerp is een veelzijdig onderzoeksplatform met een diesel motor, hydraulische transmissie, vierwielaandrijving en vierwielbesturing. De robuustheid van het voertuig en de open software architectuur staan een groot spectrum aan onderzoek toe ten aanzien van intra-rij onkruid detectie en wied-actuators. Het concept ontwerp wat betreft de navigatie is een combinatie van camera gebaseerd rijvolgen en op GPS gebaseerde navigatie in een perceel.

Het resulterende concept ontwerp identificeert de onderwerpen die verder onderzoek vereisen. Dit onderzoek concentreerde zich dan op het beantwoorden van de onderzoeksvragen gerelateerd aan autonome navigatie:

- Hoe gewasrijen te detecteren met beeldverwerkingstechnieken.
- Hoe een regeling voor padvolgen te ontwerpen voor een vierwielbestuurd robot voertuig.
- Hoe autonoom in een perceel te navigeren gegeven de locaties van de gewasrijen en de perceels- en kopakker grenzen.

Om gewasrijen in suikerbieten te detecteren met beeldverwerkings technieken, is een nieuwe benadering gepresenteerd die gebaseerd is op grijswaarde Hough transformatie op slim samengevoegde beelden resulterend in een aanzienlijke verbetering van de snelheid van beeldverwerking. Een kleurencamera is gebruikt om beelden te verzamelen van een experimenteel suikerbieten veld in een kas.

De kleurenbeelden worden getransformeerd in grijswaarde beelden resulterend in goed contrast tussen plant materiaal en de achterliggende bodem. Drie verschillende methodes om kleurenbeelden te transformeren in grijswaarde beelden zijn vergeleken. De grijswaarde beelden worden opgedeeld in drie secties die samengevoegd worden in één beeld, resulterend in een beeld met minder datapunten maar wel met informatie van drie rijen. Het is aangetoond dat het algoritme in staat is om de rij te vinden bij verschillende groeistadia van het gewas. Het maakt niet veel verschil welke van de drie transformatie methodes om kleurenbeelden naar grijswaarde beelden te transformeren wordt gebruikt. De gemiddelde afwijking van de geschatte rij ten opzichte van de echte gewasrij per meetserie varieerde van 5 tot 198 mm. De mediaan van de afwijking van de gewasrij detectie was 22 mm. De grotere fouten worden voornamelijk veroorzaakt door factoren die niet in de praktijk voorkomen, of die vermeden kunnen worden, zoals een beperkt aantal en een beperkte grootte van gewasplanten, overbelichting van de camera en de aanwezigheid van groene algen door het gebruik van een tuinbouw kas. Onnauwkeurigheden door voetstappen geven aan dat lineaire structuren op het grond oppervlak in een echt perceel zouden kunnen zorgen voor problemen die in beschouwing moeten worden genomen in aanvullend onderzoek. In twee meetseries die niet leden onder deze deze foutenbronnen was het algoritme in staat om de rij te vinden met een gemiddelde fout van 5 en 11 mm met standaard deviaties van 6 en 11 mm. De tijd die nodig was voor de beeldverwerking varieerde van 0.5 tot 1.3 seconden per beeld.

Om een pad te kunnen volgen is een nieuwe methode voor besturing van vierwielbestuurde voertuigen ontwikkeld. Om de besturing te testen, wordt de afwijking van de robot van het pad gemeten met RTK-DGPS in termen van positie en orientatie. De afwijking van de robot tot het gewenste pad wordt aangeboden aan twee hoog niveau regelaars die de orthogonale afstand en de orientatie ten opzichte van het pad minimaliseren. Wielhoek setpoints worden bepaald door het kinematisch model van het voertuig te inverteren. Op laag niveau wordt iedere wielhoek geregeld door een proportionele (P) regelaar gecombineerd met een Smith predictor. De Smith predictor werd geïntroduceerd om het probleem van tijdvertraging in het systeem op te lossen. Een verfijnde afstellingsmethode berekent settings voor de hoog niveau regeling die de robot zoveel mogelijk langs het zelfde pad naar zijn setpoint laten rijden, maar ook de versterkingen bij hogere snelheden beperkt om te voorkomen dat het gesloten lus systeem onstabiel wordt door de tijdvertraging in het systeem. Resultaten laten goede regelaar prestaties zien bij het volgen van verschillende pad-vormen waaronder een stapfunctie, een hellingsfunctie, en een typisch kopakker pad. Gemiddelde, minimale en maximale

orthogonale fouten bij het volgen van een recht pad op een verharding bij een snelheid van 0.5 m/s zijn respectievelijk 0.0, -2.4 en 3.0 cm en de standaard deviatie is 1.2 cm. De gepresenteerde regelmethode voor vierwielbestuurbare voertuigen heeft de unieke eigenschap dat zij het besturen van een door de gebruiker relatief ten opzichte van het robot frame gedefinieerde positie mogelijk maakt en dat zij om kan gaan met beperkingen op de wielhoeken. De methode is heel goed praktisch toepasbaar voor een fabrikant: alle benodigde parameters zijn bekend bij de fabrikant of kunnen gemakkelijk worden bepaald, gebruikersinstellingen hebben een gemakkelijke interpretatie en het enige complexe deel, de model inversie, kan beschikbaar gesteld worden als een generieke software module.

Tenslotte is een navigatie systeem ontwikkeld voor autonome navigatie op een perceel die de perceelsgrenzen en de kopakker grenzen nodig heeft als voorinformatie. In de uitgevoerde veldtest waren ook de robot paden langs het gewas suikerbieten beschikbaar in absolute coordinaten. De veld navigatie methode is ontwikkeld om zowel absolute navigatie mogelijk te maken gebruik makend van bekende gewas rij locaties met RTK-DGPS, als relatieve navigatie gebruik makend van op beeldverwerking gebaseerde gewasrij detectie. De veld navigatie omvat verder detectie van het oversteken van veldgrenzen, kopakker detectie en automatisch keren op de kopakker door een automatisch gegenereerd kopakker pad te volgen met RTK-DGPS. Twee proeven zijn tegelijkertijd uitgevoerd in het veld met het robot platform: navigatie langs de gewasrijen gebaseerd op RTK-DGPS en het vastleggen van gewasrijen door op beeldverwerking gebaseerde rijdetectie te combineren met RTK-DGPS informatie. Standaard deviatie, gemiddelde, minimum en maximum orthogonale afstand van de actuator tot het pad bij het volgen van een rechte gewasrij in het veld met RTK-DGPS bij een snelheid van 0.3 m/s zijn respectievelijk 1.6, 0.1, -4.5 en 3.4 cm. Voor detectie in welk deel van het veld gegeven coordinaten zoals de actuator positie of het zichtveld van de camera zich bevinden, heeft het point in polygon algoritme bewezen een passende methode te zijn. Een vloeiend kopakker pad wordt gegenereerd in realtime met een op splines gebaseerd algoritme, dat de opeenvolgende paden langs het gewas mooi verbindt. De hybrid deliberate software architectuur met een behavior based reactive layer maakt evaluatie van de robot prestaties gemakkelijk. Resultaten van veld experimenten laten zien dat de robot autonoom kan navigeren in een perceel.

Curriculum Vitae

Tijmen Bakker was born on December 30th, 1975 in Ede, The Netherlands. After completing high school at the Van Lodenstein College in Amersfoort, he studied Agricultural Engineering at Wageningen University. His first MSc thesis concerned object orientated design of an ISO 11783 based Virtual Terminal, and the second thesis concerned spread pattern modeling of centrifugal fertilizer spreaders. In 1999 he finished his studies and started as Project Engineer at Kverneland Mechatronics BV in Nieuw-Vennep, the Netherlands. His work concerned the development of electronic control systems for agricultural machinery with precision farming related applications as area of special attention. In 2002 he started his PhD research at the collaborating groups Systems and Control and Farm Technology of Wageningen University. The research concerned the design of an Intelligent Autonomous Weeder and the results are presented in this thesis. In 2008 he founded the company Tyker Technology, by which he targets on research and development of technology for (semi) autonomous vehicles.

List of Publications

Lokhorst, K., Achten, V., Bakker, T., Goense, D., Vermeulen, B., 2003. Wieden zonder handwerk: wat mogen we van de onkruidrobot verwachten? Ekoland 23 (3), 12–13.

Bakker, T., Van Asselt, C. J., Bontsema, J., Müller, J., Van Straten, G., 2004. The design of an autonomous weeding robot. In: Proceedings 6th EWRS Workshop on Physical and Cultural Weed Control. Lillehammer, Norway, p. 94.

Bakker, T., Wouters, H., Van Asselt, C. J., Bontsema, J., Müller, J., Van Straten, G., Tang, L., 2004. A vision based row detection system for sugar beet. In: Computer-Bildanalyse in der Landwirtschaft. Workshop 2004. Vol. 37 of Bornimer Agrartechnische Berichte. Institut für Agrartechnik Bornim e.V., Potsdam-Bornim/Braunschweig, Germany, pp. 42–55.

Bakker, T., Van Asselt, C. J., Bontsema, J., Müller, J., Van Straten, G., 2005. An autonomous weeding robot for organic farming. In: Preprints of the International Conference on Field and Service Robotics. Port Douglas, Australia, pp. 580–591.

Bakker, T., Bontsema, J., 2005. An autonomous weeding robot for organic farming. In: Proceedings EWRS Workshop in Spatial and dynamic weed measurements and innovative weeding technologies. Bygholm, Denmark, p. 16.

Bakker, T., 2005. Control of a weeding robot. In: 25th Benelux Meeting on Systems and Control. Heeze, The Netherlands, p. 106.

Bakker, T., Wouters, H., Van Asselt, C. J., Bontsema, J., Müller, J., Van Straten, G., Tang, L., 2005. A vision based row detection system for sugar beet. In: 24th Benelux Meeting on Systems and Control. Houffalize, Belgium, p. 138.

Bakker, T., 2005. Weeding robot is autonomous. Resource 12 (7), 14.

Bakker, T., Van Asselt, C. J., Bontsema, J., Müller, J., Van Straten, G., 2006. Autonomous navigation with a weeding robot. In: Rothmund, M. (Ed.), Proceedings of the 1–2 September 2006 Conference ATOE, Automation Technology for Off-road Equipment. Bonn, Germany, pp. 51–57.

Bakker, T., Van Asselt, C. J., Bontsema, J., Müller, J., Van Straten, G., 2006. An autonomous weeding robot for organic farming. In: Corke, P., Sukkarieh, S. (Eds.), Field and Service Robotics. Vol. 25 of Springer Tracts in Advanced Robotics (STAR). Results of the 5th International Conference, Springer-Verlag Berlin Heidelberg, pp. 579–590.

Bakker, T., Van Bergeijk, J., Biesenbeek, S., Van der Bijl, M., Dhaene, M., Govers, M., Jansen, R., Knol, J., Kroon, B., Speetjens, B., 2006. First universal wheel unit for field robots - poster. In: Field Robot Event 2006. Hohenheim, Germany.

Straten, G., Bakker, T., Van Asselt, C. J., 2006. Robotisering in de landbouw: Autonome agrarische voertuigen. Agro-Informatica, 10–12.

Bakker, T., Van Asselt, C. J., Bontsema, J., Müller, J., Van Straten, G., 2007. Path following with a robotic platform. In: Agricontrol 2007. 2nd IFAC International Conference on Modeling and Design of Control Systems in Agriculture. Osijek, Croatia, pp. 153–158.

Bakker, T., Van Asselt, C. J., Bontsema, J., Müller, J., Straten, G. v., 2007. RTK-DGPS based path following with a robotic platform. In: VDI-MEG. Proceedings of the Land Technik AgEng 2007. Hannover, Germany, pp. 183–184.

Bakker, T., Yaman, M., 2007. Wegen vegen met een robot, kan dat? Eerste resultaat innovatieprijsvraag AGI. GeoNieuws 1, 32–33.

Bakker, T., Van Asselt, C. J., Bontsema, J., Müller, J., Van Straten, G., 2008. Autonomous navigation in a sugar beet field with a robot. In: Proceedings of the AgEng 2008. Crete, Greece, p. 19.

Bakker, T., Van Asselt, C. J., Bontsema, J., Müller, J., Van Straten, G., 2008. Autonomous navigation in a sugar beet field with a robot. Biosystems Engineering, Submitted for publication.

Bakker, T., Van Asselt, C. J., Bontsema, J., Müller, J., Van Straten, G., 2008. Path following with a robotic platform. Autonomous Robots, Submitted for publication.

Bakker, T., Van Asselt, C. J., Bontsema, J., Müller, J., Van Straten, G., 2008. Systematic design of an autonomous platform for robotic weeding. Journal of Terramechanics, Accepted for publication.

Bakker, T., Wouters, H., Van Asselt, K., Bontsema, J., Tang, L., Müller, J., Van Straten, G., 2008. A vision based row detection system for sugar beet. Computers and Electronics in Agriculture 60 (1), 87–95.

136

Patent

Bakker, T., 2007. Wiedinrichting. Octrooiaanvraagnummer: NL2001003, Ingediend: 13-11-2007. Aanvrager: Wageningen University.

Reports

Bakker, T., 2003. Autonomous weeding. Literature review. SCO report 03-01, Wageningen University, Systems and Control group, Wageningen, 43 p.

Kok, J. P. B., Bakker, T., Lokhorst, C., 2003. Programma van eisen voor een intelligente autonome wieder. Report, Instituut voor Milieu- en Agritechniek (IMAG), Wageningen, 68 p.

Bakker, T., Van Asselt, C. J., 2006. Precies positioneren van een rooiunit voor struiken. SCO report 06-01, Wageningen University, Systems and Control group, Wageningen, 36 p.

Bakker, T., Bontsema, J., 2007. Een intra-rij wieder met een nieuwe actuator. Haalbaarheidsstudie naar de Speed-IRW. SCO report 07-02, Wageningen University, Systems and Control group, Wageningen, 47 p.

Bakker, T., Van Asselt, C. J., 2007. Robotiseren van het dagelijks onderhoud aan wegen via geo-informatie. SCO report 07-01, Wageningen University, Systems and Control group, Wageningen, 81 p.

Completed training activities

Discipline specific activities

Intelligent technologies for future farming	2003
3rd EWRS workshop on Site Specific Weed Management	2003
Intelligent Vehicles - From Concept to Confidence	2003
6th EWRS Workshop on Physical and Cultural Weed Control	2004
Workshop Computer-Bildanalyse in der Landwirtschaft	2004
AgEng 2004 International conference on agricultural engineering	2004
24th Benelux Meeting on Systems and Control	2005
Delft Science in Design	2005
FSR '05 International Conference on Field and Service Robotics	2005
Spatial and dynamic weed measurements and innovative weeding technologies	2005
25th Benelux Meeting on Systems and Control	2006
ATOE 2006 Automation Technology for Off-road Equipment	2006
Symposium besturingen in de hydrauliek	2006
Workshop geïntegreerde navigatie	2006
Workshop Agrobots	2007
2nd IFAC International Conference on Modeling and Design of Control Systems in Agriculture	2007
Land.Technik - AgEng 2007	2007
AgEng 2008 International Conference on Agricultural Engineering	2008

Courses

Scientific writing	CENTA	2002
Biology and Control of Pests and Diseases I	CWE	2002
Design methods for control systems	DISC	2003
Project and time management	WGS	2003
Procesbegeleiders Academic Master Cluster	OWU	2004
Projectmanagement voor gevorderden	KIVI	2005
Afstudeervak organiseren en begeleiden	OWU	2006
Interpersonal communication for PhD students	WGS	2007